Tampere University

Jesse Salmi

DEVELOPING COMPUTER VISION-BASED SOFT SENSOR FOR MUNICIPAL SOLID WASTE BURNING GRATE BOILER

A practical application for flame front and area detection

Master of Science Thesis
Faculty of Engineering and Natural Sciences
Examiners: Prof. Risto Ritala
Prof. Esa Rahtu
Supervisors: M.Sc. (Tech.) Timo Ojanen
M.Sc. (Tech.) Vesa Nieminen
September 2021

ABSTRACT

Jesse Salmi: Developing computer vision-based soft sensor for municipal solid waste burning grate boiler – A practical application for flame front and area detection
Master of Science Thesis
Tampere University
Master's Degree Programme in Automation Engineering
September 2021

Waste is incinerated in grate boilers to produce energy that is then converted to electricity and heat. Even though grate boilers can use low-quality waste as fuel, the grate combustion is proven to be harder to control compared to other combustion technologies. Earlier studies have shown that an optimised combustion process is in a key position increasing energy efficiency and lowering environmental impacts and operating costs. Computer vision-based approaches have been applied successfully for combustion diagnostics but there is a limited number of research from waste combustion in grate boilers.

This study aims to develop a practical computer vision application for detecting flame area and position and explore how computer vision-based combustion diagnostics in a grate boiler environment. The thesis is divided into a literature review and empirical research. The literature review explores waste incineration, grate combustion, primary control loops and computer vision applied in combustion processes. In the empirical research part, experimental video, process and survey data were collected from an industrial grate boiler and its specialists. The research method of the study was a single case study.

The study presents a data-driven computer vision-based model that detects flame area and flame front position from the video of the combustion chamber. The proposed system utilises a similar approach model and algorithms as earlier studies which were found in the literature research. The model was evaluated against the available process data with cross-correlation and statistical analysis methods. The study found that the flame front location correlates the most with the process parameters while the flame area predicts the signal changes the earliest. The results indicate that the model provides useful metrics of the combustion that is applicable for monitoring and control purposes.

Qualitative research shows that the most important state variables for the grate boiler are related to modelling chemical and physical combustion dynamics. The most suitable combustion characteristics that camera systems can automatically recognise are flame area, position, intensity, movement, temperature and unburned objects. The results suggest that the highest improvements for power plant operation are possible by modelling the combustion process more accurately. Building accurate models require collecting new data in which computer vision provides additional information on the operation conditions of the grate boiler. Our findings are supported by prior research.

Keywords: computer vision, soft sensor, grate boiler, control system, waste-to-energy

TIIVISTELMÄ

Jesse Salmi: Konenäköön perustuvan ohjelmallisen anturin kehittäminen jätettä polttavalle arinakattilalle – Käytännön sovellus liekkirintaman ja paloalueen havaitsemiseen
Diplomityö
Tampereen yliopisto
Automaatiotekniikan diplomi-insinöörin tutkinto-ohjelma
Syyskuu 2021

Arinakattilat tuottavat sähköä ja lämpöä jätettä polttamalla. Vaikka arinakattilat pystyvät käyttämään heikkolaatuisia jätteitä polttoaineena, arinapolton on todettu olevan vaikeammin säädettävissä verrattuna muihin polttotekniikoihin. Aikaisemmat tutkimukset ovat todistaneet, että polton optimointi on avainasemassa energiatehokkuuden lisäämisessä sekä ympäristövaikutusten ja käyttökustannusten vähentämisessä. Konenäköpohjaisia lähestymistapoja on sovellettu onnistuneesti polton diagnosoinnissa, mutta laajempia tutkimuksia arinakattilaympäristöissä on rajatusti.

Tämän tutkimuksen tavoitteena on kehittää käytännöllinen konenäkömalli liekin alueen ja sijainnin havaitsemiseksi sekä selvittää, kuinka konenäköä voitaisiin hyödyntää kattavammin polton diagnosoinnissa arinakattilaympäristössä. Diplomityö on jaettu kirjallisuuskatsaukseen ja empiiriseen tutkimukseen. Kirjallisuuskatsaus tutkii arinakattilan jätteenpolttoa, arinapolttoa, pääsäätöpiirejä ja konenäköä palamisprosesseissa. Empiirisessä tutkimuksessa kerättiin kokeellista video-, prosessi- ja kyselydataa teollisuusluokan arinakattilasta ja prosessiasiantuntijoilta. Tutkimuksessa käytetty tutkimusmenetelmä on tapaustutkimus.

Tutkimus esittelee konenäköpohjaisen mallin, joka tunnistaa paloalueen ja liekkirintaman sijainnin arinakattilan tulipesästä kuvatusta videokuvasta. Esitetty malli hyödyntää kirjallisuustutkimuksessa löydettyä lähestymistapaa ja algoritmeja, jotka perustuvat aikaisempiin tutkimuksiin. Mallia arvioitiin ristikorrelaatiolla ja tilastollisen analyysin menetelmillä kerättyyn prosessidataan. Löydösten mukaan liekkirintama korreloi eniten prosessimittausten kanssa, kun taas liekin alue ennustaa signaaleiden muutoksia aikaisintaan. Löydökset osoittavat mallin tuottavan tärkeää informaatiota palamisesta, jota voitaisiin käyttää valvonta- ja säätötarkoituksiin.

Kvalitatiivinen tutkimus osoittaa, että arinakattilan tärkeimmät tilamuuttujat liittyvät polttoprosessin mallintamiseen fysikaalisten ja kemikaalisten reaktioiden kautta. Sopivimpia polttoa kuvaavia parametrejä, joita kamerajärjestelmät voisivat automaattisesti tunnistaa, ovat liekin alue, sijainti, intensiteetti, liikehdintä, lämpötila ja palamattomat esineet. Tulokset osoittavat polttoprosessin tarkemmalla mallintamisella olevan eniten vaikutusta voimalaitoksen toimintaan. Prosessin tarkempi mallintaminen vaatii uuden datan keräämistä, jossa konenäkö voi tuottaa lisäinformaatiota arinakattilan käyttöolosuhteista. Aikaisemmat tutkimukset tukevat löydöksiämme.

Avainsanat: konenäkö, ohjelmallinen anturi, arinakattila, ohjausjärjestelmä, energiajäte

PREFACE

Six years of studies, three universities, two continents, a lot of good memorable events and a countless number of ups and downs are some of the characteristics that describe my life while pursuing a master's degree. All the hard work and effort I put in has culminated in this paper.

Clean technology has an important role in fighting against climate change, especially in energy and process industries. Recently, artificial intelligence has shown great promise enabling advanced possibilities in numerous industry sectors. I feel honoured for being a forerunner combining these two separate fields in my study. I hope this thesis will be a precursor for enabling cleaner and more efficient energy production.

Firstly, I would like to express my sincerest gratitude to Valmet for providing an interesting topic to work with. I want to thank my talented colleagues Timo Ojanen for providing excellent guidance and support in every circumstance; Vesa Nieminen and Matts Almark for offering deep insight into combustion process and controls; Anna Hakala for meaningful discussions about computer vision and data analysis; Module 55 occupants for joyful lunch and coffee breaks; and all the other valmeteers and automagicians who helped me during the thesis – the list could go on.

The education gained from Tampere University has remarkably helped me finishing this thesis. When even more knowledge was required, I gained invaluable mentoring from my examiners Risto Ritala and Esa Rahtu. I am beyond grateful for their devoted time and effort in sharing part of their vast knowledge with me. I want to also thank Ville Koljonen who assisted me in typesetting issues that influenced how this thesis looks like.

The thesis would have not been possible without data collection from the industrial-size grate boiler. I strongly appreciate the support given by Tammervoima process specialists with a special mention to Mika Pekkinen, Mika Pasula and Ville Leskinen. Much obliged for you making the measurement campaign possible even during the global pandemic.

Finally, I wish to thank my friends and family for all the unconditional love and support they have given me during my studies. It has been a pleasure to experience unforgettable – yet never unbearable moments with all of you. You are the reason I have made it this far.

Tampere, 20th September, 2021

Jesse Salmi

CONTENTS

1. Introduction 1
1.1 Background and research motivation 1
1.2 Objectives and research questions 5
1.3 Methodologies and research scope 6
1.4 Structure of thesis 7
2. Grate combustion 9
2.1 Waste incineration 9
2.2 Combustion process 11
2.3 Grate structures 14
3. Control systems 16
3.1 Primary control loops 16
3.1.1 Combustion control 20
3.2 Imaging based soft sensors 22
3.2.1 Flame characteristics 24
4. Computer vision applications in combustion processes 27
4.1 Process 27
4.1.1 Image formation 28
4.1.2 Pre-processing 29
4.1.3 Segmentation 30
4.1.4 Feature extraction 31
4.1.5 Model and fitting 33
4.2 Camera features 35
5. Research methodology 37
5.1 Research method and approaches 37
5.2 Description of power plant 39
5.3 Overview of measurement campaign 43
5.3.1 Measurement equipment 44
5.3.2 Visible light camera installation 46
5.3.3 Infrared camera fixed installations 47
5.3.4 Infrared camera mobile inspections 50
5.3.5 Process data collection 53
5.4 Power plant expert surveys 56
5.5 Data analysis 57
5.5.1 Soft sensor parameters 58

5.5.2 Surveys 61
6. Soft sensor implementation 63
6.1 Development choices 63
6.2 Image formation 64
6.3 Pre-processing 65
6.4 Segmentation 66
6.5 Feature extraction 68
6.6 Video data processing 70
7. Results 75
7.1 Soft sensor model 75
7.2 Surveys 76
8. Analysis 80
8.1 Computer vision soft sensor 80
8.2 Process state variables 91
8.3 Combustion characteristics 92
9. Conclusion 95
9.1 Main findings 95
9.2 Contributions and implications 97
9.3 Future research 98
References 100
Appendix A: Data sheets of cameras 112
Appendix B: Collected process values 116
Appendix C: Survey questionnaire. 121
Appendix D: Signal analysis results 122

LIST OF FIGURES

1.1 Imaging system structure and highlighted scope of the thesis. (Courtesy of Valmet) 4

2.1 Example layout of a solid waste incineration plant for municipal waste. [32, p. 35] 10
2.2 Combustion process of solid fuel in inclined stepped grate boiler. Adapted from [39]. 12
2.3 Stationary sloping and travelling grate layouts. 14

3.1 Arrangement of the coordinated control system in steam generating plant. [41] 19

4.1 Simplified image analysis process. Adapted from [71]. 27

5.1 Cross-section of the municipal solid waste grate boiler of the test campaign. [99] 42
5.2 Camera installations at the end of the grate. The visible camera on the left and the infrared on the right side. 44
5.3 The camera equipment of the measurement campaign. (Courtesy of Valmet) 45
5.4 Example image from the end of the grate with VIS camera. 46
5.5 Thermopile image from visible light camera system. 47
5.6 Example images from MWIR camera. 48
5.7 Heat map from end of the grate with infrared camera. 50
5.8 Superheater section recorded with mobile infrared camera. 51
5.9 Top of the combustion chamber recorded with mobile infrared camera. . . 52
5.10 One of the operator process displays during data collection. 54

6.1 Camera captured image. 64
6.2 Histograms of the colour channels. 65
6.3 Median filtered image. 66
6.4 Histogram of preprocessed image. 67
6.5 Segmented image with tested methods. 67
6.6 Segmented and morphological operated image. 68
6.7 Feature extraction sequence. 69
6.8 Detected flame front and feature points of the flame location. 70
6.9 Logged soft sensor features. 71

6.10 Filtered flame area with three tested moving averages. 73

8.1 Cross-correlation of the minimum flame point and primary air flow. 81
8.2 Primary air flow and minimum flame point. 82
8.3 Cross-correlation of the minimum flame point and secondary air flow. . . . 83
8.4 Secondary air flow and minimum flame point. 84
8.5 Primary air flow and maximum flame point results. 85
8.6 Cross-correlation of the flame area and primary air flow. 86
8.7 Primary air flow and flame area. 87
8.8 Flue gasses intercepting camera vision. 90

LIST OF TABLES

3.1 Measured flame characteristics by soft sensors. 25

5.1 Technical data of the power plant. Adapted from [96]. 41
5.2 Summary of the collected process values. 55
5.3 Survey themes and codes. 62

8.1 Main data analysis results for the primary control loop state variables. . . . 89

B.1 Collected process values. 120

D.1 Results with extracted flame front minimum point. 125
D.2 Results with extracted flame front maximum point. 129
D.3 Results with extracted flame front average point. 133
D.4 Results with extracted flame front coefficient b. 137
D.5 Results with extracted flame front coefficient a. 141
D.6 Results with extracted flame area. 145
D.7 Excluded signals. 145

ABBREVIATIONS

Artificial Intelligence (AI)	Field of study for simulating human intelligence with machines
Artificial Neural Network (ANN)	Computing system designed to simulate human brain
Charge Couple Device (CCD)	Integrated circuit image sensor in visible light cameras
Combined Heat and Power (CHP)	Generation of power and heat from energy
Complementary Metal Oxide Semiconductor (CMOS)	Integrated circuit structure in semiconductor devices
Computer Vision (CV)	Scientific field for simulating human vision system
Density Based Spatial Clustering of Applications with Noise (DBSCAN)	Data clustering algorithm
Distributed Control System (DCS)	Decentralised control system architecture
Fluidized Bed Combustion (FBC)	Combustion technology
Frames Per Second (FPS)	Unit of frame capturing rate
Gaussian Mixture Model (GMM)	Probabilistic clustering method
Genetic Programming (GP)	Technique of evolving programs
Hidden Markov Model (HMM)	Statistical model based on Markov chain
Industrial Waste (IW)	Waste generated by manufacturing or industrial processes
K-Nearest Neighbour (KNN)	Supervised classification algorithm
Machine Learning (ML)	Data analysis method for building automatic analytical models
Middle Wavelength Infrared (MWIR)	Wavelength in range of 3–8 µm
Model Predictive Control (MPC)	Model based control strategy
Multivariate Image Analysis (MIA)	Methodology for analysing multivariate images
Municipal Solid Waste (MSW)	Community discarded waste

Open Source Computer Vision Library (OpenCV)	Python's computer vision library
Ordinary Least Square (OLS)	Linear regression model
Principal Component Analysis (PCA)	Data dimensionality reduction method
Proportional Integral Derivative (PID)	Controller with proportional, integral and derivative blocks
Red Green Blue (RGB)	Colour model that produces colour space
Refuse Derived Fuel (RDF)	Fuel produced from various types of waste
Root Mean Square Error (RMSE)	Error measurement tool for differences
Scale Invariant Feature Transform (SIFT)	Computer vision feature detection algorithm
Selective Catalytic Reduction (SCR)	NO_x emission reduction technology with catalyst
Selective Non-Catalytic Reduction (SNCR)	NO_x emission reduction technology by ammonia or urea injection
Self-Organizing Map (SOM)	Unsupervised learning algorithm for dimensionality reduction
Solid Refuse Fuel (SRF)	Fuel produced from recovered waste
Structured Query Language (SQL)	Programming language for managing relational database management systems
Support Vector Machine (SVM)	Supervised learning algorithm
Total Organic Carbon (TOC)	Amount of carbon in organic compound
Visible Imaging System (VIS)	Imaging system using visible light radiation
Waste To Energy (WTE)	Energy generation method from burning waste

SYMBOLS

α	Significance level
λ	Air–fuel ratio
a	Polynomial slope coefficient
b	Polynomial y-intercept coefficient
H_0	Null hypothesis
H_1	Alternative hypothesis
L^2	Euclidean norm
m	Signal offset
P	Critical value
$\hat{R}_{xy}$	Zero-Normalized Cross-Correlation

1. INTRODUCTION

Combustion optimisation is important for a power plant's energy efficiency. Combustion diagnostics have a crucial role in increasing power plant performance in which computer vision has shown great promise in some applications. This chapter explains the background of the research, states the research questions and outlines the research methodology. The first section briefly reviews the earlier studies, introduces the current situation of the research topic and asserts the importance of the research. The second section presents research objectives and research questions. The third section explains applied methodologies and research scope while the final section describes the format of the thesis.

1.1 Background and research motivation

Thermochemical treatment of the waste has been widely applied as a waste management process. It reduces required landfill space by changing the waste to easily disposable residues and neutralises hazardous substances. [1] Another important object of waste incineration is energy recovery which is also known as Waste To Energy (WTE). Burning the waste releases energy that produces electricity and heat [2, 3]. This helps to fight against climate change by replacing fossil fuels in energy production. Fossil fuels are known for a high amount of greenhouse gas emissions that contribute to climate warming. Patel *et al*. confirmed that waste is both an economically and technically viable option to substitute fossil fuels in energy production [4].

Waste is incinerated in grate boilers. Grate boilers offer high fuel flexibility and easy operation which is good for waste where fuel is heterogeneous [5]. However, grate boilers have lower energy efficiency and higher emissions compared to other waste incineration technologies, such as Fluidized Bed Combustion (FBC) [6]. Harmful waste to humans and the environment alike has increased the enforcement of strict directives and legislation. Waste incinerators are known for having stringent emission limits to air and water compared to other power plants. [1] This puts additional requirements for the waste incineration grate boilers. Studies have shown that the development of advanced technologies is required to overcome these challenges and make WTE a more suitable and widely applied method for energy production. Fodor and Klemeš [7] compared waste treatment

methods. According to their study grate combustion requires more research and development to make it a more widely accepted solution for energy production to fulfil strict requirements for combustion efficiency and emissions [7].

Various technologies have been researched and applied to reduce emissions, such as flue gas cleaning technologies [8]. Flue gas cleaning is an effective way to reduce emissions but it is costly and should be applied only if no other option is available. Alternating combustion conditions have been shown to have a high effect on emissions and combustion efficiency. Munir *et al*. demonstrated that right combustion stoichiometry reduces NO_x emissions and increases combustion efficiency without affecting boiler lifetime [9]. Therefore, optimising the combustion process has a significant role in providing clean and economical energy.

Waste is difficult fuel because it is highly heterogeneous and its calorific value is varying. This makes combustion harder to keep stable. Previous studies have shown that low fuel quality, such as waste causes unstable flame and incomplete combustion, reduces combustion efficiency and increases pollutant emissions [10, 11, 12]. Meeting the strict regulations requires energy savings and cutting down emissions. Here, advanced technologies for combustion monitoring and control have become the topic of research interest. One of the research fields has been utilising computer vision-based processing techniques for combustion monitoring and control.

Earlier studies have shown that the physical characteristics of the flame yield important information about the state of the combustion process inside the furnace. Lu *et al*. [13] proved that digital imaging and image processing techniques are applicable for combustion flame characterisation. Image processing techniques have been applied in industrial-size boilers to detect physical parameters of the combustion, such as flame intensity [14], temperature [15] and flame flickering [16]. Some studies have applied model-based approaches to detect the state of the combustion [17, 18].

Research indicates that image processing provides important information of the combustion process. However, it seems that there is rather little research where computer vision or image-processing methods has been applied to grate combustion analysis. Tóth *et al*. [19] predicted heat output of a small-scale biomass grate boiler with flame images. Garami *et al*. [20] studied in the same boiler how the location of the flame boundary corresponds to a couple of process measurements. Both of these papers note that there are not many studies exploring flame monitoring computer vision systems in grate boilers and further research is required [19, 20].

Even fewer studies are found from waste burning grate boilers. Strobel *et al*. [21] reported that they improved combustion efficiency by lowering excessive air with a computer vision-based control system. Martin *et al*. [22] analysed recent process control system technologies where they discussed a control system utilising an infrared camera.

Cui *et al*. [23] utilised flame location in control loops inside refuse waste incineration. The problem with these studies is that they utilise black-box models without explaining how computer vision is applied to the solutions. The models are not assessed or the significance in the process controls explained. Nevertheless, numerous other studies [15, 18, 19, 20, 24, 25, 26, 27, 28] from other combustion processes have proven that image processing and computer vision are applied to optimise and monitor combustion. Utilising computer vision-based analysing tools could benefit WTE industry and thus there is both economical and environmental motivation to research this topic.

This thesis is done in collaboration with Valmet, a publicly listed Finnish company that is a global developer and supplier of process technologies, automation and services for the pulp, paper and energy industries. They employ over 14 000 professionals in 30 countries around the globe and their net sales were 3.7 billion euros in 2020. [29] Valmet's automation business line supplies and develops automation and information management systems, applications and services. Their main products are control systems, analysers and measurement devices. Products are designed to maximise profitability and sustainability by improving production performance, cost-effectiveness, energy and material efficiency.

Part of Valmet's analyser and measurement systems are imaging systems that are designed for high-temperature processes in power generation, Waste To Energy, pulp and paper, iron and steel, petrochemical and cement industries [30]. Imaging systems provide combustion monitoring and measurements in boiler and furnace conditions. Systems contain visible and infrared cameras that are paired with thermal infrared sensors for real-time regional temperature measurement. Cameras are designed to endure harsh process circumstances. They are equipped with a heat withstanding enclosure and air-cooling system which prevents imaging units from overheating. The system is integrated into an automated retraction system that protects camera modules in case of cooling air loss if needed.

Imaging systems are controlled with specific software that enables a human-machine interface for the operators. The software provides live video stream monitoring for displays, measurement analysis tools, daily trend and video reports as well as interfaces to other systems, such as plant control systems. From the software, an operator configures live image, communication and measurement settings and take video or snapshots. Furthermore, the software contains some image-processing methods, such as frame averaging, gamma correlation and image colourisation that allows adjustment of the image quality. Cameras can be connected to plant's automation systems. Cameras provide measured values that are utilised in control rooms or stored in information systems. The typical camera system layout is illustrated in the Figure 1.1.

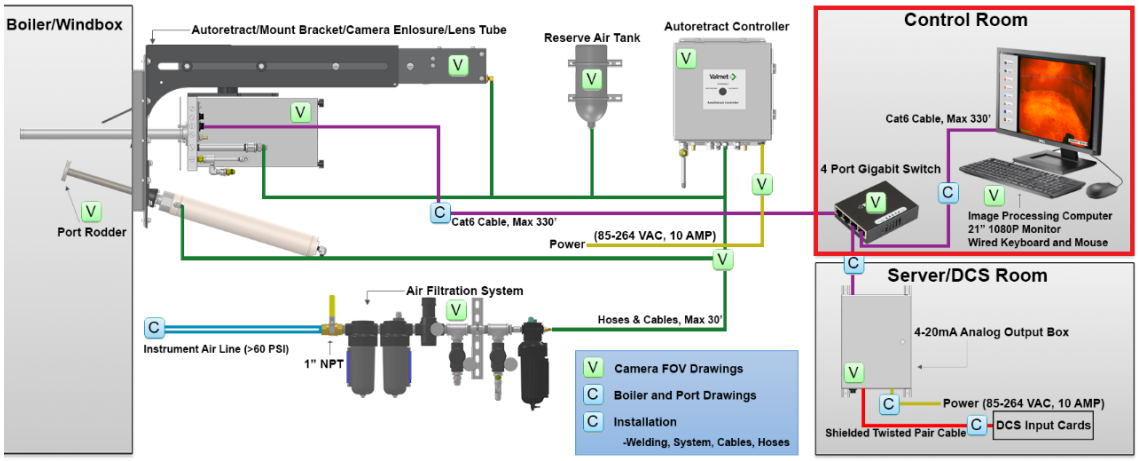

Figure 1.1. *Imaging system structure and highlighted scope of the thesis. (Courtesy of Valmet)*

Currently, basic image-processing methods, such as frame averaging, edge detection and binary mask quantifies key performance indicators of the process from the video feed. These calculated parameters include parameters, such as slag buildup in the superheater section in pulverised coal boilers, flame profile in rotary kilns and bed volume in recovery boilers. The issue with the current imaging systems is that these parameters are not widely utilised in control loops. Operators follow video stream and calculated parameters and make process control decisions based on his or her judgement manually. These choices are subject to personal biases and highly depended on a person's level of expertise. In addition, combustion process parameters from grate boilers are not currently determined from the video stream in the imaging system software. This further makes process control prone to human errors as there is no information available thus affecting the overall performance of the process and its stability.

Precise, real-time and automatic analysis for image feed is required to make imaging systems describe the combustion in more detail. Flame imaging systems need to be combined with control algorithms and loops [13]. Computer vision in control systems has potential to improve the overall efficiency of the combustion process operability and give additional information about the state of the process compared to invasive single point sensors.

Previous discussions with grate boiler manufacturers have given preliminary indications that optimising grate speed and cooling is possible if flame front location, flame shape and temperature distribution are measured from the grate. Determining these process parameters is possible with computer vision-based methods which are integrated to control systems. This potentially leads to improved process performance, energy efficiency and reduced fuel consumption. Nielsen *et al.* [31] simulated grate boiler and flame front location position in the dynamic test environment. According to their simulation results utilisation rate and load change capability of the grate increases if flame front position

is controlled. [31] Study indicates that the flame front position needs to be measured to optimise boiler efficiency. This needs to be researched in industrial size power plant to find practical usage.

1.2 Objectives and research questions

The thesis aims primarily to develop a proof-of-concept computer vision-based soft sensor for municipal solid waste burning grate boilers. The soft sensor defines flame size, flame front shape and location in industrial size grate boiler. The design of a computer vision-based application focuses to implement academically and practically feasible software that determines the wanted process variables from the video stream. In the future, advanced process controls or diagnostics can utilise information provided by the sensor. The computer vision model is developed with a Valmet imaging system image processing computer. The developed model and measured variables are evaluated with the process data available from the power plant to assess the usefulness of the model.

The secondary objective of the thesis is the study of computer vision in process control and monitoring. Valmet has delivered several grate boiler automation systems and has a wide knowledge of the grate boiler process controls. Valmet is committed to develop and offer new products for their customers that increase energy optimisation and material usage. One of the research and development focus is on advanced process controls that utilise computer vision. The thesis aims to bring objective and detailed information on computer vision-based methods found in the literature and how they are utilised in boiler monitoring and control. The applied technology and combustion process dynamics of the grate boiler are explored systematically and without bias.

The combustion process is highly dynamic and requires constant tuning to achieve high operating efficiency. Valmet's imaging systems potentially offers a real-time, non-intrusive and cost-effective choice for process analysing. The thesis aims to inspect how camera systems are adopted for process diagnostic and control purposes and exploit their full potential. A review of combustion parameters that are measurable from the image recognised in the literature is considered. The thesis investigates computer vision models utilising visible light or infrared cameras. Investigation of grate boiler control parameters are considered and a small-scale computer vision application is developed. Surveys are conducted to evaluate computer vision for process diagnostics. Research questions therefore are:

- Which process state variables are important in grate boiler control systems?
- Which combustion characteristics can be detected from the video that can be integrated to automation systems?
- How process variables can be measured automatically using infrared or visible light

cameras?

- How to determine flame front and area with computer vision?

To find answers to these questions, the thesis aims to connect academic literature, process specialists' knowledge and experimental data collected from an industrial grate boiler plant.

1.3 Methodologies and research scope

The research contains a theoretical literature review, an empirical quantitative analysis and qualitative surveys. The literature review consists of an examination of grate boiler and grate firing technologies, power plant control systems and computer vision applications applied in combustion processes. The review elaborates on grate boiler burning process characteristics, control system structures, imaging-based soft sensors and computer vision models. The main sources of the literature review are academic articles, journals, reports and a couple of books. Reliability and quality of the articles are assessed with a status of peer-review, publisher, publication year, number of references, author's area of expertise and other publications listed in priority sequence. The credibility of the books have been evaluated with parameters, such as the author's other publications, area of expertise, bibliography credentials and publishing authority. Most of the literature has been searched and accessed using Tampere University library's search services and collection databases.

The quantitative analysis is carried out in a municipal solid waste energy recovery grate boiler power plant. Video recordings and temperature distribution from the combustion process are collected with Valmet's visual light and infrared imaging systems. The computer vision model is developed based on the collected video material. To evaluate the developed computer vision model, conventional process data is collected from the plant's control and information management systems. Gathered data contains measurements from the power plant's sensors and control loops and the data set is compared to computer vision model parameters with signal analysis techniques.

In qualitative research, semi-structured surveys with open-ended questions were held to gather information from the grate boiler control room operators and the specialists. Surveys provided insight on power plant operability from the combustion control point of view and how the grate boiler utilises camera systems. Surveys are analysed with descriptive research methods and the results are reflected against the literature review when applicable.

This thesis is part of Valmet's advanced process control development project where computer vision-based control systems are demonstrated in grate boiler processes. The final developed system utilises Valmet imaging systems for image acquisition, pre-processing

and image analysing as well as Valmet control systems to control the boiler's combustion process. The development project contains both the computer vision and control model development phases. This thesis focuses on computer vision development in imaging systems and the development of the control application is omitted from the scope of the thesis. In addition, this thesis is concentrating on developing flame front and flame area detection algorithms and not other auxiliary development which is required for the final product. For instance, imaging systems require additional development to allow data connection to control systems and modifications to a user interface which are not part of this thesis. The scope of the thesis in imaging systems is highlighted with a red square in the Figure 1.1.

The thesis is limited to develop an experimental computer vision application with data available only from one specific type of municipal waste burning grate boiler. It must be acknowledged that this study is done in close collaboration with the company's research project that has a set scope and budget. This sets limitations to applied research methods in the form of level of detail in data collection and analysis stages. It is not possible to find comprehensive and generalisable results within the scope of this master's thesis.

The literature review is limited to grate boiler combustion. There are other combustion technologies for thermal treatment of the waste, such as fluidized beds, gasifiers and rotary kilns but this study focuses on waste burning grate boilers. The literature review section focusing on computer vision uses only studies from industrial boilers and burners since there is a limited number of studies from a grate boiler environment. From the camera technologies perspective, this thesis concentrates on visible light and middle wavelength infrared radiation which Valmet's imaging systems represent.

1.4 Structure of thesis

The thesis is divided into a literature review and empirical research. The literature review starts from Chapter 2 that introduces the background of the waste incineration, grate combustion and discusses grate boiler structures. Chapter 3 elaborates conventional grate boiler control loops explaining their structure and control strategies. After that, the chapter describes camera-based soft sensors and combustion characteristics that these sensors measure. The final chapter of the literature review is Chapter 4 that investigates the state-of-the-art computer vision approaches and models in combustion process diagnostics and elaborates which special requirements the combustion process sets to the camera systems.

The empirical research starts from Chapter 5 that explains applied research methods, approaches and data analysis techniques. This thesis is a case study where the research material is gathered with a measurement campaign in the grate boiler and surveys. In analysing the computer vision model against the process data, the study applies cross-

correlation analysis and Granger causality test while for the surveys qualitative content analysis was applied.

Chapter 6 presents the developed computer vision model and choices taken during the implementation phase. Chapter 7 presents the results of the study. The chapter starts by describing the main numerical results from the signal analysis and after that the surveys. The results of the surveys are explained from the combustion challenges, automation system, camera system and operation condition point of view that were identified themes of the surveys. The detailed analysis of the results is presented in Chapter 8. Results are compared to research questions and reflected to other academic literature. Finally, Chapter 9 concludes the study by discussing the implication, limitations and identified future research opportunities of this study. In addition, the chapter reviews the execution of the study and reaching the objectives of the thesis.

2. GRATE COMBUSTION

This chapter describes the grate boiler environment and the characteristics of waste incineration. First, the chapter explains waste incineration. The focus is on energy production and the role of the power plant in incineration. After this, the chapter explains the usage of the grate boiler in incineration. Thirdly, thermal treatment of the waste is discussed from the perspective of the combustion process. Finally, the end of the chapter explains different grate structures. Section 2.1 is mostly based on references [1], [2], [32] and [33] while Section 2.2 is based on [34], [35], [36] and [37] unless otherwise stated.

2.1 Waste incineration

Waste is a highly heterogeneous material that consists mostly of organic materials, minerals, metals and water. It is produced broadly in various processes in society and contains substances hazardous to both humans and the environment. Waste accelerates negative environmental impact with polluting materials and greenhouse gasses as well as increase the chance of epidemic diseases. That is why waste treatment is important. One method for waste management is incineration.

Systematic waste incineration started in Europe in the 19th century and has grown rapidly since then. In the 2010s, European member states generated a total of $350\,\mathrm{Mt}$ of waste annually. Around $31\,\%$ of this waste was burned in 470 incinerators with average capacity of $193\,\mathrm{kt/a}$. The number of the generated waste is increasing every year due to population growth and industrialisation. Moreover, new directives for waste disposal at landfills have enforced waste incineration and usage in energy production.

The main objective of waste incineration is to destroy toxic organic substances, capture possibly harmful ones and minimise the required volume capacity of the residues. Organic and inorganic substances as well as volatile heavy metals are demolished in high-temperature combustion where they turn into more easily treatable residues. Waste is important in WTE where released energy from burning the waste is recovered for electricity and heat.

European incinerators generated over $275\,000\,\mathrm{TJ}$ of heat and $110\,000\,\mathrm{TJ}$ electricity from the waste in 2013. Waste has high energy content since it consists of 60–95 $\%$ of biogenic

matter. This is especially true in Municipal Solid Waste (MSW) incinerators where waste has high calorific value. 1 Mg of MSW generates 300–6400 kWh electricity depending on the power plant structure. Burning waste substitutes fossil fuels in energy production which reduces overall carbon dioxide emission.

The principal structure of an incineration plant is shown in the Figure 2.1. The plant is in charge of the following operations:

- waste reception, pre-treatment and storing
- thermal treatment of the waste
- pollutant monitoring and control
- solid residue disposal and discharge.

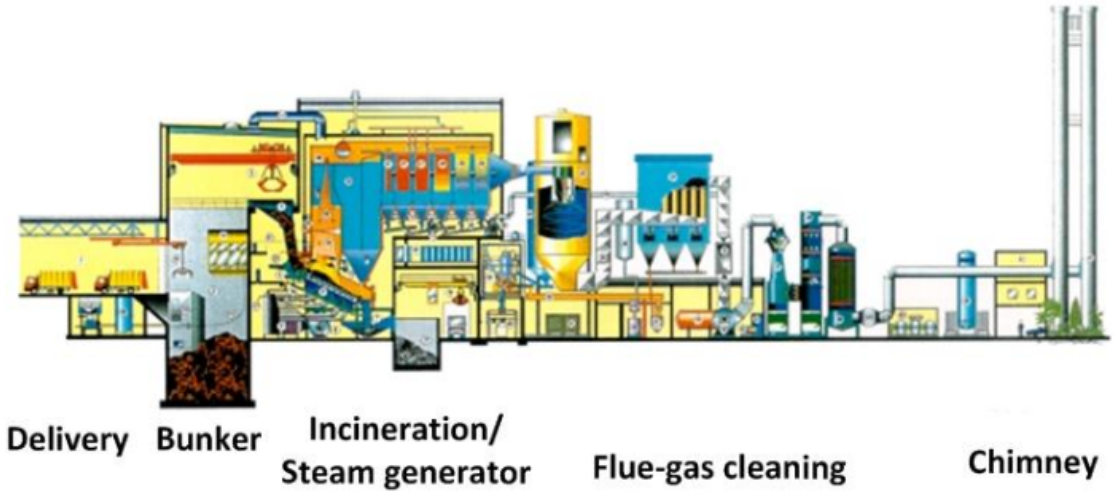

Figure 2.1. *Example layout of a solid waste incineration plant for municipal waste. [32, p. 35]*

Delivery trucks collect waste outside the incineration plant. Trucks then deliver solid waste to a plant where they unload their cargo to a delivery area. Part of the waste is pretreated before arriving at the plant. Typically, recyclable materials, such as paper, bio-waste and glass are not delivered to incineration. From the delivery area, the waste is moved to a water- and fireproof concrete bunker which holds the waste before it is moved to incineration. The bunker is ventilated to avoid gas formation and fermentation.

In the bunker, the waste is blended with fuel and homogenised. Depending on the type of waste, it is shredded, separated or solidified. Solid waste in the bunker is usually crushed into smaller pieces with shears, shredders or mills thus balancing the heat value. Big and heavy metallic or glass objects are removed from the waste. Overhead claw cranes move the waste from the bunker into the furnace hopper. From here the waste enters the furnace where the waste is burned and turned into energy.

Waste is incinerated with many technologies. One of them is grate combustion where the waste is burned in grate boilers. Over $80\,\%$ of the waste burning plants have grate boilers making grate combustion the most common technology for WTE plants [33, 34]. The second most common method is FBC technology which $10\,\%$ of European incinerators use [3]. FBC has replaced the grate firing in large plants over the last decades [32, 34] but the grate boilers are still favoured for their simplicity, reliability and cost. FBC requires more fuel preparation, it is not suitable all types of fuels such as MSW and its thermal power input is lower compared to grate boilers. [1, 3, 33, 34, 38] However, grate boilers have some limitations to the burned waste. Grate boilers cannot burn liquid, powder or melting wastes. However, a small amount of moderately dry sewage sludge can be burned mixed with other fuels. [2] Thermal treatment of the waste and combustion process are explained in more detail in Section 2.2.

Grate boilers for waste incineration are designed to burn fuels with varying heating values and qualities. Grate boiler's structure and dimensions of heat recovery are defined by the most unclean and corroding fuel properties. This ensures process operability in every situation but reduces the energy efficiency in electricity production because steam temperatures have to be limited due to the increased risk of corrosion.

The energy released from the burned waste generates steam. Steam either produces electricity in turbines or is distributed to district heat networks. Combustion creates flue gasses and other pollutants as a secondary product. Hot flue gasses leave the combustion chamber from the top of the grate from where they go to the heat recovery section. The heat recovery section improves power plant energy efficiency by utilising hot flue gasses to preheat the water. After the flue gasses have lost their heat energy they enter the flue gas cleaning section.

In the cleaning section, flue gasses are cleansed from polluting materials. Flue gasses contain pollutants, heavy metals, fly ash and other inorganic substances from the burned waste. Plant is in charge of monitoring and reducing the following emissions to the environment: CO_x, NO_x, SO_2, HCl, HF, Total Organic Carbon (TOC) and dust. Emissions are reduced with various methods, such as scrubbers, Selective Non-Catalytic Reduction (SNCR) or Selective Catalytic Reduction (SCR) and baghouse filters. Other unburned materials are removed with bottom ash. Residues are recycled or they are put to a final storage place.

2.2 Combustion process

Thermal waste treatment happens in the boilers in which waste is firstly heated to volatilization temperature followed by the combustion of organic components. Combustion of solid fuels in the grate is divided into four stages which are drying, devolatilization, char burning and ash reactions which are illustrated in Figure 2.2. Depending on the fuel, these stages

happen simultaneously or sequentially.

The burning rate of the fuel is affected by the fuel particles' physical, chemical and structural properties. Affecting physical properties contain specific heat capacity and thermal conductivity, chemical properties include reactivity, pyrolysis temperature and calorific value while structural properties include features, such as particle size, density and porosity. Chemical kinematics, such as reaction speeds as well as heat and material transfer mechanisms have also a substantial effect on combustion.

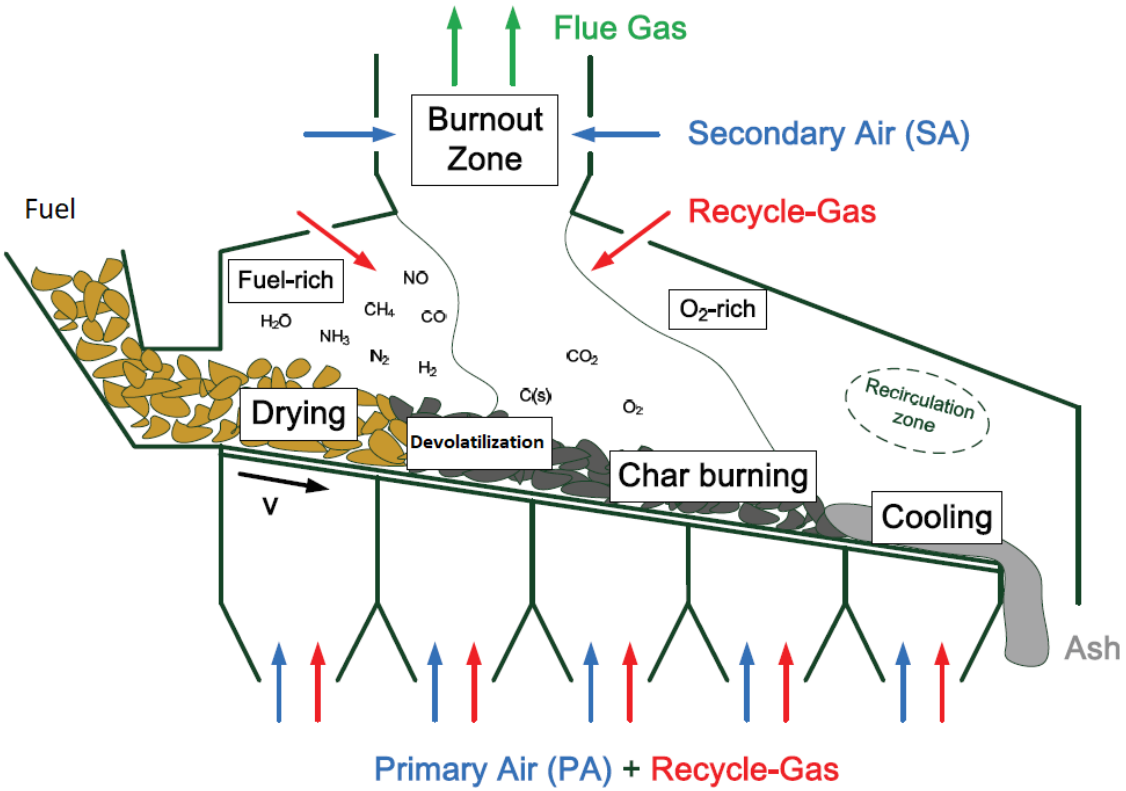

Figure 2.2. *Combustion process of solid fuel in inclined stepped grate boiler. Adapted from [39].*

In the drying phase, inserted fuel starts to dry in the furnace from absorbed heat coming from radiation and convection. As the particle's temperature increases water begins to evaporate and the size of the wet core decreases. Water vapour escapes through the pores of the fuel particles. The speed of evaporation depends on the physical properties of the fuel, such as moisture content and particle size. Moist fuels are slow to reach ignition temperatures and require large space of the grate for drying. This reduces the overall efficiency of the combustion.

The drying phase should be kept as short as possible because it lowers the temperature of the combustion chamber. Drying is enhanced with preheating of the primary air, thermal insulation or by pre-processing the fuel. Primary air is either preheated or part of the hot flue gasses is recycled and mixed with primary air to accelerate drying and ignition.

Boiler walls lined with heat dispersing and reflective materials helps to dry the fuel through radiation faster. Reducing particle size by pre-processing the fuel and designing grate dimension efficiently increases the area of evaporated fuel particles which accelerates the drying and ignition.

As the temperature increases in the particle, the devolatilization phase begins. In this stage, the lowest activation energy reactions start and fuel begins to release tars and combustible gasses such as methane, hydrogen, carbon monoxide as well as carbon dioxide. Hydrocarbons and carbon monoxide which are the quickest elements to evaporate, start to release right after the drying section but reach the ignition temperatures after the temperature has reached 500–700 °C. Heavy hydrocarbons are released the last but they start to ignite in 250–400 °C. Visible light is produced when these gasses are burned with oxygen supplied by primary air. Released heat helps ignition of the solid particles. Fuel particles lose their mass and increase their porosity as carbon is consumed. Some of the gases rise to the burnout zone above the bed where secondary air is introduced to finalise the combustion.

Devolatilization is typically an endothermic process that turns into an exothermic after the porous materials start to ignite and burn. After the devolatilization has taken place long enough and the temperature has risen, the process continues to operate without external energy. Optimal combustion is achieved when the temperature of the flue gasses is in the range of 800–1000 °C and the concentration of CO is small. This requires over 700 °C temperature, sufficient excessive air concentration and mixing of flue gasses and secondary air. Combustion chambers are designed to assist mixing of the gasses and their burning above the grate. The speed of devolatilization is affected by chemical kinematics and heat transfer with the environment.

Solid particles that are left from the devolatilization are called the carbonised residue. After the volatile materials have been released the remaining combustible carbonised residue substances, such as fixed carbon and dispersed mineral matter begin to release in char combustion. The visible flame extinguishes and the surface of the particle starts to generate carbon monoxide that reacts with excessive air forming carbon dioxide. Char combustion requires high temperatures and the right oxygen concentration to take place. This stage is slower and requires much larger space from the grate than devolatilization.

Burn time of the carbonised residues depend on the type of fuel. This reduces the controllability of the process. The burning is enhanced by reducing fuel particle size and raising temperatures. However, the temperature cannot be raised too much because high temperatures lead to the melting of the ash. [40] Right dimensioning of the grate improves energy efficiency [36, p. 468].

Ash is unburned materials that remain after the combustion has taken place. Depending on the fuel, it contains substances, such as char, alkalies, minerals and silica. Most of the

ash in grate boilers is removed from the end of the grate as bottom ash compared to other boilers where it leaves as fly ash with flue gasses. This affects the boiler dimensioning. Due to high temperatures and intensive combustion, ash is partly sintered and melted.

2.3 Grate structures

The purpose of the grate is to transport the waste from the feeder to the ash hopper and enable continuous combustion. In addition, the grate is responsible for mixing and exposing the waste to primary air to make combustion more complete. Grates are divided into sections where each combustion process phase take place. There are mainly four grate types which are stationary sloping, travelling, reciprocating and vibrating grate. [5, 38] An example of two types of grate layouts is shown in the Figure 2.3.

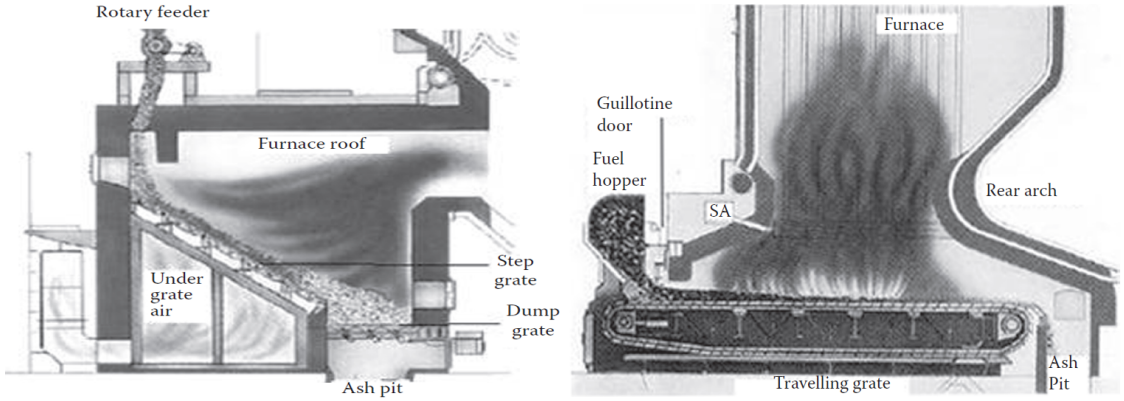

(a) *Stationary sloping grate layout. [38, p. 189]* ***(b)*** *Travelling grate layout. [38, p. 188]*

Figure 2.3. *Stationary sloping and travelling grate layouts.*

In a stationary sloping grate, the grate is fixed to a predefined tilting angle and therefore does not move. Gravity moves the waste in the grate. The angle of the grate is defined in the grate dimensioning phase and it depends on the quality of the fuel. The angle is around 35–38 ° and is usually more inclined at the beginning of the grate where the fuel feeding is located. [38, 36, pp. 472–473, 37, p. 147–148] According to Yin *et al.* [5], stationary grate combustion is more difficult to control compared to other grate types. One example is the increased risk of the fuel pile crash if the fuel feed and combustion speed are not adjusted accordingly. Stationary grates are cheap to manufacture and their lifetime is long but nowadays other types of grates are more popular due to their benefits over the stationary ones. [5]

In travelling grate, the grate is made of heat-resistant steel belts and links that are moved by front and rear shafts that acts as a conveyor. Waste is fed on top of the grate and moved forward by a mechanical structure that rolls the grate. Primary air is supplied from the small holes in the chains and bars. [5, 36, p. 476–477] A travelling grate has good carbon burnout efficiency because the fuel layer is relatively small. The length and the

width of the grate is limited to 5 m and 8 m respectively by mechanical limitations. Grate speed is controlled by shaft rotation. [38]

Reciprocating grates consist of inclined grate bars that are assembled to separate levels. Grate levels resemble steps and sometimes these types of grates are called step grates. Grate bars are inclined in range of 0–30 ° depending on the fuel. Grate motion is done by pushing grate bars back and forth. Pushing movement penetrates the fuel mass and exposes a new surface area for combustion which is better for mixing compared to travelling grate where the fuel is only carried on the top of the grate. [36, p. 484–485] Primary air is supplied from the side of the bars. Grate speed is changed by alternating the length of pushing or the speed of movement. [38] According to Yin *et al*. [5], reciprocating grates are good for bulky fuels, such as MSW because of good air and fuel mixing. Their lifetime is shorter compared to travelling grates since the grate has more moving parts that are affected by mechanical wearing and thermal stress [5].

Vibrating grates consist of leaf springs that are connected to grate frames. Grate vibrates back and forth that moves the fuel forward and spreads it evenly. They are suitable for solid fuels with small ash content, such as Refuse Derived Fuel (RDF). [38] Vibrating grates are simple to construct and have few moving parts compared to other moving grates which improves reliability and maintenance costs. They are suitable for large scale boiler units since the width of the grate is not restricted by mechanical limitations. [5]

Even though the grates are designed to withstand a harsh combustion environment, they cannot tolerate too high temperatures. Grate temperatures need to be kept under 450 °C and local hot spots should be minimised. Grates are cooled to decrease thermal damage and increase the lifetime. [1, 2] Grates are either air- or water-cooled. In air-cooled grates, the primary air is lead through the grates before entering the combustion chamber. Around 80 % of total air is lead through primary air nozzles. Fuels with heating values in range of 5–15 MJ/kg are suitable for air-cooled. Air-cooling has low operating costs. [38]

In a water-cooled grate, grate bars contain water tubes with circulating water that cools the bars. Water-cooling allows more flexible controls and optimised combustion since cooling is separated from the primary air. In water-cooling grates only 60 % of the air is primary air. A higher amount of air is supplied from the secondary air level which enhances combustion increasing boiler efficiency and lowering emissions. Lowering primary air flow results in fewer combustible particles leaving the combustion chamber with flue gasses which reduces unburned substances. [2, 38] Water-cooled grates are suitable for fuels with heating values in range of 10–20 MJ/kg. Water-cooling is good for wastes, such as Industrial Waste (IW) that require over 1100 °C to burn hazardous substances. Water-cooling is more expensive compared to air-cooling because of the more complicated cooling system. [5]

3. CONTROL SYSTEMS

This chapter explains the control system of the power plant. The first section explains primary control loops which are the main process systems in the power plant. Combustion control is explained in more detail. The second section discusses camera based soft sensors and their utilisation in the control systems. The end of the section presents which combustion characteristics earlier computer vision-based soft sensors have measured from the combustion processes.

3.1 Primary control loops

Waste incineration plants are designed to operate continuously with minimum downtimes in the process. Automation systems have an important role in securing the availability of the plant. [1] They increase the efficiency of the operation, provide good operability of the power plant and allow interface for process operators to oversee the energy production [41]. In the automation system, the control system operates actuators through control loops, and supervises and optimises power plant operations [42, p. 147, 41].

The main function of the boiler is to produce live steam with desirable pressure and temperature securely and economically. Steam then generates electricity in a turbine or heat in the heat exchanger to a district heat network. The most typical usage of steam is in Combined Heat and Power (CHP) plants where the turbine creates electricity from the superheated steam and the leftover thermal energy is recovered for heating. [37, p. 262–263] To achieve stable production of the energy, the power plant needs to work harmoniously and the process needs to be kept within safe limits. The automation system controls and monitors the process through the control loops. [1, 37, 42]

The primary control loops of the condensing power plant are:

- live steam pressure and temperature
- feedwater flow
- combustion power
- furnace chamber flue gas pressure
- electric power. [37, p. 262, 42, p. 147]

It is important that steam going to the turbine is at the correct pressure. The live steam pressure has lower and upper limits depending on the technical specifications of the turbine manufacturer. Too high deviations from these values cause damages to the turbine. Live steam pressure is controlled with two boiler operation modes which are constant and sliding steam pressure. [43] In constant operation mode the pressure of the live steam is kept constant in every power level by regulating thermal power and turbine valve position [42, p. 158]. Changes in live steam or steam drum pressure give control signal to fuel flow controller unit or turbine control valve. Control difference variable composes of live steam pressure setpoint and steam pipe pressure sensor measurement difference. [37, p. 263–264] Fuel flow controller is achieved with two-level control where the first level controls the setpoint of thermal power based on pressure and the second level combustion air and fuel feed flow which produces required thermal power. The setpoint of the second controller consist of the control output of the first level control. [42, pp. 158]

In sliding pressure operation mode, turbine's control valve position is kept close to maximum opening and steam pressure is controlled only by regulating thermal power. Changes in thermal power setpoint affect directly to fuel feed speed and that way to produced thermal power. Control has a slow response because changes in fuel feeding speed take time before it affects the steam mass flow rate. Furthermore, thermal storage capacity of the boiler slows the energy release to the water. [37, p. 265] The turbine control valve position is adjusted only a little in start-ups and in maximum thermal power production. [42, p. 158]. According to Milovanović *et al*. [43], sliding control has good energy efficiency in partial loads, good stability and component lifetime is higher due to reduced stress compared to a constant operation mode.

Steady and efficient plant operation requires live steam temperature control. The temperature needs to be as close to the ideal designed value as possible. Too low steam temperature causes losses in boiler efficiency while too high temperatures increase the risk of overheating and failure in heater tubes as well as turbine blades. [41] Steady live steam temperature reduces thermal stress of the tubes and increases boiler load balancing [42, p. 165]. Steam temperature alternates depending on the boiler load, air flow, burner operation, feedwater temperature, fuel and heating surface heat transfer coefficient [41].

Live steam temperature controller keeps the temperature at its setpoint. The setpoint is defined by the required thermal power. [41] Live steam temperature is controlled by changing steam flow in the superheater section, alternating gas recirculation flow or by spraying water to the steam [37, p. 273]. The most common method is water spraying because it is simple, inexpensive and easily controllable [42, p. 166]. In this type of control, water nozzles are installed between the superheater sections. Water is injected through the nozzles to high-temperature steam which vaporises and cools the steam. [41] This is achieved by cascade control with two Proportional Integral Derivative (PID)-controller

blocks. The controlled variable is steam temperature measured after the heaters and the control variable is the position of the injection valve that feeds water to nozzles. Sometimes additional measurement from steam temperature before heaters is utlised. [42, p. 166-167]

Feedwater flow control regulates that there is enough water to vaporise in the steam drum. The amount of required water depends on boiler type, capacity and load. [41] Having enough water in the steam drum is important for boiler efficiency and preventing pipeline damages. Control is implemented by changing the feedwater valve position which regulates how much water is going to the steam drum. [37, p. 263]

Control is achieved with one, two or three-element control loops. [42, p. 152–153] In one element loop, feedwater valve is controlled with only drum level measurement [41]. This does not consider the amount of fed water or leaving steam and therefore is not suitable for high load changes [37, p. 263, 42, p. 154]. The generated steam is taken into account in two-element controls where feedback loop consists of steam flow and drum level. This control loop handles the swelling and shrinking effects of the steam and is more robust compared to one element control loop. The best controllability is achieved by a three-element control loop where the flow is controlled with system's main steam flow, drum level and feedwater flow measurements. Control utilises two control difference variables that are the water level difference and the steam and water flow difference. A setpoint of a PID controller is the sum of these variables. [42, p. 155-156] This is the most typical control strategy [37, p. 263].

The main task of the combustion control is to keep adequate thermal power so that the required steam is generated. Thermal power setpoint is determined by deviations in live steam pressure, electric power or turbine control valve position. [37, p. 266] Combustion control loops which include fuel speed, combustion air flow and combustion chamber flue gas pressure controls are discussed in more detail in Subsection 3.1.1.

The main function of the electric power control is to keep the generators created electricity matched to the requirements of an electric power network. Electric power network voltage, frequency and waveform need to be kept inside boundaries or the turbine starts to oscillate and needs to be taken off from the network. [42, p. 168] Setpoint is the load demand of the network. Control is achieved with boiler follow, turbine follow modes or coordinated control. [42, p. 149–151]

In the boiler follow mode, electric power is controlled by changing the position of the turbine control valve. Stored energy in the boiler gives an immediate load response but causes pressure drops in the live steam. To maintain the pressure setpoint, the boiler increases thermal power output. In the turbine follow mode, the control is opposite. Electric power causes changes to the thermal power setpoint which increases pressure in live steam. The turbine control valve keeps the pressure constant by opening and closing

the control valve. [42, p. 150, 41] In these control types, the turbine and boiler controls are separate and they do not communicate with each other. This is not the case in a coordinated control system where boiler sub-processes are connected with each other to achieve a quick response time. [41] Structure of coordinated control system is illustrated in the Figure 3.1.

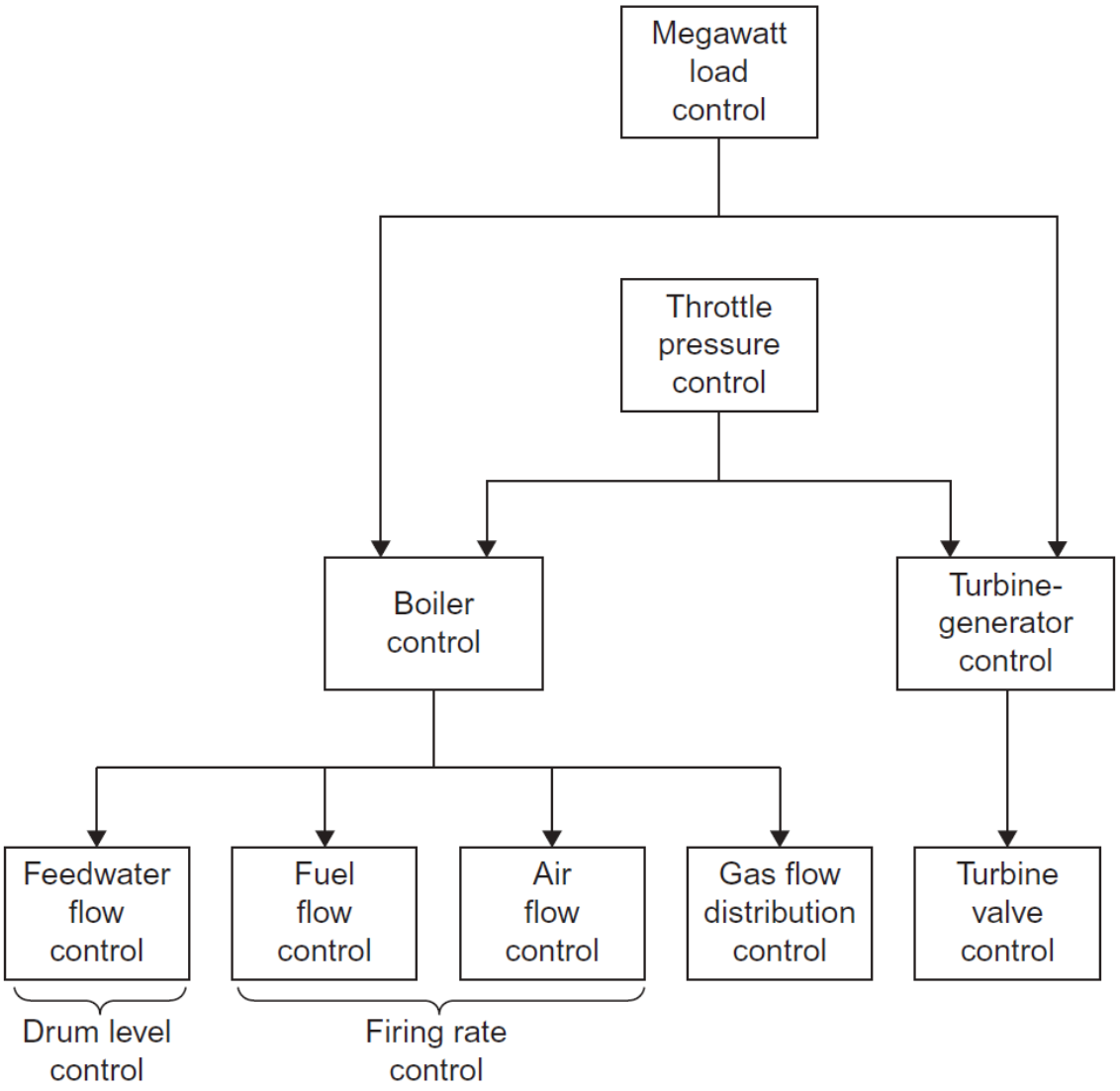

Figure 3.1. *Arrangement of the coordinated control system in steam generating plant. [41]*

In a coordinated control system, sub-process controls are harmonised to work together. The master controller calculates required control variable values based on their pre-set limits and sends commands to other boiler control loops. [41] Coordinated control system calculates optimal setpoints for the control loops and releases the operator from the decision making [42, p. 151–152].

3.1.1 Combustion control

A stable combustion process requires three conditions to take place which are the presence of the fuel, sufficient temperature and oxygen [36, p. 186]. Alternating fuel quality of the waste requires constant controlling of the combustion. Control loops have to be able to follow the uncertain energy content of the fuel and control the air flow and the grate speed to enable optimal combustion circumstances. [36, p. 486] Waste incineration has stricter emission limits compared to other fuels and power plants [1]. This puts special requirements for combustion controls. Combustion is regulated in grate boilers with combustion air flow rate, fuel feeding speed and combustion chamber pressure [41].

The main function of combustion control is to keep adequate thermal power dictated by the load demand. Control difference unit compares load setpoint to live steam flow signal, turbine pressure setpoint to signal from the turbine steam pipe and electric power setpoint to the measured one. The error signal is then fed to combustion controllers. [41, 37, p. 266] Thermal power is regulated either by air or fuel flow controls [42, p. 159].

Combustion air flow and fuel feeding speed controls are either in series or parallel adjusted. In the series type of control, the changes in thermal power setpoint cause changes in air flow which then affects the fuel feeding. In parallel type, the response of both control setpoints is immediate if the thermal power setpoint changes. Wired controls are common in grate combustion because of the dynamics of the combustion chamber. [42, p. 161]

Fuel flow controls adjust the amount of burning material in the furnace. Fuel should be spread evenly to minimise air flow disturbances and allow proper mixing. [36, p. 471] Controlled variables are grate movement speed and fuel feeding from the bunker to the furnace. Depending on the boiler structure, the grate speed is adjusted separately in grate sections or the whole grate moves at the same speed. Grate and fuel feeding control parameters are dependable on the calorific value of the fuel. [37, p. 266] Alternating movement speed of the grate or the fuel feeder has a long response time to thermal power because it takes time before the inserted fuel starts to release energy. However, the grate contains a pile of dry fuel that is easily ignited by introducing more air to the furnace. [42, p. 159] That is why fast changes to thermal power are controlled by changing the air flows but the fuel flow is the most important controllable variable for thermal power [36, p. 186]. If the air flow and fuel flow are not in balance, the bed inventory starts to deplete and at some point, the combustion extinguishes.

The function of the air flow control is to maintain a proper air level so the combustion process keeps happening. Controllable variables are fan speeds or single leaf damper positions in the regions of the boiler [37, p. 267]. In grate boilers, air flow control is staged to primary and secondary air levels. Primary air is further divided into grate sections where air flow is controlled separately. Most of the primary air is blown from the

grate where the devolatilization takes place. [36, p. 474, 487] Complete stoichiometric combustion requires specific amount of air that is described with air–fuel ratio (λ). The higher the ratio, the more excessive air there is in the combustion which is not required for complete combustion. [42, p. 160] Air-fuel ratio is adjusted in the feedback loop of the air flow control with O_2 concentration measurement from the flue gasses and thermal power load. Desired O_2 level is not constant but depends on the boiler load [41]. Having the correct ratio boosts boiler efficiency and keeps the process stable. Too small air-fuel ratio causes imperfect combustion. Combustion does not get enough air and fuel starts to pile in the furnace. In serious cases, this causes explosions in the furnace. Having too high a ratio is not desirable because it increases flue gas losses, emissions and affects efficiency. [42, p. 160] Other parameters that affect the air flow controls are fuel calorific value, its mixture as well as furnace temperature [41].

The function of the furnace pressure control is to keep negative pressure inside the furnace. Negative pressure is required so the flue gasses do not leak to the boiler room. [37, p. 269] Having balanced pressure inside the furnace helps to stabilise combustion because fluctuations in pressure disrupt the air flow. This affects the amount of combustion air and makes combustion incomplete. In serious cases, unstable pressure extinguishes the flame. [42, p. 164] Negative pressure is created by induced draught fan. Fan's pre-rotation vane position, rotor blade pitch or revolution speed are controlled variables. Interferences caused by air flow and fuel feed to combustion are mitigated with feed-forward controls which take into account disturbance variables from a combustion air blower. [42, p. 164–165]

The other function of the combustion controls is to optimise combustion efficiency by reducing unburned fuel and flue gas losses. The most effective way to achieve better combustion is to reduce excessive air. Lowering the amount of excess air by $1\,\%$ increases combustion efficiency the same amount while reducing NO_x emissions. [42, p. 160, 21] On the other hand, having small excessive air ratio increases emissions, such as CO [21]. The speed of the primary air flow affects particle emissions. Lowering the air flow velocity reduces small particles that leave the combustion chamber. [36, p. 487] Stable flame is mainly maintained by optimising fuel flow control [41]. Optimised combustion is important for reducing emissions. Waste contains substances, such as dioxins and furans that require complete combustion conditions. Better combustion process reduces the secondary cleaning methods of the power plant, such as the investment and operating costs of the flue gas cleaning. [36, p. 485] Combustion efficiency is controlled with the air flow of the secondary air level by furnace temperature, O_2 and CO measurements [8].

3.2 Imaging based soft sensors

As discussed in the last section, most of the control systems in practical industrial size power plants are implemented with traditional PID control loops. However, this is not the optimal solution. Grate boilers are complex systems that contain high nonlinearities. Seeber *et al*. [44] reason why conventional PID control systems are not suitable for today's combustion plants. According to them, PID controls are not suitable for dealing with multiple inputs and outputs which reduce the achievable performance levels. They state that this is especially true when power plants want to achieve low emissions while having good efficiency combined with load and fuel flexibility. [44] Similar observations have been reported in other studies as well [7, 21, 45, 46] Garami *et al*. stated that reliable control configurations are required to achieve high operating efficiency [20].

Achieving better combustion circumstances has led to developing new control strategies such as predictive models. These approaches model the combustion process from multiple process data measurements and assess process parameters more efficiently. According to Nielsen *et al*. [31], models are derived either from computational fluid dynamics and reaction kinematics or simplified simulated transient models. According to them, models related to chemical reactions are hard to adopt for control purposes since they are complex and require high computational power [31]. Miljković *et al*. [46] demonstrated in their paper how their developed numerical model improved the predictions for bed inventory and combustion circumstances. The model utilised additional measurements from the process compared to the conventional system [46]. The performance of these models is dependable on the attainable data. According to Kortela and Jämsä-Jounela [47], advanced process controls and their dynamic models require additional information from the process so control systems make correct actions. This requires improved control and process monitoring methods [20]. One way to get new information from the process is to collect data with more sensors.

Soft sensors have been proven to be an effective way to achieve this. Kadlec *et al*. defined a soft sensor as a computer program based predictive model that measures chemical or physical properties from the process [48]. They explained that the benefits of the soft sensors are the capability to measure various process conditions with lower costs compared to conventional hardware-based sensors [48]. Ballester and García-Armingol [49] argued how imaging-based sensors are better than hardware-based ones. According to them, practically every monitoring and control systems utilise input variables, such as temperature, oxygen content and fuel characteristics to measure combustion. However, these parameters are giving only indirect information about combustion outputs, such as the chemical substances, flame and the global efficiency of the furnace which is not enough for precise diagnostic and control purposes. [49]

Soft sensors are categorised into the model- or data-driven approaches. Model-driven

approaches are based on first principle physical models that rely on prior knowledge of the process. Contrary to this, data-driven models are derived empirically from historical data. [50] According to Kadlec *et al*. [48] data-driven models are more popular in the combustion process industry for their adaptability. Soft sensors change their models dynamically to match the changes of the environment. [48] Lin and Jørgensen [51] claimed that the model-based soft sensors are harder to adopt in real-time applications since they require more computational power.

Vision-based soft sensors have been applied in grate boiler automation systems for diagnostic purposes. Tóth *et al*. [19] researched how to automatically detect operating problems from the video feed. They proposed a new camera-based soft sensor model that predicts the temperature of the output water. The tests were conducted in an inclined reciprocating grate-fired biomass boiler with a nominal capacity of a $3\,\mathrm{MW}$. They captured images from the combustion flame with the colour camera. They computed features from the images that describe the combustion conditions. These features were then fed to Artificial Neural Network (ANN) along with a couple of process measurements from the Distributed Control System (DCS). The model predicted $30\,\mathrm{min}$ ahead of time the out-coming water temperature within ± 1 ℃ accuracy. [19]

Garami *et al*. [20] studied detecting the combustion reaction zone for combustion monitoring in the same grate boiler and data set. They introduced a computer vision system that determined the flame boundary and location from the combustion chamber. Flame location was compared to process data available from the plant. They observed that the changes in the fuel feeding and grate motion are seen in the flame endpoint location. Garami *et al*. conducted a cross-correlation analysis between flame location and collected process measurements. The study suggests that the location of the edge correlates strongly with O_2, CO_2 concentrations in the flue gas as well as combustion chamber and flue gas temperature process parameters. Some correlation was also found between NO_x and CO concentrations. Garami *et al*. stated that flame boundary could be applied for control purposes. [20]

Matthes *et al*. [52] investigated detecting empty regions of the grate. They captured images with Middle Wavelength Infrared (MWIR) camera to monitor fuel distribution in the grate. They proposed a new computer vision algorithm for detecting empty grate sectors. They showed that regions correlated with steam production and the disturbances in the steam generation are automatically detectable. In the same study, Matthes *et al*. argued how Visible Imaging System (VIS) and MWIR cameras are suitable in burnout monitoring tasks in grate boilers. According to their analysis, flame dimensions and burning intensity are monitorable from VIS images while measuring bed temperature distribution and the location of the burning zone is possible from MWIR images. [52]

In addition to a diagnostic tool, soft sensors have been applied in grate boiler control

loops. Strobel *et al*. [21] studied excessive air reduction in commercial WTE grate power plant. They estimated fuel quality with a 3D laser scanner, video analysis to determine fire curvature and the endpoint from the camera images, waste composition from the flue gas and grate's pressure difference for bed volume estimation. These variables were utilised in the control loops. Study showed that their advanced combustion control model was able to reduce excessive air to $1.2\,\lambda$ which reduced NO_x and CO emissions. At the same time live steam flow fluctuation was reduced and a lower continuous operation setpoint for O_2 was achieved. [21]

Martin *et al*. [22] investigated the newest control system concepts for WTE grate-based systems. One of the examined systems has a MWIR camera integrated into control loops. This control system increases boiler efficiency by reducing flue gas losses and enhancing ash quality. This is accomplished by adding more oxygen to combustion air and control fuel bed temperatures. Lower emission combined with higher efficiency and increased residues quality in the large-scale pilot plant was reported in this study. [22]

Cui *et al*. [23] applied digital image processing in an industrial refuse incineration plant. They controlled grate speed by the flame endpoint. The location of the flame was determined from the images taken with a visible light camera. The grate travelling speed was controlled with the additional measurement of the location of the flame endpoint. They found out that the controller was able to keep the flame location in the centre of the grate. They stated that better combustion conditions, reduced labour and waste disposal costs as well as the improved lifetime of the equipment is achieved with controls that utilise flame location information in the feedback loops. [23] Nielsen *et al*. [31] study supports this statement. They investigated how flame front information enhances boiler controls. Their tests with simulated grate boiler model showed that the utilisation rate of the grate is optimised with the information of the flame front. They proposed PID control strategy that controlled fuel flow and primary air flow setpoints with the soft sensor's flame front position. [31]

3.2.1 Flame characteristics

Soft sensors provide measurements from quantities that might be otherwise impossible to measure. Finding relevant and informative variables to measure is important in applying soft sensors to boiler processes. [48] Finding features that correlate with physical and chemical properties helps to improve combustion quality and reduce emissions [53]. Suitable variables that describe the combustion in more details is active work and applying vision-based systems to monitor and control combustion has been a growing field of research.

Previous studies have concentrated on measuring the characteristics of the flame from the images. Imaging-based sensors that measure flame which is the output of the com-

bustion give information about the quality of the process. Huang *et al*. stated that reliable information of the flame helps to understand and react better to the combustion process, pollutant formation and other combustion problems [15].

According to Hernández and Ballester [54], measured variables from the flame are divided into geometrical, radiation, physico-chemical or fluid mechanic parameters. Based on their research, these features extract distinctive physical characteristics that are interpretable. Determining these features is important because images contain a lot of data that is difficult to analyse in real-time. [54] Measured characteristics of the flame from the other studies are combined in the Table 3.1.

Parameter type	**Measured characteristics**	**References**
Geometric	Flame position	[20, 21, 23, 31, 55]
	Shape	[10, 12, 14, 21, 23, 24, 27, 51, 52, 54, 56, 57, 58, 59]
	Area	[24, 52, 54, 55, 57, 59, 60, 61]
Radiation	Intensity	[10, 12, 19, 51, 57, 58, 59, 62]
	Emissivity	[49, 63]
Physico-Chemical	Temperature	[15, 18, 22, 49, 52, 55, 60, 61, 64]
Fluid mechanics	Flow/oscillation frequency	[10, 13, 14, 16, 18, 24, 28, 58, 61, 63, 65]
	Stability	[10, 66]

Table 3.1. *Measured flame characteristics by soft sensors.*

Characteristics listed in the Table 3.1 are collected from the studies where computer vision soft sensors are applied for combustion diagnostics and control. Characteristic have been extracted from images taken with VIS or MWIR cameras from combustion processes. Based on the earlier studies, multiple parameters have been measured from the camera images.

Geometrical parameters describe the structural characteristics of the flame and radiational ones emission and transmission of the energy. These attributes are known to correlate with process measurements. Lin and Jørgensen [51] calculated features from the image based on flame size, intensity and luminous. They demonstrated how NO_x emission measurement accuracy is improved with video images [51]. Wang *et al*. [12] showed that it is possible to detect unstable operating conditions from the flame images by analysing flame characteristics, such as flame area and intensity. Li *et al*. [58] rea-

soned that the colours of the flame present important information about the state of the burning. They studied how to recognise abnormal burning conditions from the flame images. They found out that flame colour is a useful feature to determine from the images. [58] Szatvanyi *et al*. [62] found that the colouration of the flame provides information both fast and slow dynamics of the combustion.

For physico-chemical parameter measuring temperature has been researched due to its physical indication of the combustion. It gives direct information about the state of the process [63]. Jiang *et al*. [63] proposed a way to measure temperature from the colour camera images. They were able to measure a 2D temperature map from the industrial size power boiler. The measurement error was less than $10\,\%$ compared to thermocouple measurements. Smart *et al*. [18] calculated flame temperature and oscillation frequency from high-speed Charge Couple Device (CCD) camera images. They found out that the temperature of the flame is highly controlled by the flue gas recycle ratio in a combustion plant [18]. Image processing is proven to provide non-intrusive measurement method that offers information about temperature distribution [15, 18, 63]

Fluid mechanics parameters have focused on quantifying parameters that describe flame fluctuation. Fleury *et al*. [24] determined spatial frequency and geometrical features of the flame. Additional frequency characteristics from the image were calculated with the 2D Fourier transform. They found out that their model was able to detect and classify sudden changes in the combustion parameters. [24] Toth *et al*. [28] researched measuring optical flow for monitoring and control purposes in the combustion chamber. They capture images from the burner with VIS and MWIR cameras. After this, they applied an optical flow algorithm to calculate flame flow and compared them to process measurements. They demonstrated that the changes in a couple of process parameters, such as stoichiometry and thermal ones, were detected in optical flow velocity transient magnitudes. [28] Study suggests that optical flow techniques are applicable for monitoring and control purposes.

The table contains only features that have been manually designed to be extracted from the images. However, analysing images does not always require human interference in the design phase. Bae *et al*. [67] applied ANN model to detect stability of the flame of the burner. They did not choose measured characteristics manually but fed the whole images to the network. The neural network learned to predict flame state from the images at the same accuracy as the human operator. [67] Similar kind of approaches where features are not handcrafted have been applied in other studies [25, 26, 68, 69] as well. Hernández and Ballester [54] proposed Self-Organizing Map (SOM) based algorithm that estimated NO_x emissions from the full images. They also tested a model based on calculated geometrical parameters but concluded that it was not as effective a model compared to SOM [54].

4. COMPUTER VISION APPLICATIONS IN COMBUSTION PROCESSES

In this chapter, the image analysis process is explained. Primarily, the chapter describes the simplified image analysis process phases. In each phase, applied methods from the previous studies are discussed in more detail. After that, the chapter explains the special requirements that infrared and visible light-based camera technologies have in combustion monitoring systems. The combustion process is a harsh environment that puts additional requirements for the camera systems.

4.1 Process

Images needs to be understood for process monitoring and control purposes. The human operator interprets video camera data with eyes and brains to make actions. The objective of the Computer Vision (CV) is to make the machine understand and interpret the content of the image [70]. This information is then applied in problem-specific applications which are referred as machine vision [71]. It should be noted that these two terms are closely related to each other and are sometimes used interchangeably.

Computer vision problems require various techniques and approaches depending on the nature of the tasks to be accomplished [70]. However, there is a generic approach model that can be broken down into computer vision processing phases. The main phases of the 2D image analysis are illustrated in the Figure 4.1.

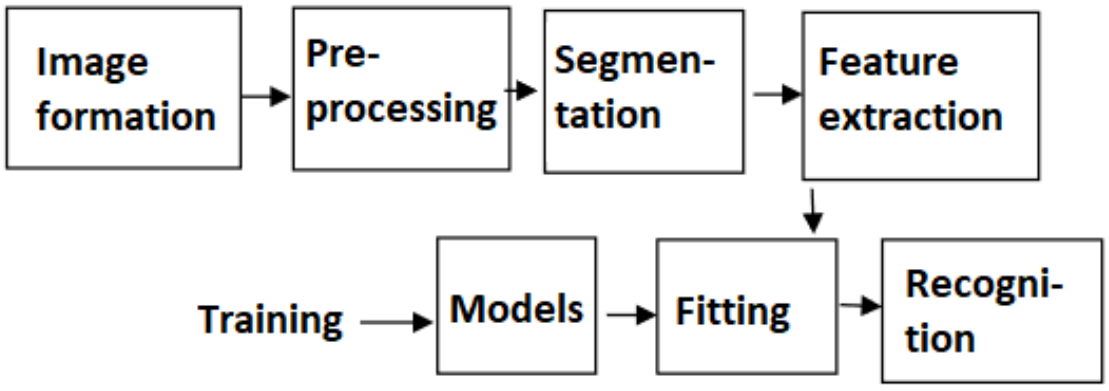

Figure 4.1. *Simplified image analysis process. Adapted from [71].*

It should be noted that the illustrated process is a simplified version of the classical computer vision method that solves practical cases. Depending on the applied approach, the process steps differ, for example in deep learning methods. [71] According to Szeliski deep learning systems do not require manually designing segmentation and feature blocks because networks learn to identify these characteristics by themselves [70].

4.1.1 Image formation

The first step in image analysis is image formation. A camera collects electromagnetic radiation from emitting or reflecting objects at a specific spectrum. Light flows through the camera optics that focuses them into a single point sharpening the image. Collected light enters to imaging sensor unit that transfers the light to a digital image. [70]

Multiple wavelength sensors are applicable in the boiler environment. Visible light sensors have either CCD or Complementary Metal Oxide Semiconductor (CMOS) sensors [70]. Garami *et al*. took flame images with CCD camera flame from the grate boiler [72]. Sawicki recorded flame images from combustion chamber with high-speed CMOS camera [73].

Infrared radiation cameras are suitable for monitoring combustion processes. Matthes *et al*. [52] explain in their study the benefits of the MWIR camera compared to the visible light camera in grate boilers. Visible light cameras cannot see through the flame and they are affected by the radiation of unwanted particles. Combustion chamber contains gaseous components, such as CO, H_2O, and soot. The spectral scattering and radiation of these substances are at the highest in visible light spectrum. Particle scattering is lowest in wavelength range of 3.8–$4.0\,\mu\text{m}$. Measuring this radiation and creating images is achieved is possible with microbolometer chips with a band-pass filter in that range. [52] A combination of wavelength sensors is possible. Sun *et al*. [10] estimated stable flame from the spectral bands with a camera that had ultraviolet, visible and infrared photodetectors.

According to Szeliski [70], aperture size, focal length, shutter speed, sampling pitch, fill factor, chip size, analog gain, sensor noise and resolution affect the quality of the digital images. Sun *et al*. [10] investigated how exposure time, aperture size and camera placement affect temperature measurements. In their test, calibrated aperture size provided $1.4\,\%$ more accurate temperature measurements compared to uncalibrated one. [10] Correct imaging setups during the image recording improve later image analysis phases [71]. Bael *et al*. [67] point out in their study that radiating light from the flame, firebricks and water-pipe walls causes inaccurate segmentation in detection tasks during the image formation phase. Tóth *et al*. [19] minimise pixel saturation and image streaking with short exposure time of $0.75\,\text{ms}$.

4.1.2 Pre-processing

After the camera has created a digital representation of the imaged scene pre-processing methods are applied to the image. Pre-processing manipulates images to be more suitable for interpretation in the further analysis steps. [71] Earlier studies have argued why images should be pre-processed. Combustion is a rapidly changing process that contains dynamic disturbances which affect the quality of the data [60]. Raw image data contains high-frequency noise and fluctuating interference signals that increase measurement uncertainty [58]. Images contain a large amount of data that reduces the performance of online systems or even impede their operation without bringing additional information of the process [20]. That is why it is important to apply pre-processing methods to the image data.

Pre-processing operations include methods, such as noise reduction, colour balancing and image manipulation. Various pre-processing techniques enhance features of interest based on the application requirements. [70] Methods improve the performance of the algorithm [16], decrease the response time of the system [19] and reduce the influence of the noise [15]. Studies have also shown that pre-processing is not only helping computer vision algorithm to perform better but they provide more reliable visual information for the process operators about the state of the combustion process [23, 58].

Gray-scaling reduces the amount of processed data and removes noise [67]. Grayscale images have been composed of all three colour channels [58] or information from separate colour channels is utilised [72]. Garami *et al*. [20] separated colour channels to reduce the amount of processed data since they found out that only the red colour channel provided relevant information of the flame. Another method for data reduction is image downsampling. Tóth *et al*. [19] subsampled images before feeding them to ANN to increase the speed of the application.

Filtering methods help to eliminate image noise, enhance image quality and make detection algorithms execute faster. Approaches, such as median, average and Gaussian filtering are applied depending on the task [12, 27, 60]. Ruixuan *et al*. [27] compared filtering algorithms in detecting fuel feed flows in the furnace. Median filtering was shown to give the best results for reducing the noise while preserving the quality of the features such as edges [27]. Median filtering has also shown better performance in noise removing compared to average filtering in other studies as well [12, 53, 60]. Morphological filtering methods have been applied in noise reduction, such as in the articles [16, 23, 27]. Cui *et al*. [23] filled the small holes and connected flame boundaries with corrosion and expansion operators. Zhang *et al*. [27] applied opening operation to separate flame regions from the background.

4.1.3 Segmentation

In the segmentation phase image is divided into regions that have a similar appearance. The goal is to find and extract objects from the image based on their characteristics. [71] Segmentation algorithms group pixels based on distinguishable characteristics and find boundaries of these regions. This is done for every pixel in the image [70]. According to Szeliski segmentation methods are divided into a semantic, instance or panoptic segmentation. The goal of semantic segmentation is to accurately label pixels to classes, instance segmentation outlines separate objects while panoptic segmentation combines both semantic and instance segmentation. [70]

Earlier combustion process studies have concentrated on applying semantic segmentation. The main object has been to divide images into flame and background classes. One of the methods is grey-level thresholding. It has proven to be an effective way to segment images since combustion regions have bright intensity values which are easily distinguished from the background. Zhou *et al*. [14] thresholded grayscaled images to separate flame area from the background. Sbarbaro *et al*. [74] applied the same threshold principle but they determined threshold value only from the blue colour channel.

Zhang *et al*. [27] compared segmentation algorithms in detecting the flame of the blast furnace. One of the compared algorithms is called Otsu's method [75]. The algorithm segments the image into two classes by maximising the discriminant separability value of the two classes. The value is chosen from the distributions that represent the classes. The optimal value maximises the distance between the variances of the distributions [75]. Zhang *et al*. [27] found out that Otsu's thresholding algorithm provided the best result compared to four other thresholding algorithms. Wang *et al*. [12] searched flame regions by segmenting images with logarithmic entropy multi-threshold segmentation method proposed in the article [76]. The image was classified into three classes where two classes represented the flame. They stated that this provided better results compared to binary image segmentation methods. [12]

Lin and Jørgensen [51] applied Multivariate Image Analysis (MIA) methodology to monitor flame in a burner. They applied 3×3 Principal Component Analysis (PCA) kernel to calculate histograms from each of the colour channels to detect flame areas. [51] Tanaś and Kotyra [16] applied Gaussian Mixture Model (GMM) to extract flame boundaries from the combustion chamber in their paper. Wu [55] applied boundary detection to segment flame regions based on pixel's geometric similarities. Temperature profile was then calculated from the segmented flame [55]. Marques and Jorge [56] detected the flame of the burner with two contour methods. Images taken with MWIR camera were segmented into flame regions and background. Intensity profile and Bayesian probability distribution methods segmented the image into the background, outer and inner flame boundaries. [56] Matthes *et al*. applied template matching to detect empty grate regions from the grate

[52].

Pietikäinen and Silvén [71] state that segmentation is one of the critical phases in solving computer vision tasks. Poor segmentation hinders analysis and makes the following steps harder to perform [71]. Wang *et al*. [12] reported how flame luminosity and intensity as well as reflecting light from furnace walls lowers the performance of the flame extraction from the images. Other studies have also reported similar problems where boiler walls and other reflective materials make accurate segmentation hard task [56, 72].

Image segmentation is not always required to analyse the flame. Silva *et al*. [65] did not segment images but calculated properties from the pixel regions of the image and applied them in modal analysis. They stated that this helps to reduce image processing in turbulent combustion environment while achieving good flame analysis capability in classification systems. [65]

Applying new methodologies for image segmentation is an active field of research. One of the researched topics is superpixel techniques that are based on pixel clustering by their similar appearances. Shen *et al*. [77] describe how superpixels are useful for many computer vision problems, such as segmentation, classification and object detection. They proposed a new superpixel algorithm applying a clustering method called Density Based Spatial Clustering of Applications with Noise (DBSCAN) for image segmentation. The data clustering algorithm was firstly proposed by Ester *et al*. in the article [78]. Shen *et al*. algorithm outperformed other applied segmentation algorithms in accuracy and computational cost [77]. Their paper findings give a preliminary indication that these methods are applicable in computer vision-based applications in a combustion environment which require accurate measurements and real-time performance. Likewise, connected components algorithms have been applied to segmentation tasks. Grana *et al*. proved that a decision trees-based method is effective both in segmentation accuracy and speed [79].

4.1.4 Feature extraction

To group and match the objects from the segmented areas in the image, features that describe and distinguish objects from one another needs to be found. Finding these characteristics from the image is called feature extraction. [71] The goal of this phase is to find useful keypoint features such as edges, lines and contours that describe the content of the segmented areas. Feature extraction transforms images to feature vectors which represent image accurate enough while reducing the dimensionality of the data. [70] Tóth *et al*. [19] were unable to feed full images to their ANN model because raw images contained too much data that was not processable with limited computing resources. They reduced the size of the data by calculating features from the images that were then fed to neural network [19]. Similar issues with image data sizes have been reported in other studies as well [17, 68].

Features need to reliably differentiate objects from one another while describing corresponding ones [71]. Szeliski states that good features have good repeatability across images, they are scale, rotational and orientation invariant as well their performance is not reduced by affine transformation [70]. Feature extractions are divided into hand-crafted and learned features. Algorithms created by humans determine hand-crafted features, while learned features are discovered characteristics and fine-tuned model parameters that deep learning pipeline systems learn by themselves. [70]

Geometrical parameters, luminosity distributions and colours have been detected with hand-crafted features in the earlier computer vision applications. Detecting geometrical parameters requires describing image scenery with lines, curves, surfaces and points and these features are calculated based on pixel values. Hernández and Ballester [54] calculated intensity, width, length, orientation and eight other geometric parameters from the pixels of the segmented flame that were then fed as inputs to an ANN model. Sujatha *et al*. [53] extracted flame area, intensity and orientation from segmented flame images for their application. Wang *et al*. [80] defined flame combustion area by applying contrast difference to before and after images from the combustion chamber.

For detecting the edges of the flame, the widely adopted method has been the Canny edge detection algorithm [81]. The algorithm is multi-staged. First, the image is filtered with a 5×5 Gaussian filter to reduce noise. The next stage searches edge gradients and directions by filtering with the Sobel operator both in horizontal and vertical directions and then calculating gradients. Kernel size of the Sobel operator and image gradient algorithm can be modified. After that, the algorithm removes pixels that do not belong to the edges by checking each pixels gradient direction and determining if it is a local maximum. Finally, the algorithm thresholds the image with lower and upper threshold values that remove weak noisy edges. [81] Zhang *et al*. [61] extracted the boundaries of the flame from the blast furnace with Canny edge algorithm. Contour detection algorithms have identified closed shapes in earlier studies. Fleury *et al*. [24] determined contours from Otsu thresholded images and calculated features that described the shape of the flames. Omiotek and Kotyra [82] calculated contour areas and their respective sizes and centroids with the active contour method.

Toth *et al*. [28] applied optical flow algorithm proposed by Brox *et al*. in the article [83] to calculate burner flame optical velocities. They extracted spatial velocity magnitudes from different sections of the flame images taken from the combustion chamber [28]. Tanaś and Kotyra [16] calculated velocity vectors and orientations with Lucas-Kanade optical flow algorithm from the images taken in pulverised coal and biomass burning boiler.

Luminosity, brightness and colour characteristics help to describe the flame of the image. The characteristics are evaluated from the pixel values of the colour channels. Li *et al*. [58] projected image pixels to colour score space with MIA and retrieved the sim-

ilar colours from the image space. They also applied Scale Invariant Feature Transform (SIFT) with K-Nearest Neighbour (KNN) clustering to extract other features from the image. Castiñeira *et al*. [84] obtained flame brightness, uniformity and number of colours along with PCA feature vectors for their application. Brightness was calculated by integrating luminous intensity levels which were defined as a weighted coefficient vector over the colour channels [84]. Sun *et al*. [10] evaluated flame stability from luminous region, brightness and non-uniformity characteristics.

The flame temperature has been a topic of interest in feature extraction. Determining flame temperature is possible by measuring thermal radiation of the object. Objects emit black-body radiation based on their physical characteristics and the temperature is related to spectrum of the radiation. [85] For determining temperature, Wien's approximation of the Planck formula has been applied to construct temperature fields in various types of boilers [15, 18, 49, 55, 60]. Wu [55] proposed a way to calculate the temperature field and monitor the combustion process in his paper. The temperature distribution was calculated with the Wien approximation of the Planck formula, where spectral radiance from each of the colour channels was estimated separately. An isothermal three-dimensional temperature map was obtained from the flame which worked in real-time and provided information about the combustion [55]. Two-colour method, where radiation between two wavelengths determines temperature, has been proposed in a couple of studies [15, 18, 49, 60]. Huang *et al*. [15] measured flame temperature from the furnace burning coal. Temperature field was determined from the CCD images with a two-colour approach. They found out that this method was able to measure the temperature distribution within the same accuracy as thermocouple and the algorithm performed calculations in real-time. [15]

There are plenty of characteristics that have been quantified from the images as seen from the Table 3.1. Even more methods have been applied to extract these features from the images. There seems to be no consensus on what features should be determined and with what methods from the image but they are based on the experience of the implementer. There is a limited number of studies where the performance of the methods has been compared and evaluated.

4.1.5 Model and fitting

The next step involves making recognition actions with the processed images [71]. This involves classifying, measuring, predicting or controlling output variables. Computer vision problems are in general inverse problems where the situation is to estimate unknown parameters with the given measurements [70].

The computer vision model takes inputs and produces outputs based on its internal set of rules. Derived feature vectors from the images are fed as input to the models [71].

Typically, models utilise other parameters as input, such as process measurements from the automation systems. For instance, Li *et al*. fed measured NO_x values as an input along with processed images to their model [68]. Utilising both process measurements and information available from images as model inputs appears to make models more effective. Garami and Tóth [72] evaluated two models to predict output water temperature. One model utilised only process measurements while the other extracted additionally reaction zone features from the images. They reported that the model with flame features predicted output temperature $5\,\%$ more accurate compared to the other model. [72]

According to Szeliski models are categorised into scientific, statistical and data-driven approaches [70]. Scientific models are derived conceptual models representing real physical phenomenon. Solutions are formulated with probabilistic methods in statistical models while the data-driven approaches are based on collecting data and teaching model to represent it. [70] For combustion monitoring and control purposes, most of the applied methods have either been probabilistic or data-driven models.

Szeliski argues that many computer vision problems require estimating unknown quantities from noisy data. Therefore, uncertainties and unknown parameters are modelled with statistical techniques. [70] Graphical models have been applied in probabilistic approaches. Chen *et al*. [69] applied Hidden Markov Model (HMM) to detect abnormal conditions for flame process controls. According to their research, the HMM was able to associate changes in the flame flickering to abnormal behaviour [69]. Chen *et al*. [17] proposed new control strategy where the air-fuel ratio is controlled with Gaussian process model and image data. Qiu *et al*. [86] compared probabilistic models in predicting combustion conditions. They reported the best results with the HMM based approach with total accuracy of $95\,\%$. The other tested models were GMM, k-means and c-means. [86]

Since Artificial Intelligence (AI) has gained research popularity during the last decades so has the number of data-driven approaches to combustion monitoring and control increased. Numerous Machine Learning (ML) models have been applied for image processing flame analysis. Earlier studies have confirmed that these approaches are suitable for classification [27, 53, 58, 59, 65, 67, 69, 82, 87, 88], measurement [14, 57, 74, 89], prediction [17, 19, 51, 68, 80] and control [25, 62, 84, 90] purposes in combustion processes.

From ANN based approaches the feed-forward back-propagated networks seem to be the most common method [20, 25, 49, 53, 54, 55, 72, 91]. Allen *et al*. [25] fed full-size images to the feed-forward neural network which outputs the combustion load controller utilised. Their study demonstrated that the controller achieved satisfying results utilising only information from the neural network's outputs [25]. Hernández and Ballester [54] predicted NO_x emissions with self-organising feature maps. Deviation of the classification was less than $3\,\mathrm{ppm}$ compared to measurements available from the traditional sensor

[54].

Supervised methods have been applied to classification and clustering tasks. Zhou *et al*. [14] estimated fuel properties with Support Vector Machine (SVM) from the flame images. They reported over $99.1\,\%$ identification accuracy. SVM has been applied in other studies as well [73, 92]. Sawicki [73] analysed three classification methods, which were KNN, Naive Bayes Classifier and SVM, in determining state of the combustion. KNN was the most accurate method in this study, resulting in average accuracy of $83\,\%$ in detecting if the combustion was stable or not [73].

Models are trained with test data which needs to be collected from the model development [71]. After the data collection the data is pre-processed and fed to the model. The model fits the data and learns to interpolate it. Data fitting requires loss function that minimises the fitting error. [70]

4.2 Camera features

The furnace chamber of the grate boiler is exposed for high temperatures and volatile substances that affect the quality of the data available from the camera. Additionally, combustion process is known to be a harsh environment because of physical and chemical properties of the energy release mechanisms. This puts cameras under additional stress that they might not be suitable for. Toth *et al*. [28] mentioned that conventional cameras are not designed to withstand dust, vibrations and temperature making them unfit for combustion process. Marques and Jorge [56] debated that special cameras are required if combustion needs to be diagnosed with cameras. To achieve continuous operation in these circumstances, cameras require additional features to withstand the environment.

In devolatilization phase the temperature rises to $1000\,^{\circ}\mathrm{C}$. Camera modules and lenses are not designed to withstand long periods of time in such circumstances and protecting camera hardware parts from the heat is necessary. According to earlier studies, metallic enclosures cover camera components from the radiating heat. Stainless steel containers have been applied in the articles [15, 28, 93]. Tóth *et al*. [19] designed new enclosure from two nested metallic tubes and special lens to withstand high temperatures in their study.

In addition to protective closure the camera needs to be cooled. The electronic parts of the camera, such as signal processing board, need to keep their ambient temperature at certain limit to avoid malfunctions. According to earlier papers, both air- [19, 28, 56, 93] and water-cooled [10, 15, 52] systems have been applied. Both methods work in the same principle where cooling media flows through sealed jacket and transfers heat out from the camera.

Dust, soot and other particles foul camera's lens or electronics. This prevents accurate

imaging. Compressed air keeps parts dust-free and reduce the risk of contamination of the electronics [10, 15, 19, 28, 52, 56, 93]. Air flow creates positive pressure inside the camera and purges lens. Furthermore, camera systems can be equipped with auxiliary systems that do not affect imaging but camera's overall operability. Matthes *et al*. [52] reported that their camera was equipped with retraction system. The retraction system moved the camera out of the combustion chamber in case of cooling system breakdown to protect the camera parts from overheating [52].

Besides protecting camera from the temperature and dust, combustion process puts additional requirements to imaging units as well. Sun *et al*. commented that the cameras with high Frames Per Second (FPS) are required since the combustion contains fast-changing objects, such as flame [10]. Accurate analysis of these objects demands high-speed cameras, such as the one Toth *et al*. [28] applied in flame flow analysis. Fast response rate is needed from the image processing components too. Huang *et al*. [15] and Sun *et al*. [10] both argued that special made embedded signal processing boards helps to achieve real-time data analysis capabilities which are essential for combustion diagnostic applications.

5. RESEARCH METHODOLOGY

The main goal of this study was to develop a proof-of-concept soft sensor for grate boilers using waste as fuel. The functional requirements for the soft sensor are that it automatically determines the flame shape, flame front and its position on the grate from the Valmet imaging systems video feed. Non-functional requirements are that the soft sensor should operate in real-time and it should follow the disturbances in the flame with reasonable accuracy.

The second goal of this study was to assess imaging systems computer vision development requirements. The task was to investigate how computer vision applications improves diagnostic and control applications in a boiler environment. This requires a detailed understanding of what issues grate boilers have during operation and what benefits they achieve from the cameras. This information is then reflected to findings of the literature review.

This chapter describes the research methodology of the study. The beginning of the chapter considers the chosen research approaches and explains the nature of the research. After this, the chapter describes applied data collection methods. Finally, the chosen research methods for analysing results are explained.

5.1 Research method and approaches

A single case study was chosen to be the research method of the study. Yin describes a case study as "an empirical enquiry that investigates a contemporary phenomenon within its real-life context, especially when the boundaries between phenomenon and context are not clearly evident" [94, p. 13]. According to Williamson the goal of the case study is to find both academically and practically viable answers to research questions that are formulated with ’why’, ’what’ and ’how’ questions [95, p. 114].

The case study was conducted in an industrial-size power plant that burns MSW in a grate boiler. The executed literature review discovered that the research of a computer vision in WTE grate boilers is a quite new field of study. Most of the studies where computer vision was applied to detect flame front were either tested in small-scale pilot or biomass burning grate boilers. Few studies were found from boilers that burn waste but the research did

not articulate what computer vision model they developed, how the model was applied or what data set they had collected. There seems to be no single consensus on how camera systems should be utilised for process monitoring and control purposes. Previous research papers have not utilised data available from an industrial-size power plant burning waste. Williamson articulates that a case study is a good approach to develop and test theories in a research field where common methods are not widely accepted or the development is at their early stages [95, p. 112–113]. Therefore, utilising data available from the real-life combustion process seems to be an appropriate approach method.

A single case study was chosen after evaluating the requirements set for the thesis. In addition to the literature review, Valmet wanted to develop a computer vision application that is both feasible and practically viable solution. The developed algorithm should work in the real-life process environment without heavy modifications. Working close to the actual process system gives us reliable information and helps us to develop computer vision application and investigate the development requirements of the cameras. Thus, a case study seemed to be an appropriate research method to combine academic research and practical development.

A case study was chosen to collect data only from one power plant after considering the resources and time constraints of the research. It must be understood that this research is part of the company's research and development project that has a set budget. Additionally, collecting data from closed power plant systems is resource-intensive and requires careful preparation. This is especially true during the COVID-19 pandemic when the operational reliability of the power plant had to be secured at all times.

A case study combines both qualitative and quantitative research approaches to collect and analyse applied methods in the research [95, p. 111]. The quantitative approach was conducted in the form of a measurement campaign. The campaign collected video feed from the physical grate boiler power plant and process data available from the plant's automation and information systems. The proposed computer vision algorithm is developed based on the collected video feed. The soft sensor is then evaluated against the collected process data available from the automation and information management systems of the power plant. The measurement campaign was chosen to be a quantitative data collection method since Valmet did not have prior video data available from the waste burning grate boilers. Also, to our knowledge, there is no open database that fulfils the requirements for the soft sensor development. Therefore, quantitative data collection was required. The measurement campaign is explained in more detail in Section 5.3.

Furthermore, this study investigates combustion characteristics and process parameters that are important for the grate boiler's operation. There is not a large number of publicly available quantitative data from the market. There is a limited number of research on how grate boiler operators utilise camera systems and what are the biggest challenges

of the combustion process. Since there is no exact information available about the issues grate boiler customers encounter and camera utilisation for combustion diagnostics the study must rely more on qualitative analysis on this side of the research. To gain a better general view of the camera systems in the combustion process a online survey was conducted. The survey collected information from the grate boiler process experts from the same power plant as the measurement campaign. Responses are then analysed to find faced challenges in the operating combustion process and development requirements for the cameras from the grate boiler end-user perspective. The surveys also complement literature review and quantitative data analysis. The conducted surveys are explained in Section 5.4.

Since the surveys are part of the research sample, interpretive side of the research needs to be considered as well. As Williamson states researcher's subjective observations needs to be considered when analysing the survey results [95, p. 93–94]. This means that a researcher's personal opinions, attitudes, feelings and personal understanding of the subjects affect the results. Likewise, the accuracy of respondents self-reported data and the applied sampling technique needs to be recognised when analysing the generalisability of the results.

Because this study combines surveys, the developed soft sensor and collected process data to literature review findings, this study's research type is also multimethod research. Multimethod research utilises and combines data from multiple data sources to find answers to research questions. Since our study merges both qualitative and quantitative approaches, the study utilises a multimethod research approach.

5.2 Description of power plant

The data in this thesis is collected from the CHP waste incineration plant located in Tampere, Finland. The power plant has been operating since 2015 and its nominal production capacities are $12.5\,\mathrm{MW_e}$ electricity and $45\,\mathrm{MW_{th}}$ thermal energy. The construction of the power plant started to comply with the Finnish Waste Act of 2011 that prohibits the disposal of biodegradable and other organic waste to landfills. The power plant has reduced waste collection fees and enabled moving to a circular economy in the local regions. After the boiler started its operation, less than two per cent of the waste is deposit into landfills. [96] Power plant has decreased $60\,000\,\mathrm{t}$ CO_2 emissions and $600\,\mathrm{GWh}$ natural gas consumption annually [97].

The power plant generates energy from waste that is collected from 650 000 residents around local regions. Small amounts of clinical and commercial waste are also used as fuel. The generated energy provides district heating and electricity for the residents and buildings covering over $15\,\%$ of the usage in Tampere. [97] In 2015 the boiler burned $160\,000\,\mathrm{t}$ of waste that generated $310\,\mathrm{GWh}$ of district heat and $95\,\mathrm{GWh}$ of electricity [98].

The power plant's operational efficiency is 95 %.

The power plant is equipped with a flue gas condenser and heat accumulators that improve the power plant's district heat production and flexibility. The boiler is equipped with a SNCR and a semi-dry flue gas cleaning system. The plant has two auxiliary oil burners that are utilised in the start-ups or if the fuel quality is not adequate to keep the combustion stable. The utilisation rate of the bottom ash is 97 % since the metals and minerals are recovered from the bottom ash and the remaining ash is sieved. These substances are then recycled or disposed of. [96] The technical data of the main components of the power plant is shown in the Table 5.1.

Boiler	Steinmüller Babcock Environment GmbH
Number of units	1 unit / grate system, boiler and steam generator
Throughput per unit	20 Mg/h
Throughput total plant	160 000 Mg/y
Design heating value of the waste	10.5 MJ/kg
Thermal capacity	58.5 MW
Grate system	air cooled forward moving grate
Grate area	73 m^3
Type of boiler	4-pass horizontal
Production of steam per unit	73.8 t/h
Steam pressure	42 bar
Steam temperature	402 °C
Production capacity	electricity/heat
CHP operation net	12.5 MW / 45 MW
Heat only mode net	0.5 MW / 57 MW
Internal electricity load	1.6 MW
Heat storage	15 MW
Flue gas cleaning	Lühr GmbH
Procedure	Semi dry system | scrubber, upper and lower circulation | ESP and SNCR
Flue gas volume flow	110 000 Nm^3 humid
Turbine	MAN Energy Solutions SE
Type of turbine	District heating turbine with none stage DH-exchanger
Steam parameters	40 bar, 400 °C, 22 kg/s
Cranes – 2 units	Kone Cranes Oyj
Nominal capacity per unit	46.8 t/h

Table 5.1. *Technical data of the power plant. Adapted from [96].*

The power plant utilises grate technology in waste incineration. The boiler's type is for-

ward moving inclined step-grate. A cross-section of the power plant is shown in the Figure 5.1. The grate is divided horizontally into two segments that are controlled separately. Both grate lines are further separated into five grate sections where the burning process happens. The grates are moved with hydraulic pistons. Cooling of the grate is done with primary air. There are ten air nozzles in each grate level that are controlled separately. The boiler is equipped with manholes and inspection ports to monitor the combustion process visually.

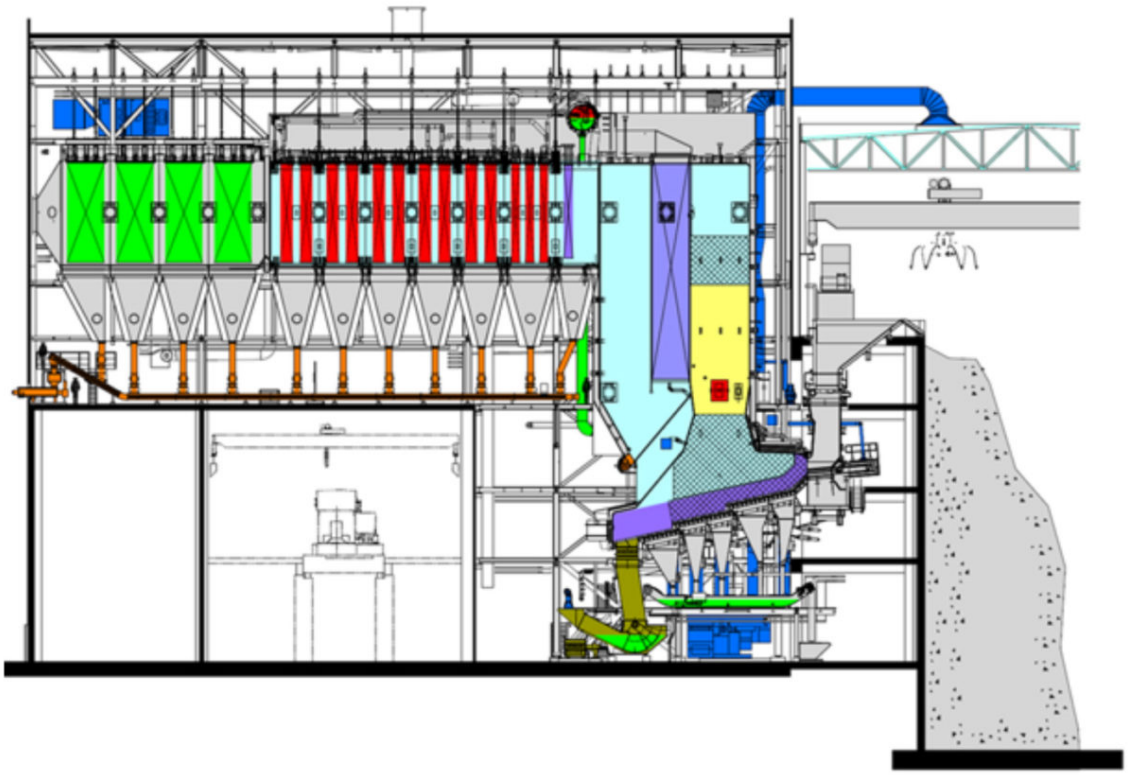

Figure 5.1. *Cross-section of the municipal solid waste grate boiler of the test campaign. [99]*

The power plant is equipped with Valmet DNA automation and information management systems. DCS automation system contains reporting, monitoring and emissions control applications and safety systems. The automation system operates the boiler in a boiler follow mode. The fuel feed rate is controlled based on the live steam and primary air flow rate. The combustion controller controls air flow and fuel feeding speed in a series type of control architecture. Part of the combustion control logic is done with advanced control strategies.

Information system stores and processes data available from the analogue sensor measurements, process variables, set points and control variables of the controllers, device statuses, alarms and operation tracking. It provides interfaces for calculations, reporting as well as data analysis and retrieving. As a part of the information system, there is Val-

met DNA Historian software that offers a process interface and databases for querying historical process values [100].

5.3 Overview of measurement campaign

The data collection was divided into two parts, the live imaging session at the power plant's boiler and the remote collection of the process data from the plant's information system. During the live imaging part, video material was collected from the various sections of the grate boiler with Valmet's camera systems. This helped us to collect data for developing a computer vision model, evaluating the camera technologies in the grate combustion environment and finding the best imaging location for the long-term camera-based process diagnostics. The camera systems are described in Subsection 5.3.1. Before going to the site, we had predefined filming locations from the boiler's cross-section images and taken initial security training which was required by the power plant operatives.

The imaging data collection was performed while the boiler was fully operating over a seven-day period. During the first days, we inspected the filming locations, assembled our filming equipment and designed the supporting equipment for the cameras. For filming the combustion process, we utilised the grate boiler's inspection ports and manholes for the camera installations. Some of the predefined imaging locations were unreachable when we went to the site. For instance, we were unable to record videos from the inspection port close to the fuel feeding, drying and ignition of the fuel at the front of the grate since the inspection port was sealed.

Because we did not have spare mountable camera units, we had to use two mobile versions of the cameras in the tests. Since these cameras are not designed for long-term installations, we had to create supportive bearings for them. We welded mechanical structures from clasps and bars that allowed rotational and linear movement of the cameras. Because cameras with their supporting structures were too heavy, we supported them with scaffolds during the installation. Scaffolds offered a stable mounting platform for a long period of data collection. They also provided a working area when we had to reach imaging ports that were unreachable from the ground, such as the inspection ports in the secondary air level.

In addition, we took some initial videos from the inspection ports during the first days. This was done to check if the inspection port or manhole is suitable to collect any informative video data or was the combustion process too turbulent affecting the quality of the video in that location. After we were done with the inspection of the ports, securing the cameras and taking the first videos we installed cameras to their filming locations. Typical long-period installation of the cameras is shown in the Figure 5.2. Inspection ports and manholes were sealed with mineral wool pieces together with flame and spark resistant

covers. This blocks possible flame bursts from the grate and excessive air flow to the combustion chamber that disturbs the combustion. The installations and gained video material are explained in more detail in Subsections 5.3.2 and 5.3.3.

Figure 5.2. *Camera installations at the end of the grate. The visible camera on the left and the infrared on the right side.*

After the live video collection on the site, we collected the power plant's process data from the power plant's information management system. Validating the developed model's practicality, performance and reliability was done with the process data available from the power plant's control loops and measuring instruments. The remote data collection is described in Subsection 5.3.5.

5.3.1 Measurement equipment

Video material and temperature measurements from the combustion process was collected with two Valmet imaging systems. One of the cameras is a digital thermal MWIR equipped with a microbolometer imaging sensor that detects infrared radiation with a wavelength close to the 4 µm. It produces 640 $\times$ 480 image resolution with a refresh rate of 30 Hz. Part of the collected emission is guided to the embedded board that determines pixelwise temperature measurements from the scenery. The camera's focal range and aperture need to be adjusted manually from the camera's adjustable screws.

MWIR camera needs to be equipped lens and there are many options to choose from. Tests were done with three lens, the 120° with infrared temperature measurements, shorter 120° lens without temperature measurement and 360° rotating lens with a field of vision of 30°. The most used lens was 120° with temperature measurement which was utilised when the camera was installed to collect long-term video material. The other two lenses were mainly reserved for shorter mobile inspection imaging.

The other camera is a digital VIS colour camera that is equipped with a CMOS detector. The camera produces a full HD image quality with a frame rate of 30 FPS. The camera has automatic gain and level adjustment options. The camera is equipped with an infrared detector probe for temperature measurements and with 64° field of vision lens. Infrared probe measures predefined zonal temperatures with the resolution of 640 × 480. The zones need to be defined from the software. The data sheets of the cameras are available in Appendix A.

Both imaging systems are equipped with an imaging module, an air-cooled electrical board, a heat-absorbing enclosure, an air filtration system and an image processing computer. Pressurised instrument air of the power plant cooled imaging systems. Vortex-cooled and purified air is applied to prevent the system from overheating and to keep electrical parts clear from impurities while the camera is close to the combustion process. The enclosure is made from stainless steel which contains holes for lens insertion. The electrical board controls the camera sensor and temperature measurements. The cameras are illustrated in the Figure 5.3.

(a) *Visual light camera.* ***(b)*** *MWIR camera.*

Figure 5.3. *The camera equipment of the measurement campaign. (Courtesy of Valmet)*

Cameras were connected to image processing computers through twisted-pair Ethernet cables that transferred image data from cameras to the computers. Computers were rugged laptops with normal computational power. Computers contain Valmet Furnace Thermal Viewer software which modify camera system parameters, read and display the video stream, log temperature measurement trends and record videos. The more detailed settings during the imaging are explained in Section 6.2.

5.3.2 Visible light camera installation

The visible light camera was installed to the left side sight glass of the manhole located at the end of the grate. The camera collected videos from this location during the whole measurement campaign. The tip of the camera is right above the ash hopper. The camera was positioned to capture the fourth grate level horizontally as much as possible. Capturing the whole grate was not possible since the field of vision of the lens was not large enough, although most of the combustion flame was within the camera's field of view. A snapshot from one of the recorded videos is shown in the Figure 5.4.

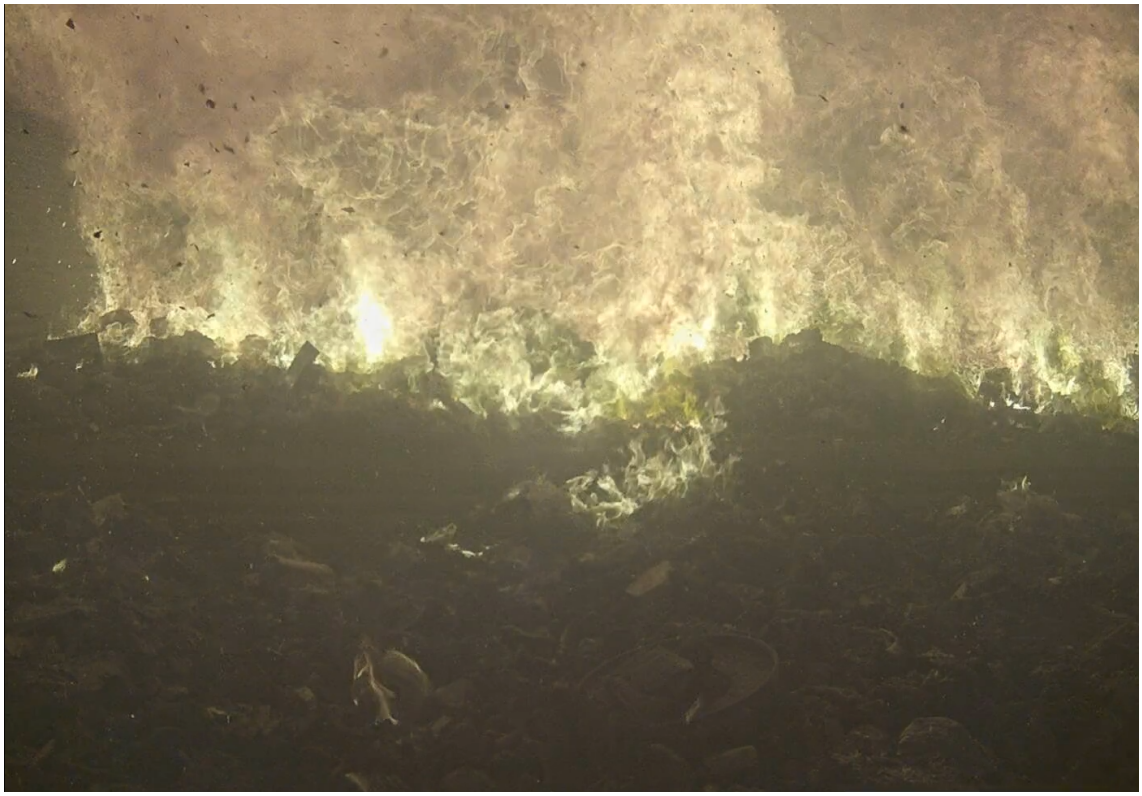

Figure 5.4. *Example image from the end of the grate with VIS camera.*

The fifth grate level is shown in the front of the image which cools the carbonised residues. The end of the flame front is in the fourth grate level in the Figure 5.4. The flame front is a little bit uneven and slightly tilted towards the right side of the image. It seems that the left side is burning a little bit more intensively compared to the right side. There is still small amount of burning material at the middle of the last grate level. Unburned metallic objects are visible at the bottom of the image.

In addition to video recordings, we defined eight temperature zonal measurements from the thermopile's heat maps. Both the fourth and the fifth grate level were divided into four segments from where the software calculated the average temperatures of the segments. Segments were defined by hand so that the segments covered the whole width and height

of both grate levels respectively. Furthermore, we stored software-generated heat maps. An example heat map is shown in the Figure 5.5.

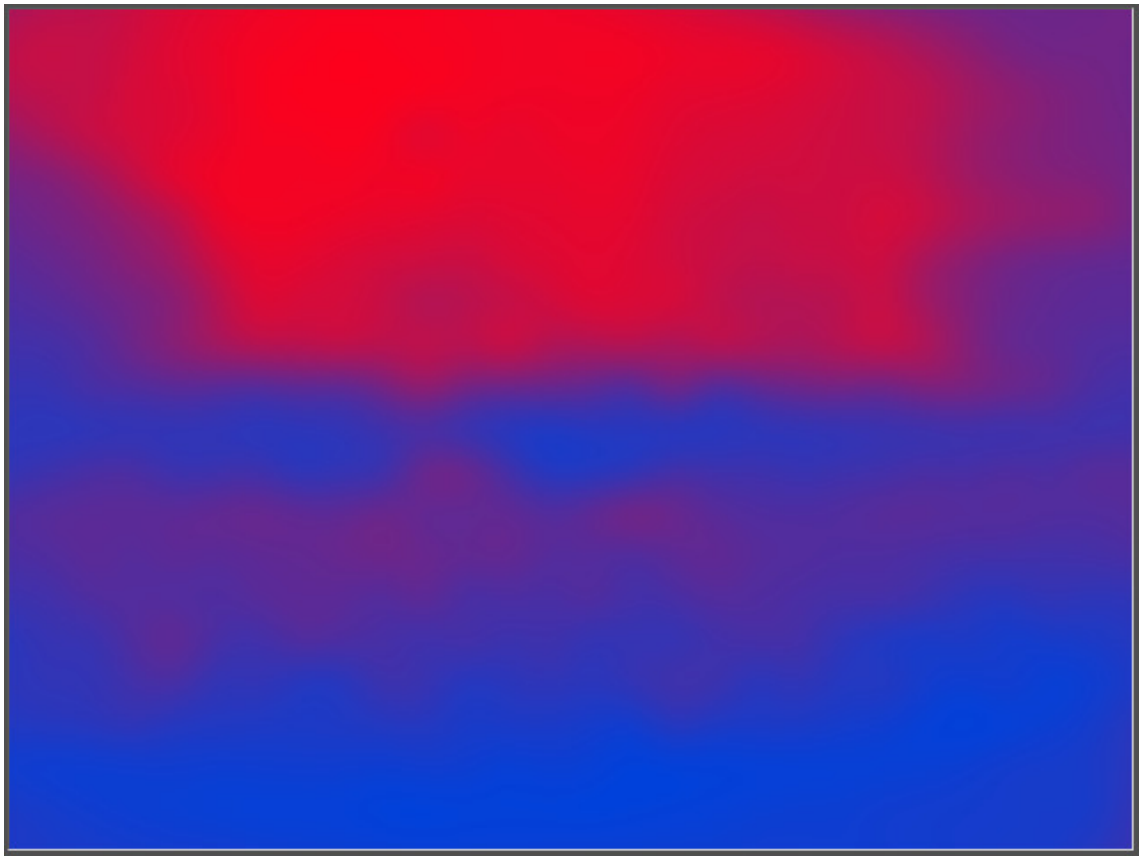

Figure 5.5. *Thermopile image from visible light camera system.*

Temperature data from zones and thermopile's heat map images were measured and stored every ten seconds. Temperature data was stored in a comma-separated values text file while the heat maps were stored as bitmap images. Overall, we acquired over 156 h of video material from the VIS camera.

5.3.3 Infrared camera fixed installations

The infrared camera collected video material from a couple of sections at the boiler. Since the camera sees through the flame it provides a convenient way to monitor combustion compared to a visual light camera. At the beginning of the measurement campaign, we installed the MWIR camera to four locations. The Figure 5.6 illustrates the gained video material from these spots.

(a) *Secondary air level inspection port.*

(b) *Top of the combustion chamber.*

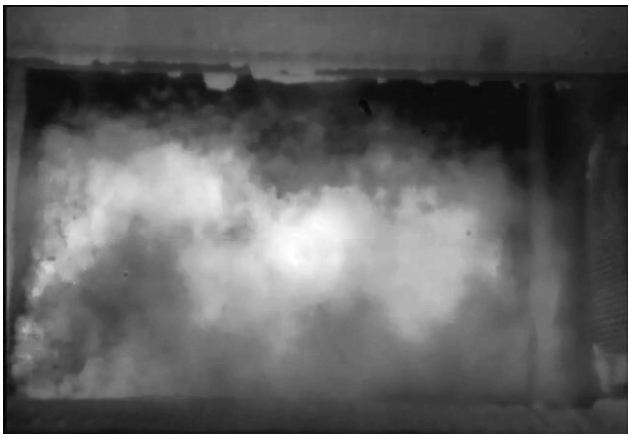

(c) *Combustion chamber towards the second pass.*

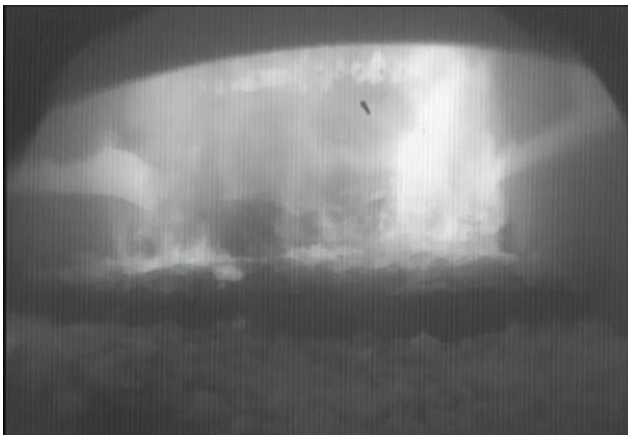

(d) *End of the grate.*

Figure 5.6. *Example images from MWIR camera.*

Firstly, the camera was installed at the inspection port located on the secondary air level. The port lies right at the top of the third grate level. Snapshot from this location is shown in the Figure 5.6a. The fuel pile is at the bottom left of the image. The fuel moves from left to right towards the ash hopper which lies behind the furnace wall on the right side of the image. Swirls of the secondary air are visible in the middle of the image and air holes at the left- and right sidewalls.

Since the combustion temperature is so high at this location the tip of the camera cannot be inserted all the way to the furnace. Hence, the tip of the lens is slightly behind the walls of the combustion chamber that is shown at the right side of the image. Small slag build-up is visible on the top right of the image. This affected the quality of the video quality gained from this location as the slag build-up grew larger and blocked partly the field of view. The camera was recording video material from this location for two days. After a day we had to take the camera out and clean the tip of the lens because it had also collected slag which affected the video quality.

After two days, the camera was moved to the top of the combustion chamber where it captured videos for one day. The filming location is top of the third grate level and the fuel moves from the left to the right. The snapshot of the gained video material is shown in the Figure 5.6b. The combustion is shown in the middle of the image. Since the filming location is so far from the grate, most of the image scenery consists of combustion chamber piping and the exact details of the flame are not visible. Escaping flue gasses had a small effect on the video quality.

The next filming location was from the front wall of the combustion chamber. The camera is at the same level as the second pass passage and the camera's module is pointing towards it. We applied the rotating lens to film the grate from this location. The Figure 5.6c demonstrates the available video material from this spot. The view is centred on combustion. The fuel is moving from the bottom of the image to the top. Field of view consists of second, third and fourth grate levels as well as a small portion of the rear wall of the chamber. SNCR ammonium spraying is visible at the right side of the image. The camera was recording from this location for half a day.

For the rest of the measurement campaign, the camera was installed to the right-side sight glass of the manhole located at the end of the grate. This location was next to the VIS camera as seen in the Figure 5.2. The Figure 5.6d shows an example image from this location. The moving fuel bed is in the middle of the image and is visible through the flame. The fifth grate level step is at the bottom section of the image. Since the field of view is greater than the VIS camera's, the MWIR camera was able to capture the whole grate horizontally.

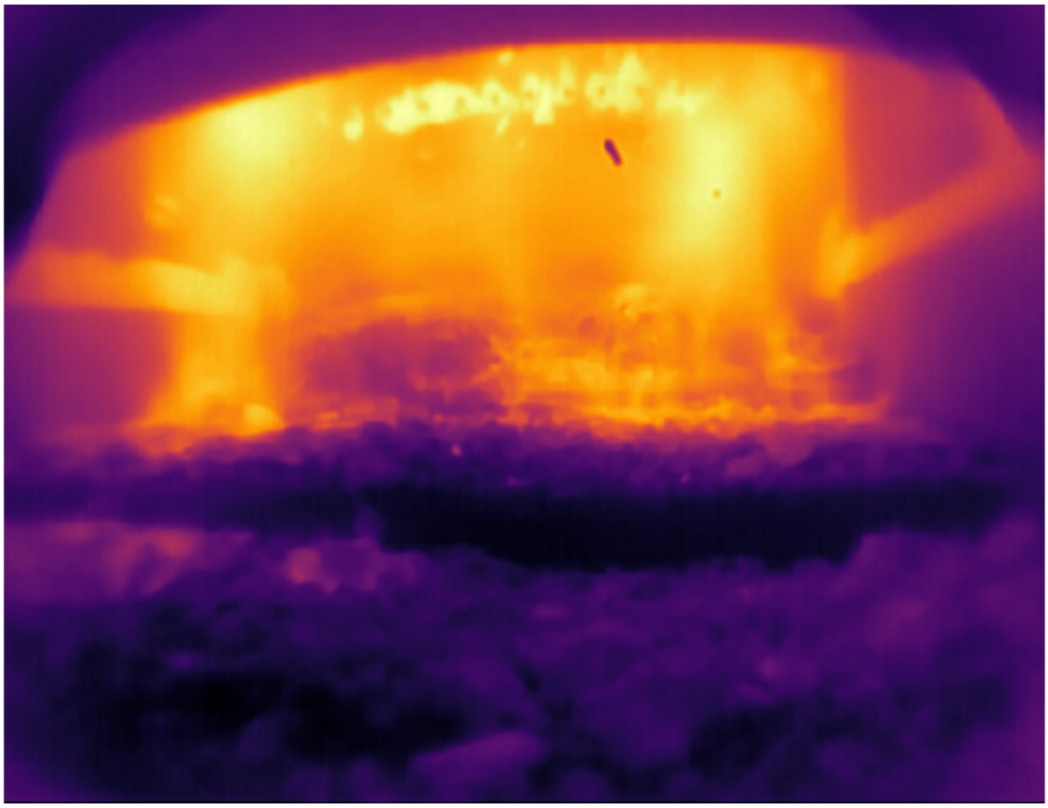

Figure 5.7. *Heat map from end of the grate with infrared camera.*

The infrared camera stores temperature data as a heat map which is illustrated in the Figure 5.7. Temperature readings are also available as numerical values. Since the infrared camera defines temperature reading for each pixel, we did not have to define temperature zones as we did with the visual light camera. The software logged temperature matrices to text files and heat maps to pixel images with the ten-second interval.

5.3.4 Infrared camera mobile inspections

During one of the data collection days, the grate boiler superheaters were cleaned with the mobile shock wave method. In this method, an ignition lance that contains explosives is inserted into the superheater section. The explosives are detonated which creates a shock wave that shakes off fouling and clinkers from the tubes. The ash falls to bottom ash extractors from where it is moved to further post-processing outside the boiler. Cleaning superheaters improves heat convection and the overall efficiency of the boiler. It also increases the lifetime of the heat exchanger tubes by reducing the risk of heat hotspots. That is why it is important to clean the superheater from the soot and slag at frequent intervals. The mobile shock wave method removes fouling from the superheaters that other boiler's cleaning methods are not able to clean.

Because earlier cleaning events had not been recorded with the cameras, we decided to

dismount the MWIR camera and take videos from the cleaning process. The intention of the imaging was to investigate, can cameras monitor the effectiveness of the cleaning and condition of the tubes. We could not record with the visible light camera since the superheater sections do not contain the source of the emitting light. That is why only mobile MWIR camera recorded videos with 360° rotating and 120° straight lenses of the cleaning. The camera was inserted into the boiler from the inspection port located at the beginning of the primary superheaters. Videos before and after the cleaning operation were recorded with both lenses. Snapshots from the videos taken with a straight lens are shown in the Figure 5.8.

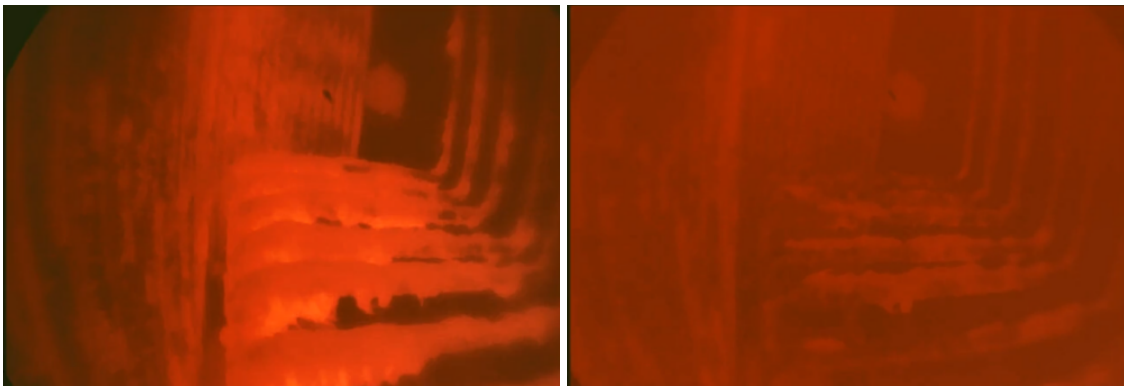

(a) *Superheaters before cleaning.* ***(b)*** *Superheaters after cleaning.*

Figure 5.8. *Superheater section recorded with mobile infrared camera.*

As the images show, the videos provided visual information about the effectiveness of the cleaning. Evaporator tubes are in the middle of the images. As illustrated in the Figure 5.8a, the evaporator tubes contain a lot of soot and slag. Residues are much hotter than other tubes because they are glowing more than the background. Comparing to the Figure 5.8b there are still some fouling and clinkers located at the tubes but most of the soot and slag has fallen off. The temperature distribution is more even after the cleaning since there are no more hot glowing objects in the image.

During one of the days at the plant, the boiler had issues with the clogging of the superheater. One of the superheaters had accumulated wet soot and slag which had blocked the ash extractor conveyor system that transfers the soot and slag out of the superheaters. The reason behind this was unclear. One possible cause is a damaged tube from the explosion cleaning that caused excessive water that caused wetting of the soot that led to clogging.

We decided to inspect this case with the camera. The purpose of the imaging was to try to detect the abnormality that caused the clogging. MWIR camera was assembled to mobile configuration. First, we took videos from the superheater section. First, we recorded videos from the same inspection port as in the Figure 5.8 that was the closest one near

the clogged conveyor. No leakages or tube damages were found from this port. After that, we took videos from the combustion chamber through the inspection port located at the rear wall of the combustion chamber. The port lies on top of the bed at the same height as the second pass passage. Video snapshot from this inspection port is shown in the Figure 5.9.

Figure 5.9. *Top of the combustion chamber recorded with mobile infrared camera.*

The dividing wall of the second pass is in the middle of the image. Three water jet nozzles are located at the combustion chamber ceiling which is shown at the top of the image. During the water cleaning, a high-velocity water jet is pumped to the spinning nozzles. The rotating nozzles spread the water evenly over the whole ceiling which forces soot and slag to drop from the tubes due to the high velocity and evaporation of the water. Water jet should spread evenly over the whole ceiling to maximise the amount of removed dirt. However, the dark trails on the ceiling gave an indication of clogged nozzles. The nozzles go through a predefined path without spinning motion that creates the symmetrical tracks to both sides of the ceiling that are shown in the image. The same kind of pattern was seen on the other parts of the chamber walls when inspecting with the rotating lens. Because the nozzles are not dividing water evenly some parts of the tubes get too much water that reacts with the soot. Excessive water creates wet soot that sticks to pipe surfaces easier than dry ones.

5.3.5 Process data collection

At the next phase of the research, we collected process data available from the power plant. Judgmental sampling was chosen to be the sampling method. This means that we limited the scope of our collected process data set to contain only the relevant process measurements that we estimated to have an influence on the combustion process or plant's overall operation. Judgmental sampling was applied since we are measuring combustion parameters, such as flame volume and combustion location with the developed soft sensor and we want to study their signification compared to conventional process measurements. The power plant automation and information systems contain every measurement available from the plant's equipment and programs. Comprehensive data collection which includes every single process measurement requires extensive data collection. We need to consider our limited resources and our scope since we are only interested in the combustion process dynamics. As an example, the district heating network or bottom ash treatment and their relative control systems do not directly influence the combustion process and therefore collecting these measurements for combustion data analysis purposes is redundant.

Assessment of the collected process measurements was done in collaboration with Valmet's advanced process control experts. Experts are working as process specialists, application developers and product managers for advanced control applications. They have years of experience in implementing and developing process control loops to various processes and energy plants including WTE grate boilers. Based on our and their prior knowledge, we chose to gather only process measurements that indicate the combustion chamber circumstances, plant's overall operability or that combustion controls utilise. Process variables described in Chapter 3 served as a basis for our collected measurements.

Power plant's DCS contains process displays that serve as a user interface for the sections of the power plant. Displays consist of control panels and process data pictures that represent the boiler status visually. User interfaces allows to retrieve process measurements and configurations. Process displays contain information about the control loops, process sensor measurements and physical device statuses. It is possible to access operating and production information through the displays and control the process. Process displays include built-in tools, such as alarms, history, report modules and configuration editors which provide additional information on the power plant elements. Process display is illustrated in the Figure 5.10.

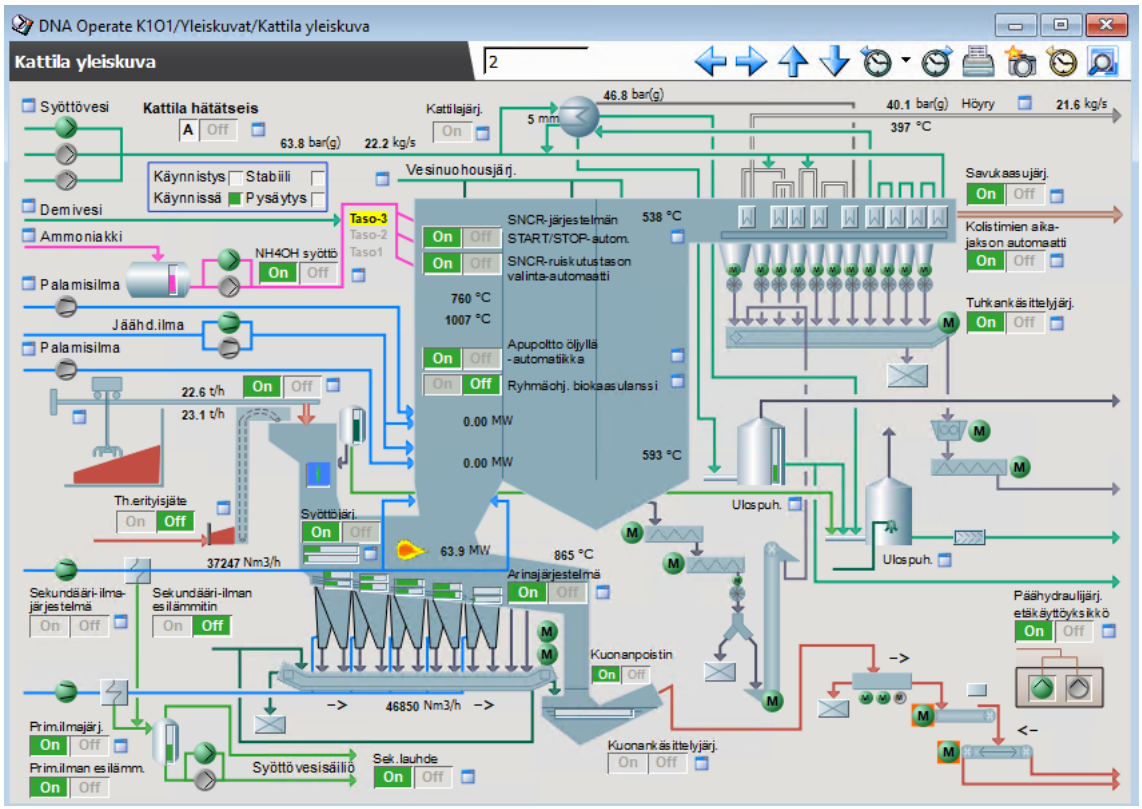

Figure 5.10. *One of the operator process displays during data collection.*

We took the remote connection to the process operation machine to gain access to the process displays. We located tag positions from the operator process displays that indicate the physical location of the measurement devices or controller configurations, such as setpoints and outputs. Information of the tag points is required to collect history data of that element from the plant's information system. From here we decided to collect tag positions based on our formerly described criteria. This means that we chose to limit our sample and collected 119 process measurements available from the power plant DCS. The compressed list of the collected measurements is shown in the Table 5.2. The section names in the table are mainly derived from the operator process displays.

Section of boiler	Measurement	Unit
Steam production	Produced live steam flow	kg/s
	Active power	MW
	Average live steam temperature	°C
	Average live steam pressure	bar
	Feedwater temperature	°C
Control loops	Process variable	SI unit
	Setpoint	SI unit
	Control variable	% / SI unit
Primary air	Total air flow	Nm^3/h
	Air flow in grate zone	Nm^3/h
Secondary air	Total air flow	Nm^3/h
	Flue gas O_2 content	volume %
Combustion	Burnout temperature	°C
	Primary air volume	Nm^3/t
Feeders	Average feeder speed	mm/s
	Feeder speed left/right	mm/s
Grates	Level zone speed	mm/s
	Left/right zone speed	mm/s
Combustion chamber	Combustion chamber temperature	°C
	Flue gas temperature first/second/third pass	°C
	Thermal load	MW
	Auxiliary burner power	MW
Emissions	Flue gas NO_x	ppm
	Flue gas flow	m^3/h
	Crude gas emissions	mg/Nm^3
	Emission limits	mg/m^3

Table 5.2. *Summary of the collected process values.*

It should be noted that the table does not specify every single measurement explicitly since it would make the table unreadable. Some of the values have been bundled to-

gether, such as emission limits for each of the flue gas compositions, grate blocks and control loops. A comprehensive list of the collected process tags with their respective descriptions and units are described in Appendix B. Tag names, descriptions and units are named as they are defined in the automation system tag configuration. Tags which name ends with 'av' are analogue values coming typically from a sensor while 'me' tags are the controller's process variable, 'sp' setpoint and 'con' or 'pos' control variables.

After we had discovered the tag positions for the measurements, we took the remote connection to the process operation machine that is connected to the plant's information management system. This operation machine allows to make queries to history databases and retrieve historical values of the tags. We created the Structured Query Language (SQL) query script that allowed us to fetch the data of the tags. Data were collected from the same duration of the measurement campaign with a sampling rate of ten seconds. We then transformed the queried data into comma-separated values text file for further processing.

5.4 Power plant expert surveys

For the executed online surveys of the research, we chose descriptive surveys as a research method. According to Williamson [95] descriptive surveys are well suited for characterising phenomenon. The goal of the descriptive survey is to collect data that lists and interprets the researched topic. They have a more explanatory data analysis perspective and they do not attempt to form inferential statistics. [95, p. 91–93]

We chose online surveys as our research method after the discussions with the power plant about the research. Coronavirus COVID-19 pandemic situation made the power plant take special caution to ensure safety and security of the plant. This compelled us to choose research methods that do not jeopardise the safety of the energy production facility. Moreover, we must recognise the usable resources and priority of the research. Qualitative data collection and analysis is known to be costly and time-consuming and the chosen methods should fit the research constraints [101]. Therefore, only online surveys were possible.

Surveys helped to gain broader apprehension of industrial-size grate boiler operation and camera utilisation from the end-user point of view. Some of the earlier studies found in the literature review have applied computer vision to small-scale pilot or biomass boilers. Evaluating computer vision-based approaches for diagnostic and control purposes from the end-user perspective helps us to assess their significance in a real-life process environment.

Surveys focused on two themes. The first theme addressed combustion control and monitoring for power plant's operability. The second theme covered camera systems and

their role in the power plant. Themes were further divided into topics. The first topic of the first theme concerned the challenges in the burning waste and operability of the boiler. The second topic focused on the role of the automation system in combustion control while the third topic concentrated on how combustion affects the other parts of the power plant. The questions related to the camera systems addressed their usage and improvement in the combustion analysis. Surveys had predefined questions. Questions of the survey were iteratively reformed based on the feedback from thesis supervisors and examiners to their final form before conducting the surveys. The survey form is shown in Appendix C.

The target group of the survey is grate boiler process specialists who work in administrative or operative positions in grate boiler power plants. The sampled group of the survey were grate combustion process experts working in the same power plant where the measurement campaign was held. Sampling was done with discretionary sampling. We decided to focus our sample to process experts who oversee the plant's maintenance, operation or automation systems. This ensured to gain a diverse sample group with different viewpoints on the subjects.

Potential respondents were firstly contacted directly to ask their willingness to participate in the survey. After the approval survey form was sent through the email to potential twelve respondents. Answers were then collected through email for further analysis. We received eight responses to our surveys. Three of the respondents work in management roles as executive director, maintenance manager and plant manager. The rest of the respondents are power plant operators.

5.5 Data analysis

We evaluated the developed computer vision model with quantitative analysis tools. Hamilton [95] explains that quantitative data analysis requires data coding, analysis and interpretation. First data needs to be transformed into a form that a computer processing software understands. Secondly, data is analysed with the chosen statistical methods and finally, the results are interpreted. [95]

We applied moving average filtering to process and soft sensor signals. The reason behind this is explained in Section 6.6. We evaluated the strength of association and statistical significance between the soft sensor parameters and the collected process data with statistical inference approaches. Applied data analysis methods are explained in the next subsection.

For interpreting the conducted surveys, we applied content analysis which is a methodology in qualitative studies. Based on the definitions described by Bengtsson in [101] content analysis is a research method that systematically and objectively interprets writ-

ten data to describe and quantify phenomena. Content analysis requires choosing a data analysis method [101]. For this, we had to rely more on inductive reasoning when analysing the results since there is no earlier research-based hypothesis to test and we wanted to identify new perspectives rather than drawing definite general conclusions.

According to Bengtsson [101], the analysis method is separated into the manifest and latent analysis. In the manifest analysis, the researcher describes the research phenomena with the collected data that the informants say about the subject while the latent analysis tries to find the underlying meaning of the data [101]. In this research, we apply latent analysis. We interpret the surveys reflecting them to found topics in the literature review and our former experience. We chose to apply latent analysis since we did not have a large sample group in our surveys and the questions, as well as answers, were more descriptive by their nature. Content analysis requires data decontextualization, recontextualization, categorisation and compilation [101]. These steps are explained in Subsection 5.5.2.

5.5.1 Soft sensor parameters

Firstly, we applied cross-correlation analysis to evaluate linear correlation and time delay of the soft sensor parameters to operational parameters. Cross-correlation measures similarity between two signals when the other signal is displaced compared to the other. Cross-correlation analysis estimates the linear correlation with the ratio between covariance and root-mean variance of the signals as a function of delay. We calculated correlation coefficients and time lag between the time signals with unbiased Zero-Normalized Cross-Correlation (ZNCC) ($\hat{R}_{xy}(m)$). Unbiased cross-correlation is defined in [102]. Unbiased cross-correlation was applied since we want to interpret the acyclic cross-correlation of the signals. This is a more realistic case compared to cyclic cross-correlation because signals are analysed as time series in the time domain [102].

According to Alessio [103] zero-normalization is required in our case since we wanted to eliminate the effect of different ranges of numerical values and measurement units as well as scale correlation coefficients to the range $[-1, 1]$. In addition, zero-normalization influences the statistical properties of autocorrelation [103]. The zero-normalization formula is explained in more detail in [103]. By combining these two formulas explained in the formerly mentioned papers unbiased ZNCC is defined as

$$\sigma_x = \sqrt{\frac{1}{N}\sum_{i=0}^{N-1}(x_i - \overline{x})^2}$$
$$\sigma_y = \sqrt{\frac{1}{N}\sum_{i=0}^{N-1}(y_i - \overline{y})^2} \tag{5.1}$$
$$\hat{R}_{xy}(m) = \frac{1}{N-|m|}\frac{\sum_{i=0}^{N-1-|m|}(x_i - \overline{x})(y_{i+m} - \overline{y})}{\sigma_x \sigma_y},$$

where σ is a standard deviation, N is the signal length, $\overline{x}$ and $\overline{y}$ are the sample mean of x and y respectively for all the lag (m) values.

Before the next analysis step, we rejected the lag values which are more than half of the length of our time series. This was decided after considering the process dynamics. It is highly unlikely that these large lag values are really a correlation between the sensor and operational parameters but more likely coincidences generated by how process operating point has been changed. This also eliminates the fluctuation of the expectation value of the time series sum as seen in the Equation (5.1). When the lag value m is close to the signal's length, the divisor $N-|m|$ and the dividend $\sum_{i=0}^{N-1-|m|}(x_i-\overline{x})(y_{i+m}-\overline{y})$ become small which causes fluctuations in correlation coefficients. This happens since we try to calculate the sum with few values divided by a value close to one.

It is not possible to calculate cross-correlation if the standard deviation of the signal is zero. This would cause division by zero in the formula. It is possible that some of the signals did not change during the measurement campaign, such as controller setpoint, so we reject these signals from our analysis.

Since cross-correlation measures only linear dependence between two variables, we cannot truthfully identify correlation, lag-lead relationship and how much information the one signal contains compared to the other one. It is possible that time series are dependent of each other but the cross-correlation appears to be close to zero. Therefore, we applied the Granger causality test to evaluate our parameters.

According to Hamilton [104], Granger causality test validates if one variable and its previous values help to predict the other variable more accurately compared to the other's variable previous values. This tells how useful time series are for forecasting each other. The test was firstly proposed by Granger in the article [105]. Given two stationary time series x_t and y_t, the test assumes a simple linear regression model between them. If one signal and its past values help to predict the other one better, the test says that the first signal Granger-causes the second one. If both signals Granger-causes one another there is a feedback relationship between the signals. [105]

For testing if one series Granger-causes another series, we conducted an F-test of the null hypothesis as proposed by Hamilton [104]. We estimate the autoregressive model between the two time series with Ordinary Least Square (OLS). We then defined a significance level (α) of 5 $\%$ in testing our null hypothesis. The null hypothesis (H_0) assumes that the lagged values of y do not explain the variation in x. Therefore, the alternative hypothesis (H_1) indicates that the y signal helps to predict the signal x more accurately. This is expressed as

$$\begin{aligned} x_t &= c_1 + \alpha_1 x_{t-1} + \alpha_2 x_{t-2} + ... + \alpha_m x_{t-m} \\ &\quad + \beta_1 y_{t-1} + \beta_2 y_{t-2} + ... + \beta_m y_{t-m} + u_t \\ H_0 &: \beta_1 = \beta_2 ... \beta_m = 0 \\ H_1 &: \beta_1 = \beta_2 ... \beta_m \neq 0 \\ S_1 &= \frac{(RSS_0 - RSS_1)/m}{RSS_1/(T-2m-1)} \\ \alpha &= 0.05, \end{aligned} \tag{5.2}$$

where β_m is a coefficient corresponding to past values of the second time series, m is lag length, T is signal length, RSS_0 and RSS_1 are sum of square errors and S_1 is linear regression model. To reject the null hypothesis we compared if S_1 is greater than the 5% critical value (P) for an $F(m, T-2m-1)$ distribution [104].

Granger causality test can be calculated for any lag values m. We wanted to test Granger causality only for the lag values of ZNCC where the absolute correlation coefficient is at the highest meaning the lag where two signals are the most similar. Therefore, we tested the null hypothesis only for the OLS model that contains lag values $m_1 ... m_{max}$ which is defined as

$$\begin{aligned} & m_{max} = \underset{m}{\operatorname{argmax}}\, f(m) := \{m : |\hat{R}_{xy}(m)| \; \forall m \subset S\} \\ \implies & H_0 : \beta_1 = \beta_2 ... \beta_{m_{max}} = 0 \\ & H_1 : \beta_1 = \beta_2 ... \beta_{m_{max}} \neq 0, \end{aligned} \tag{5.3}$$

where S is all the lag values.

Granger causality test requires defining causality relationship between the signals. If the changes of the signal y_t happens prior x_t we should test if y_t Granger-causes x_t and vice versa. We determined which way we should calculate the Granger causality test between

the signals from the sign of the cross-correlation lag values. This is expressed as

$$\begin{cases} x_t \rightarrow y_t, & \textit{if } m_{max} > 0 \\ y_t \rightarrow x_t, & \textit{otherwise.} \end{cases} \tag{5.4}$$

If the maximum cross-correlation peak happened with the lag value more than a zero when comparing y_t to x_t we tested Granger causality y_t to x_t.

Granger causality test requires moderate computational resources. The OLS model matrix multiplications and the density function of the F-distribution computational complexity grows exponentially with the lag length. Large lag values hinder our analysis. We did not calculate Granger causality test if the maximum lag value of the cross-correlation was over 2000 units which is $5.6\,\mathrm{h}$. The value was decided based on the available computational resources. Likewise, it is highly unlikely that this long cross-correlation would be practically viable in control applications.

5.5.2 Surveys

The content data analysis starts with decontextualisation where collected data is broken into smaller units to find patterns in the data [101]. We searched recurring words, sentences and paragraphs from the answers of the survey and highlighted them as well as marked their occurrence to the document to text encode the responses. Coding was done inductively meaning that we created the codes during the analysis process and not beforehand.

After this, we recontextualised the texts which is described as a process where main points are searched from the original texts [101]. We checked texts and compared them to our codes. By counting the occurrence of the codes and considering unmarked text we distinguished units that appeared to form certain groups. Texts that had small occurrences or did not answer the research questions were deemed unimportant and were excluded in this part of the analysis.

The next phase is categorisation where data is grouped into similar classes [101]. We categorised surveys into themes and codes. Themes were derived from the topics of the surveys and answers while for the coding we combined codes found in the decontextualization phase. Categorising was done iteratively. First, we analysed all the codes found from the survey answers. After this, we grouped similar codes into themes and eliminated recurring codes. We continued categorising and coding until we had reduced the number of themes and codes to a satisfactory level. Research questions and analysis' level of detail were deciding factors when we selected the number of themes and codes. Themes and codes are shown in the Table 5.3.

Theme	Code
Operation condition	Fuel quality
	Temperature
	Waste composition
	Other
Automation system	Optimisation
	Control
	Monitoring
Camera system	Flame
	Unburned material
	Automatic recognition
	Air mix
	Temperature
Maintenance challenges	Grate
	Flue gas
	Corrosion

Table 5.3. *Survey themes and codes.*

For validating the findings, we compared the results to the literature review when it was applicable. If the identified key themes of the surveys can be grouped to the topics found in the literature review it increases the credibility of the finding. However, given the qualitative and inductive sides of the survey analysis, we cannot make a too broad comparison of the identified themes to the literature review. This is notably true when analysing answers related to camera systems where previous research is limited.

It must be noted that the survey data is based on the opinions of a limited number of individuals. This limits the trustworthiness of the analysis and the results should not be taken as ground truths. The reliability of the results is estimated with the number of occurring themes and ideas. The more respondents have the same opinion about the subject the more trustworthy the result is. Nevertheless, answers that differ are evaluated whether the individual's role, experience or other factors explain the results.

6. SOFT SENSOR IMPLEMENTATION

This chapter introduces the developed computer vision-based soft sensor. The implementation phase consisted of the same stages as described in Section 4.1. Each of the computer vision stages is described in its own section. The beginning of the chapter explains the chosen development choices consisting of video material and development tools. After this, the chapter describes the developed computer vision algorithm and the decisions during the development. Finally, the chapter discusses how the collected videos were processed for the evaluation of the model.

6.1 Development choices

The soft sensor was primarily developed and tested based on videos available from the VIS camera. Visual inspection of the videos verified that the imaging location at the end of the grate was the most suitable for developing flame area, flame front and shape detection algorithm. The VIS camera was recording videos from the same place the whole measurement campaign. This means that the longest period of the continuous video data was acquired. This helps to evaluate the developed model against the process data and see the long-term changes in the detected flame. After considering solution attractiveness, it was decided to use the visible camera. Most of the grate boilers have VIS camera installed at the end of the grate making the developed solution faster to deploy because no additional hardware is required. A VIS camera is less expensive compared to a MWIR camera and its technological maturity has been proven in previous research.

The soft sensor was developed using Python programming language in the Anaconda environment. Python was chosen since it is free and contains a versatile development environment. Python has comprehensive CV and ML open-source libraries, such as Open Source Computer Vision Library (OpenCV). The library contains over 2500 algorithms for solving computer vision problems and it is a widely accepted library both in academic research and business practitioners [106]. Python was also the most familiar development tool for us. This helped us to start implementing the computer vision model swiftly.

6.2 Image formation

During the first imaging day, we adjusted the settings of the VIS camera to prevent over-exposure and other imaging issues. Automatic gain was enabled and wide dynamic range settings tuned. We further checked how the camera placement affects the video quality. An example of the camera captured image is illustrated in the Figure 6.1. This same frame illustrates the functionality of our developed algorithm in the other figures of this chapter as well.

From the MWIR camera we adjusted the camera's focal length and aperture size depending on the inspection port and lens tube. Parameters were modified to sharpen the imaged fuel pile or the flame depending on the imaging location. From the software side, contrast, brightness and gamma values were modified to correct the quality of the image.

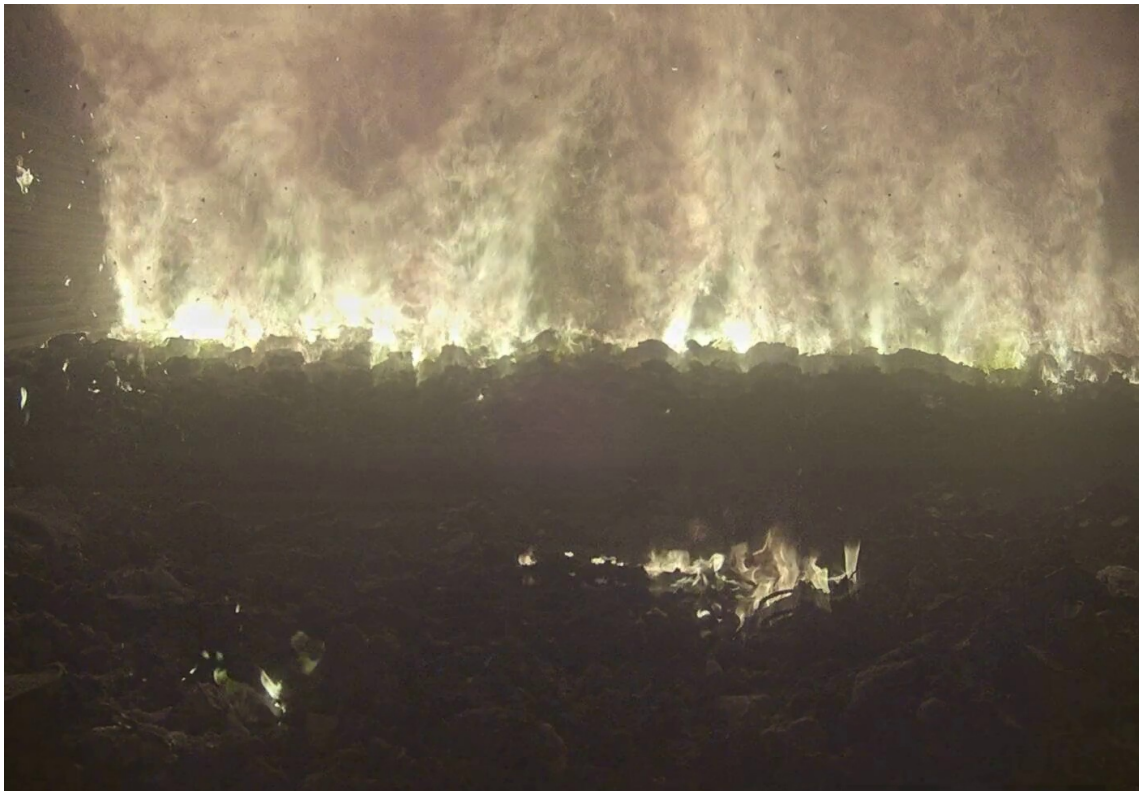

Figure 6.1. *Camera captured image.*

Finally, video capture and temperature sensor settings were verified from the camera systems software. These parameters do not directly affect the image formation side but are necessary for further analysis steps. We checked settings, such as video codec, resolution, frame rate, data logging and sensor's emissivity adjustments, refresh rate as well as running averages.

6.3 Pre-processing

In the pre-processing stage, data and noise reduction methods were applied while preserving the key information of the flame in the image. To reduce the amount of data processed, frames were converted to grayscale images. This was decided after analysing histograms of the colour channels and visually inspecting grayscale colour channel images. As shown in the Figure 6.2, a single colour channel does not provide distinct additional information when comparing them with each other. Therefore, grayscaling was a convenient way to reduce data. The conversion was done with Red Green Blue (RGB) coefficient vector based on luma luminosity encoding.

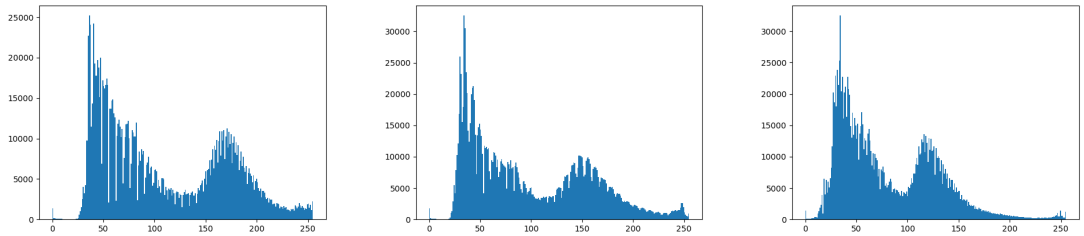

(a) *Red channel.* ***(b)*** *Green channel.* ***(c)*** *Blue channel.*

Figure 6.2. *Histograms of the colour channels.*

Visual inspection of the collected videos showed that images contain noise that prohibits further analysis steps. Flame flickering is strong owing to the influence of the primary air flow and moving fuel pile. In addition, non-burning materials in the fuel create holes in the flame that warp the flame boundaries. Similarly, the heat shield coating on the walls creates reflecting light spots that can be misclassified as a flame in the next processing steps.

Figure 6.3. *Median filtered image.*

For reducing the effect of flame flickering, median filtering in two ways was applied. First, a set of consecutive frames is added into the data buffer. Then depth-wise arithmetic mean is applied to the buffer. Making this operation reduces the fluctuation of the flame and made the frame more robust to fast changes in the image. After this, median filtering with a larger kernel aperture is applied to the buffer than what Ruixuan *et al*. proposed in [27]. Large-sized kernel provided a smoother and more uniform flame when comparing to filtering with smaller kernels. This decreased the effect of the heat shield reflection and flame warping because of the unburned material. A filtered image is shown in the Figure 6.3.

6.4 Segmentation

In the segmentation phase, the flame region is separated from the background. This required dividing the image into two separate classes where the one class represent the flame while the other the background. For this, images are binary thresholded with dynamic Otsu's thresholding. We also tested to segment images by choosing the threshold value arbitrarily. The threshold value was chosen after analysing the intensity histogram of the image and finding the sharp valley between two peaks. The Figure 6.4 present the histogram of the Figure 6.3. The threshold value was chosen from the valley between 100–130.

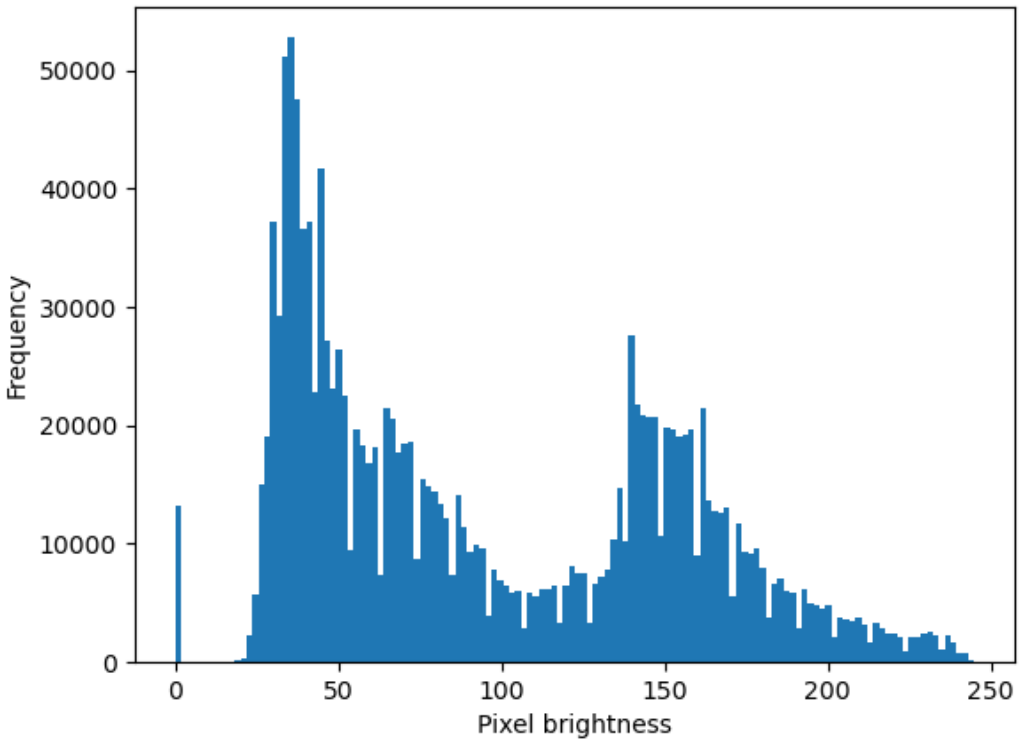

Figure 6.4. *Histogram of preprocessed image.*

Previously previously described segmentation methods were analysed by applying them to collected videos and comparing the results visually based on our judgement. The Figure 6.5 shows the results of these methods when the Figure 6.3 was segmented.

(a) *Manually segmented image.* ***(b)*** *Otsu segmented image.*

Figure 6.5. *Segmented image with tested methods.*

As seen from the image, Otsu's method is better in this case. Otsu's thresholding segments flame more accurately when the brightness of the flame altered due to changing fuel quality compared to our global thresholding value. Likewise, Otsu was more accurate

to reduce noise coming from the heat shield reflection. It can be concluded that Otsu's method was more robust in the changing environment.

Figure 6.6. *Segmented and morphological operated image.*

After the image is thresholded with Otsu's value, morphological operators are applied to the image. The image was first eroded and then dilated. Morphological operations removed noise and closed small caps from the segmented image since Otsu's algorithm was not so sharp segmenting the outer boundaries of the flame. A smaller kernel is applied compared to one proposed in [23] for the application. A segmented image is illustrated in the Figure 6.6.

6.5 Feature extraction

The calculated features from the image are the form of the flame, flame front location and its shape. Flame form information is extracted from the binary segmented image. The sum of the total number of pixels that belong to the flame class gives an approximation of the size of the flame. The larger the flame the more pixels are classified to the flame class therefore the sum will be higher.

For the flame front location and shape, flame boundaries are extracted from the image. This is achieved with Canny edge detection to the segmented image. Upper and lower hysteresis threshold values and aperture size in Sobel operator were chosen based on

segmented image histogram according to Canny's rules for optimal values [81]. L^2 distance was applied in calculating the magnitude of image gradient like in [81]. Extraction was done with Canny edge detection algorithm based on the findings of the literature review since it was clearly the most applied method for edge extraction.

Canny edge detector works quite well in detecting the edges of the flame from the segmented images but it does not segment which edges belong to the main combustion flame. As the Figure 6.7a shows, there are burning substances in the fifth grate level that is in the lower part of the image. The algorithm extracts flame boundaries from these flames that do not belong to the central combustion area. In addition, there is small noise close to the outer boundaries of the flame.

To separate small flames from the flame front additional segmentation methods are applied to the edge extracted image. A data clustering algorithm called DBSCAN is applied. Algorithm clusters data based on their density which is defined by the distance between the points. The algorithm requires two parameters, the minimum number of points in the cluster and the maximum distance between the points of the same cluster. These values were determined by the heuristic rules proposed by Ester *et al*. in [78]. The image was filtered by choosing only the data cluster that represented the main combustion flame. This data cluster had the highest density. This is illustrated in the Figure 6.7b.

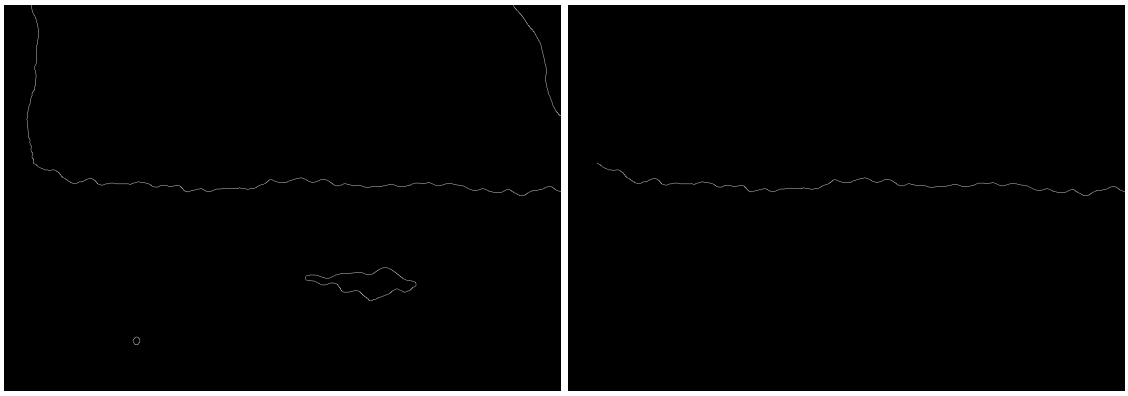

(a) *Canny edge extracted image.* ***(b)*** *DBSCAN segmented image.*

Figure 6.7. *Feature extraction sequence.*

After this, the bottom section of the detected flame is extracted that represents the flame front. The image is thresholded in the height direction based on the centre of mass. The detected flame front is illustrated with a red line in the Figure 6.8.

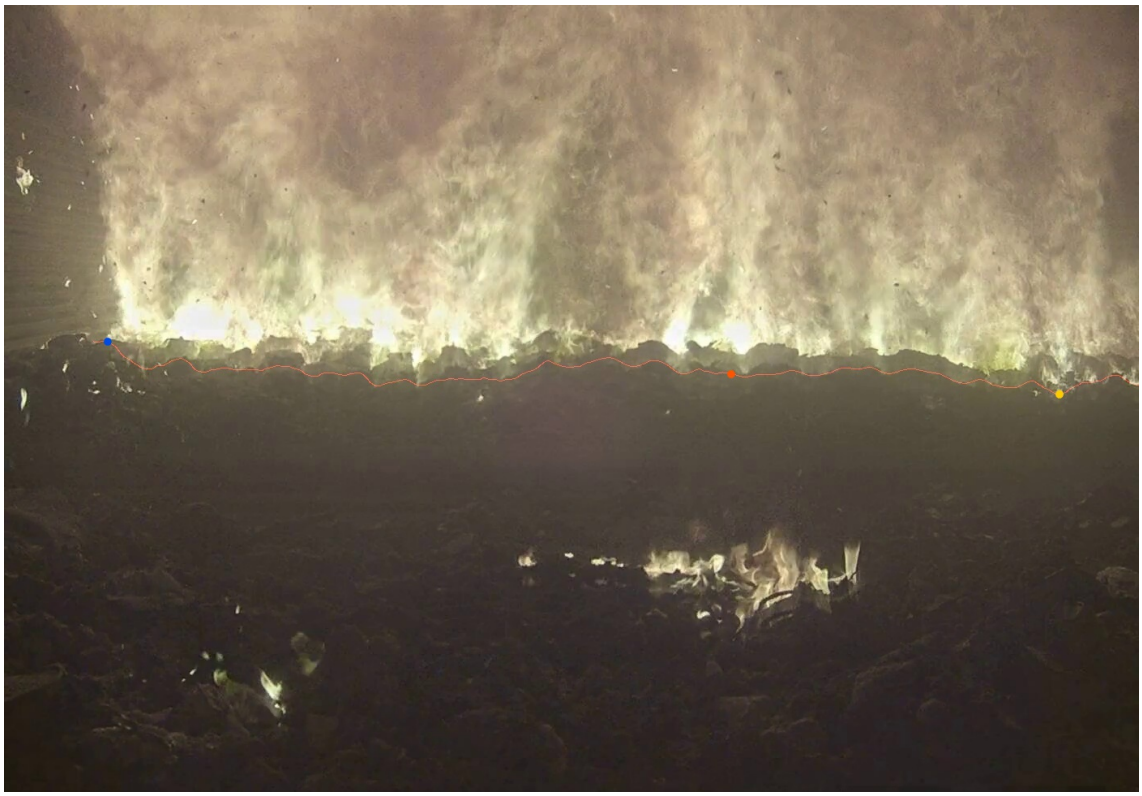

Figure 6.8. *Detected flame front and feature points of the flame location.*

Next, features that describe the flame front location and area are determined. For the location, pixel distance between the minimum, average and maximum point of the flame front to the edge of the fifth grate level is calculated. The Figure 6.8 shows the detected minimum, average and maximum points. Minimum is coloured with a blue, maximum with a yellow and average point with an orange dot. For the flame front, a first-order linear OLS model is fitted that gives us two coefficients, the slope coefficient (a) and the y-intercept coefficient (b). Therefore, there is one parameter that describes the flame area and five parameters for the flame front location and shape.

6.6 Video data processing

After confirming that the developed model handles unique combustion scenarios by running various videos through the model and analysing the outputs visually, all the collected videos with the VIS camera were processed. The videos were fed to the model which computed and reported the extracted features to the comma-separated values text file every ten seconds based on the passed time of the video. Since the camera software dynamically controls the FPS in video recording mode, the ten-second intervals had to be estimated from the length and metadata of the videos. The time series of the extracted features are shown in the Figure 6.9.

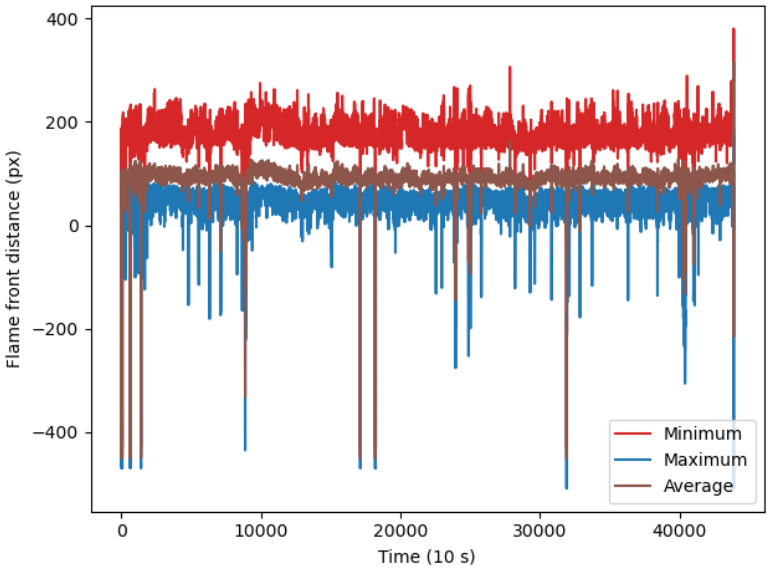

(a) *Flame front location.*

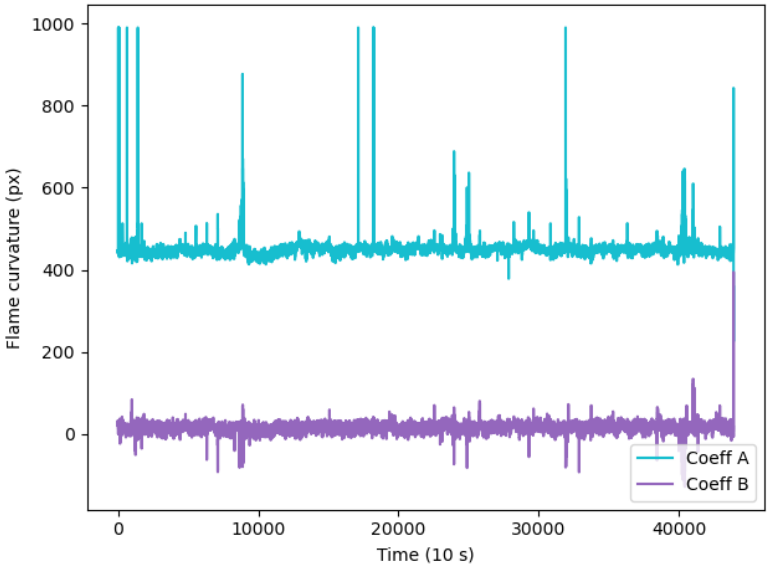

(b) *Least square coefficients.*

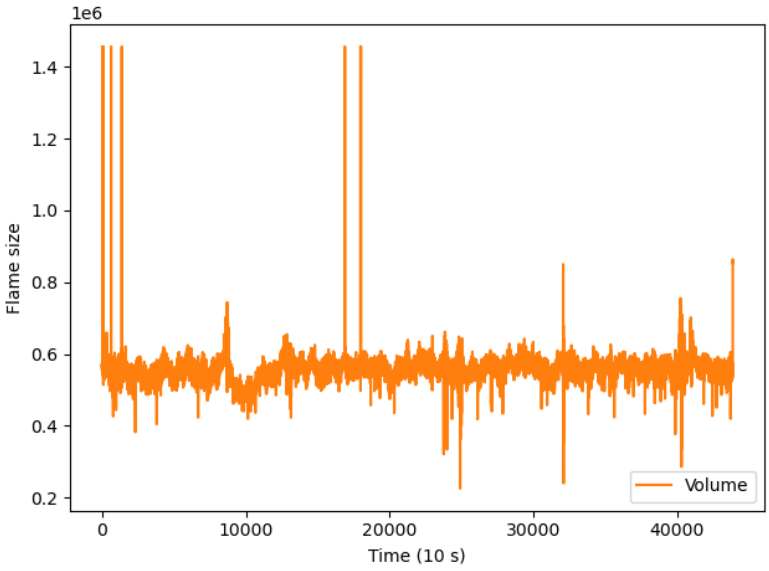

(c) *Flame area.*

Figure 6.9. *Logged soft sensor features.*

The time series contain noise that causes peaks and throughs. Time series were smoothed with the moving average for noise reduction because it has been proven to be a good technique for time series analysis. According to Hamilton [104], moving averages are good for revealing underlying trends and analysing seasonal patterns. Moving average filtering requires defining the size of the window that was chosen after testing different window sizes and inspecting responses of the smoothed signals. Tested window sizes were 15, 30 and 45 min and 1, 3 and 6 h. The Figure 6.10 shows the results of a couple of tested windows.

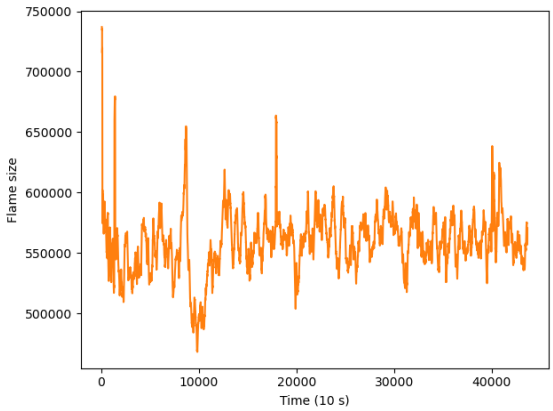

(a) 15 min *filter.*

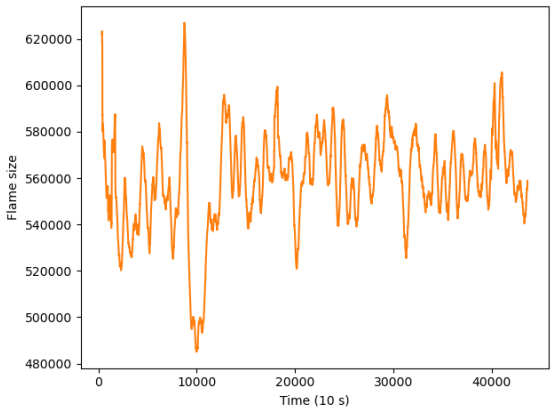

(b) 1 h *filter.*

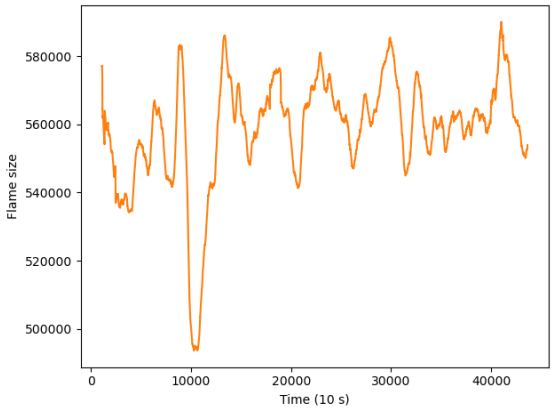

(c) 3 h *filter.*

Figure 6.10. *Filtered flame area with three tested moving averages.*

As the figure shows, the fifteen-minutes filter does not reduce noise enough while the three-hour filter attenuates and reduces the resolution of the signals. This causes loss of information. Based on the tested filters, the one-hour time window provided the most noise reduction while keeping the form of the signal. Discussions with Valmet's process experts and their apprehension of the grate boiler combustion time delay had an effect on the chosen window size. Considering the process dynamics, more than a one-hour

moving average are not feasible from the process control point of view. Therefore, signals were filtered with a one-hour window that is shown in the Figure 6.10b. Moving average filtering was done for the power plant's process measurements to make them comparable with soft sensor parameters.

7. RESULTS

This chapter describes the empirical results of the research. Results are based on the developed computer vision soft sensor model, collected process data and conducted online surveys. The first section presents the results between the extracted features of the computer vision model and process measurements. The second section explains the results of the online surveys. We use direct quotations from the surveys to support our findings. The survey results are discussed theme by theme in the same order as shown in the Table 5.3. This chapter presents only the results of the empirical research while the detailed analysis of the results is described in Chapter 8.

7.1 Soft sensor model

In the cross-correlation analysis, we compared extracted soft sensor parameters to the process signals. While computing the Granger causality tests, we calculated the results both ways but only analysed the result based on the rule in the Equation (5.4). Therefore, the process signals are marked by x and the computer vision model features by y in our analysis.

Comprehensive results of the analysis are introduced in Appendix D. The comparison of the extracted soft sensor parameters is in their respective tables. The first column of the table is the signal name. The signal name is combined with the description and suffix of the tag. This naming convention helped us to analyse the results since we did not have to look up the tag names and their description from the other tables. With this naming, we see instantly what the signal is and to which process block it belongs.

The second column of the tables is the lag length where the absolute value of the cross-correlation coefficient is at its highest and the third column is the corresponding extreme cross-correlation coefficient value. The fourth column is the Granger causality test's critical P-value when we tested soft sensor parameter to process signal while the fifth column is Granger test result done in the opposite order of the signals. The signals are sorted in the tables in descending order based on the signals the absolute value of the maximum cross-correlation coefficient. The signals for which we did not calculate the Granger causality test due to the large lag length are marked in the tables with a pound sign.

The signals that were excluded from the analysis are shown in the Table D.7. Signals happen to have zero standard deviation because of how the control loops are built or how the boiler had been operated during the measurement campaign. The setpoint signals are boiler dimensioning parameters, such as the live steam pressure, burnout temperature or excessive O_2 content in the flue gas that the boiler manufacturer has defined during the boiler delivery. Analogue measure values are auxiliary burners powers and fifth grate zone left side movement speed. Auxiliary burners were not on during the measurement campaign and there were no changes in the fifth grate level's movement speed according to this measuring unit.

The Table D.1 contains results of the extracted flame front minimum point against the process data. The highest correlation was with the combustion controller's primary air flow control variable with the correlation coefficient of 0.71 and lag 135. Signals that have absolute correlation coefficients higher than 0.6 have an average lag length of 140 meaning that the extracted soft sensor parameter is leading the process signals approximately $23.3\,\mathrm{min}$ on average.

The Table D.2 contains results of the extracted flame front maximum point while the Table D.3 contains extracted flame front average point, the Table D.4 contains the y-intercept coefficient and the Table D.5 the slope coefficient of the first-order linear OLS model against the process data. The average point and y-intercept coefficient have similar lag and cross-correlation coefficients except that the average point has positive and y-intercept coefficient negative correlation values. The slope coefficient has the lowest cross-correlation coefficients across all the extracted features. In addition, the slope coefficient has the greatest number of signals where the maximum lag length exceeds the Granger causality test limit.

The Table D.6 contains results of the extracted flame volume against the process data. The highest correlation was with the combustion controller's primary air flow control variable with the correlation coefficient of -0.68 and lag 406. Most of the signals which have an absolute correlation more than 0.55 have a negative correlation between the process measurements. Two of these signals have a positive correlation. The lag value is close to the 435 except the two signals where the lag values are -8627 and -8717 respectively.

7.2 Surveys

Based on the surveys, the fuel quality is the highest factor affecting the power plant's operability. The most recurring topic was the alternating quality of the heterogeneous waste. Characteristics, such as heating value, moisture and reactive substances changes based on the fuel. The respondents, especially process operators, pointed out that because of these reasons it is hard to predict what kind of fuel comes to the grate and how it burns.

Fluctuating fuel quality causes changes in the boiler's operation conditions where the most surfaced topics were temperature and waste composition. Four operators and the plant manager mentioned that high temperatures reduce combustion efficiency and the need for thermal load, damage heating surfaces coatings and grate grid bars while the low calorific value fuels cause sudden drops in the temperature and the combustion needs to be supported by auxiliary burners. Likewise, waste composition disturbs the combustion process. Process operators told that sometimes fuels with high content of HCl and SO_2 rises flue gas emissions and thermal load needs to be reduced. Melting metals, such as aluminium, and big unburned objects cause grate jamming or ash hopper clogging that leads in serious cases to the power plant's shutdown. The plant manager added that "Sometimes fuels for example industrial paper rolls, move like an avalanche through the whole grate straight to the ash hopper".

Based on the answers, challenges caused by varying fuel quality reflect power plant maintenance and the lifetime of the other parts as well. The most affected parts are the grate, flue gas cleaning system and piping. According to the maintenance manager and process operators, high heating value fuels rises temperature creating local hot spots which increase thermal stress of the grate. Fine-grained unburned materials cause damages in the grate bearings while metals increase mechanical stress of the grate blocks. Fuels containing high emission and suboptimal combustion put additional stress on the flue gas cleaning system and increase cleaning costs. Incomplete combustion and high content emissions damage refractory coating, cause corrosion in the piping and dirty components.

Judging from the results of the surveys, most of the issues the power plant has been facing are related directly or indirectly to waste quality and combustion optimisation. The repetitively changing fuel quality causes changes in the process conditions that have multifaceted implications. The combustion process is in a major position in dealing with the challenges. Not only it has a direct effect on the power plant's production but it affects the operating costs as well. Based on the respondents' answers, having an optimal combustion process helps to overcome the power plant's challenges.

The automation system has an important role in optimising the combustion process. One of the managers stated that the best way to influence the power plant operability is to "continuously optimise the process for achieving perfect combustion at the middle of the grate". Respondents told that the automation tries to keep the combustion in the optimal temperature range, control the combustion position at the grate and maintain the flue gas flow to be steady. Keeping the combustion process optimised helps to overcome formerly described challenges and according to respondents, the automation system has succeeded in doing it. One process operator told that "I have been optimising power plant's combustion after the commissioning ... nowadays, the automation system and combustion control has been changed so it can deal with the big changes in the combustion conditions."

Respondents told that the automation system is not perfect and the operators have an active role in operating the power plant. The operators monitor the combustion and do active corrective actions when required. One process operator mentioned that "I still have to follow that the automation response is sufficient and change settings to prevent rapid changes to combustion process conditions". Process operators mentioned that they track O_2 content, combustion chamber temperatures, pressures, power changes, steam pressures and fuel feeding from the automation system. They continued that they make changes to the air distribution, grate movement speed, thermal power and auxiliary burners when needed.

Based on the answers of the respondents, the automation system strives for optimum production capability but the process operators still have to actively control the combustion. The operators are mainly interested in what happens in the combustion chamber. They follow the process measurements related to combustion characteristics and they change mainly parameters of the combustion power control loops. This demonstrates that combustion has the highest effect on the power plant's operation conditions and thus the output.

The camera system was considered to be an effective tool for monitoring purposes. Respondents mentioned that they monitor flame front location and length, flame shape, intensity and big objects from the image feed of the camera. Five respondents told that they compare flame intensities between the grate lines. A couple of process operators further mentioned that they observer shutdowns and startups from the camera.

Respondents had a couple of ideas about how the camera system should be developed so it would bring additional value for them. The most recurring point was the automatic information of the flame front. Respondents mentioned things, such as the position of the starting and ending point of the flame as well as detecting burnout in the fourth and fifth grate levels. The second point was the temperature information of the flame. One respondent mentioned that it would be good if the temperature at the beginning of the grate is monitored. According to him, this helps to detect low-quality fuels. The plant manager and the executive director discussed that recognising big unburned objects from the grate would be beneficial for maintaining the ash hopper clear. As for the last item, one process operator wondered if the infrared camera can detect the effectiveness of the air mixing.

According to the surveys, the camera system is recognised to be a useful tool for supervising combustion. Process operators actively observe combustion and its state from the video feed. There are many characteristics, such as temperature, combustion location and unburned material that they inspect from the video. This indicates that the flame and its characteristics are important to follow. These characteristics are linked to the challenges the power plant is facing since they are indicators of the issues the respondents

mentioned. Likewise, these parameters are the ones that the process operators would like to get more information about the combustion process.

The answers by administrative respondents and process operators have some differences. The administrative respondents were more specific when describing the challenges of the grate boiler while the process operators gave more specific answers to automation and camera system-related questions. This is quite natural due to their job responsibilities. Managers oversee the power plant and are in charge of its operation, therefore they have the big picture of the challenges. Similarly, the process operators are in control of running the power plant and they have the best knowledge of the process dynamics.

8. ANALYSIS

This chapter examines the results of the study. The first section of the chapter analyses the cross-correlation and Granger causality test results, interprets the results to process knowledge as well as compares the developed model to those in the earlier studies. The second and third section examines the qualitative results of the surveys and compares them to the findings in the literature review. The second section analyses the process state variables while the third section evaluates measurable combustion characteristics with cameras. Moreover, the chapter evaluates the results, their limitations and reliability as well as sources of errors.

8.1 Computer vision soft sensor

Based on the cross-correlation analysis, the minimum point of the flame front correlates the most with the collected process signals. The highest cross-correlation coefficients are with the primary air flow signals and the relationship is positive. The Figure 8.1 shows the cross-correlation between the minimum point and combustion controller's output which is the total primary air flow. There is a clear spike in the lag value of 135 indicating evident similarity between the signals. With the other lag values, the correlation is not as strong and stays around -0.25–0.25 without clear spikes.

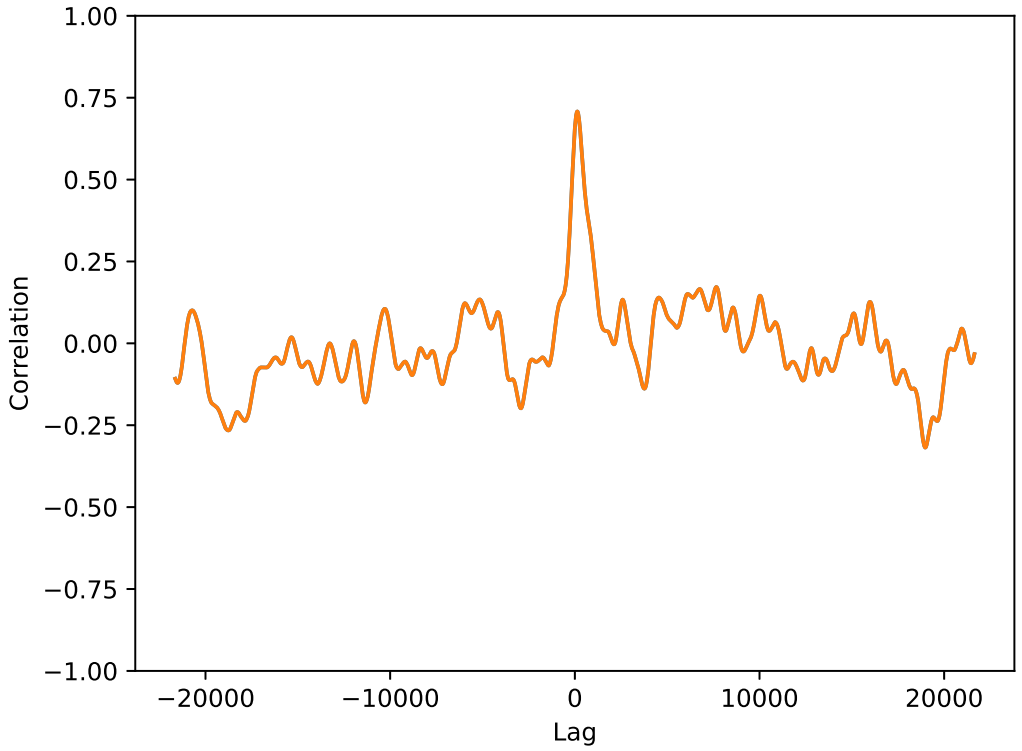

Figure 8.1. *Cross-correlation of the minimum flame point and primary air flow.*

As shown in the Figure 8.1, the minimum point of the flame is leading the process signal 22.5 min. The Figure 8.2 which shows the trends of the signals illustrates this as well. The red line is the combustion controller's primary air flow output and the blue is the minimum point of the flame. Visually inspecting, the primary air flow trend follows flame front location.

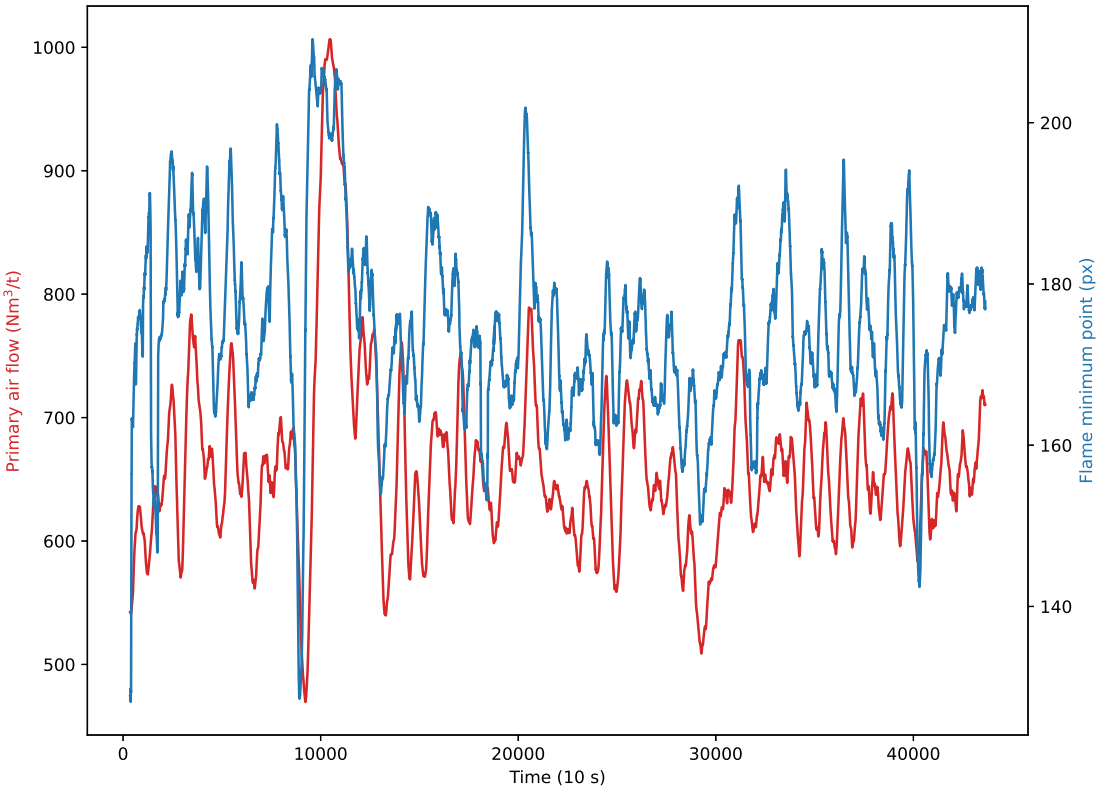

Figure 8.2. *Primary air flow and minimum flame point.*

Correlation between the flame location and primary air flows is explainable by the process dynamics. Consider flame front location to be an indicator of the bed inventory like Garami *et al*. [20] and Nielsen *et al*. [31] reasoned. When there is a lot of fuel on the bed, the bed inventory is high and the minimum flame front point should be closer to the camera as a result of waste on the grate. High bed inventory means that there is a load of combustible material waiting to combust and release energy. This pile of fuel lying on the bed requires a small amount of primary air to devolatilize and produce the required energy. Contrary, when the flame front location is farther away from the camera, that is there is not much fuel on the grate, the grate boiler needs to supply more primary air to keep the adequate energy production.

Other air flow signals have similar trends. This is reasonable since the total primary air flow is divided into predefined proportions under each grate zone. Small deviations in maximum cross-correlations are explainable with the unique tunings of the air flow controllers' parameters.

There is a negative relationship between the minimum point and the combustion controller's secondary air flow output. The maximum correlation is -0.62 and the time delay 118 units which is $19.7\,\mathrm{min}$ as the Figure 8.3 shows. The time delay is smaller compared to the primary air flow.

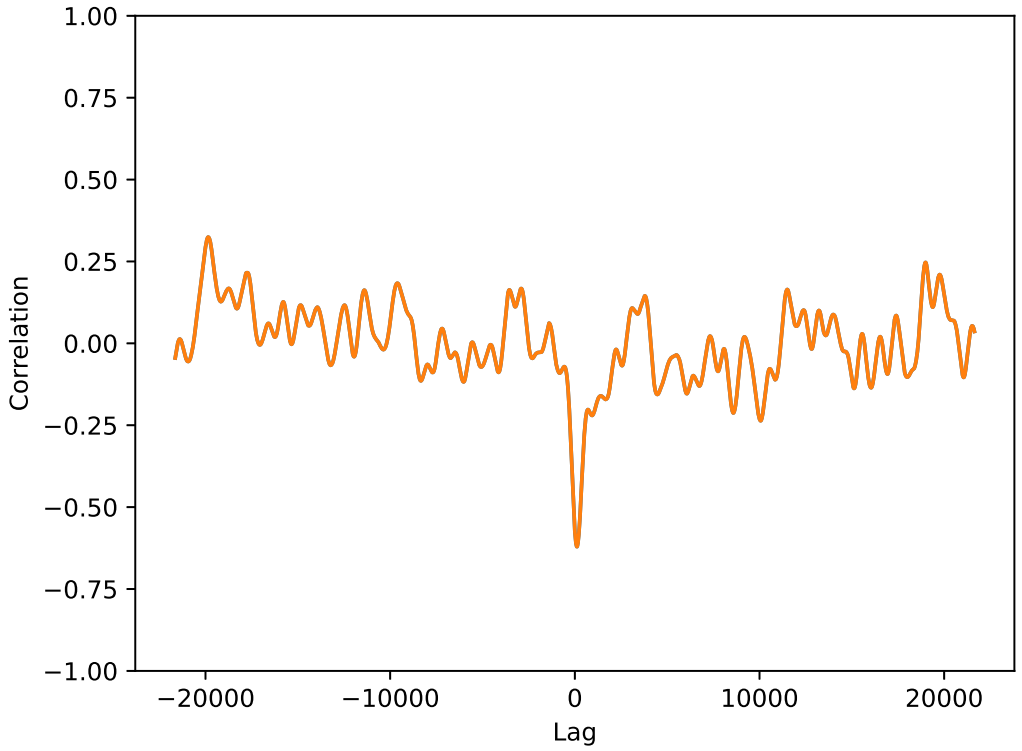

Figure 8.3. *Cross-correlation of the minimum flame point and secondary air flow.*

This matches the process dynamics. The boiler's secondary air flow controller's function is to keep an adequate air-fuel ratio that is measured from the excessive O_2 from the flue gas. As reasoned previously, the minimum point is an indicator of the bed volume. If bed volume is low, a lot of primary air flow is supplied. This reduces the secondary air flow because the primary air flow raises O_2 content. Vice versa, when the bed volume is high, more secondary air is required to maximise the combustion. Delays in the process explains the difference in the maximum lag value. Since the excess air ratio is measured from the flue gas after the first pass, the changes in the primary air flow take some time before they are visible in the sensor. The Figure 8.4 presents the secondary air flow and the minimum point of the flame.

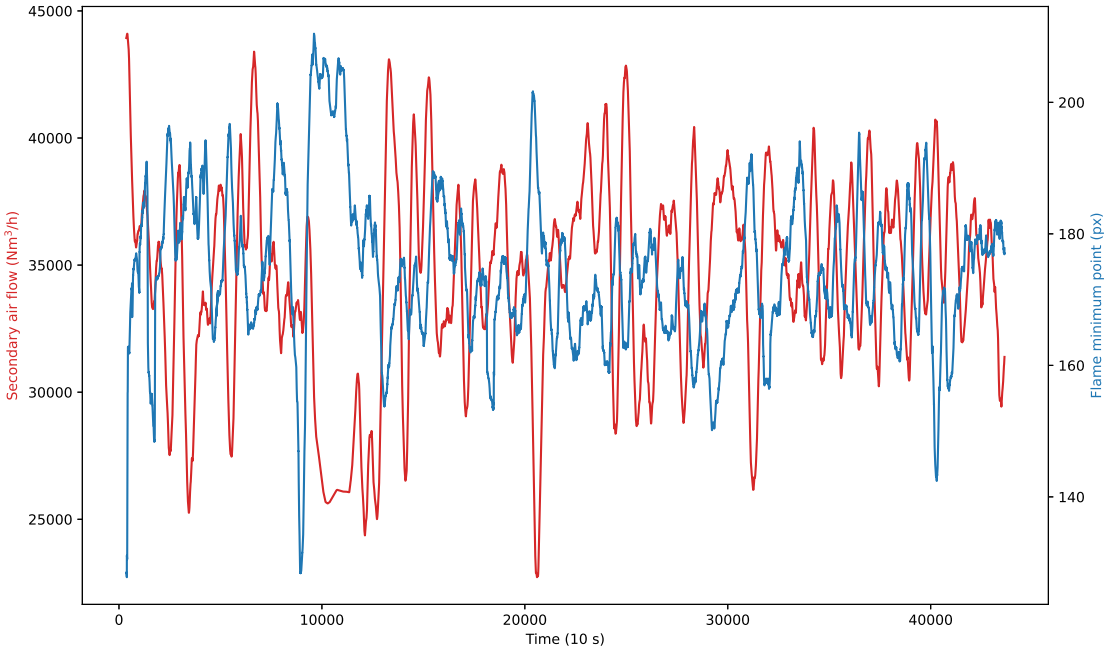

Figure 8.4. *Secondary air flow and minimum flame point.*

There is a decrease in the maximum cross-correlation values when comparing the results of the maximum and average point of the flame to the minimum point. As seen from the Figure 8.5b, the maximum point seems to have a smaller deviation than the minimum point. One explanation is that the process operators control the location of the flame location. Based on the surveys, the process operators try to keep the flame front away from the last grate level. Visually analysing the Figure 8.5b, the maximum point seems to be on average 55 px away from the fifth grate zone boundary, which is roughly at the middle of the fourth grate zone. According to the results, these parameters are not so informative compared to the other features.

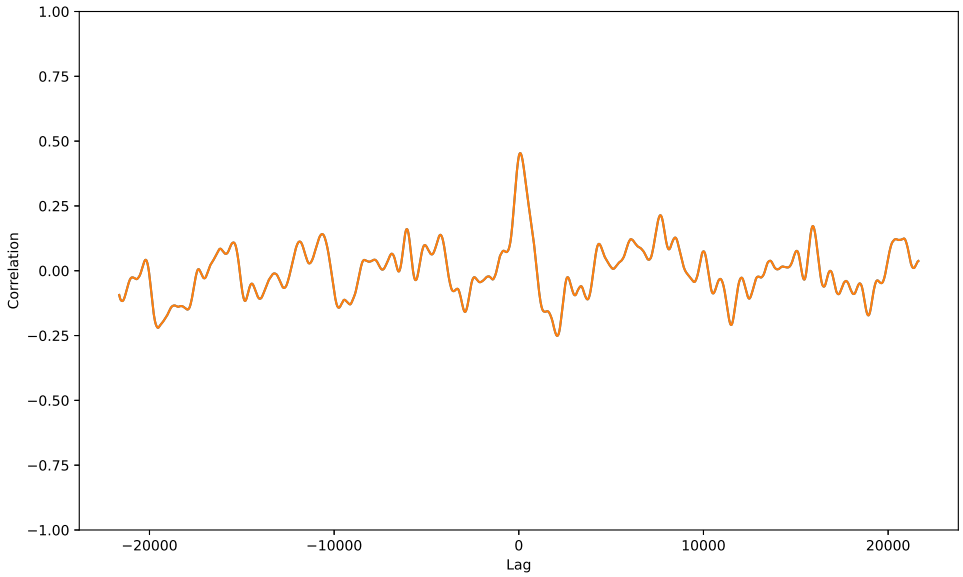

(a) *Cross correlation.*

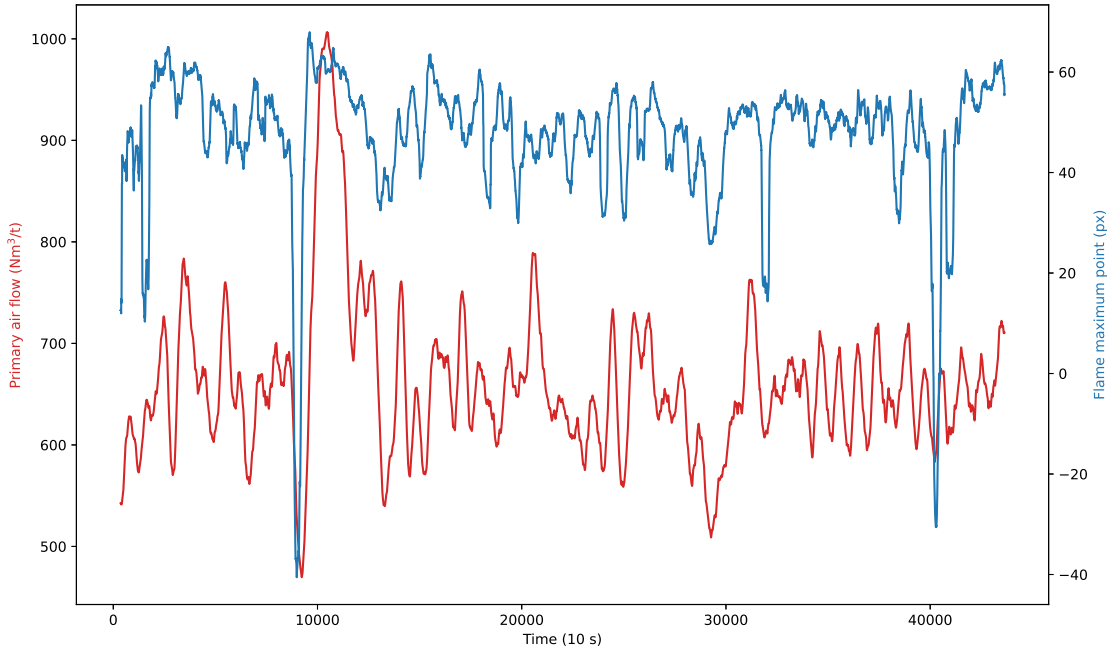

(b) *Time series graph.*

Figure 8.5. *Primary air flow and maximum flame point results.*

Based on the cross-correlation, the linear polynomial fit for the flame front does not seem to contain additional information compared to other extracted features. The correlation coefficients are lower and lag values higher than on the other features. This holds true especially for the slope coefficient a that has the most signals where the Granger causality test was not calculated. Based on the results, the linear line fit does not bring supplementary information about the combustion. This is an interesting finding since according to

surveys, the process operators monitor the shape of the flame front with a camera. They also mentioned that the flame front should be as even as possible. Reasons for poor results are that the camera position was not optimal for measuring the flame front shape or that the flame front shape does not affect the combustion as much as the process operators think. However, further research is required.

According to cross-correlation analysis, the area of the flame leads the process signals the most on average across all the extracted features. The Figure 8.6 shows the cross-correlation between the flame area and primary air flow. The correlation coefficient is -0.68 and the flame area is leading the process signal 406 units that is $67.7\,\mathrm{min}$.

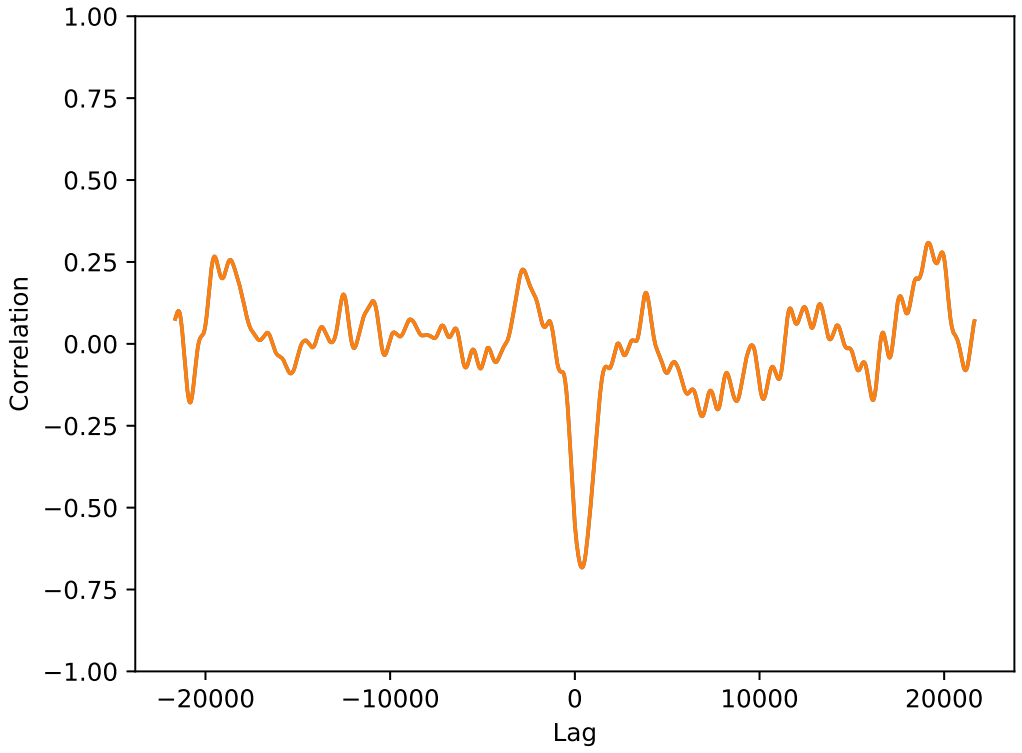

Figure 8.6. *Cross-correlation of the flame area and primary air flow.*

Even though there is a clear spike in the cross-correlation trend indicating a somewhat clear correlation, this is not explainable by the time constants of the combustion process itself. Nonetheless, performing a sanity test between the minimum point and flame area helps to analyse why the flame area has the higher maximum lag values.

Considering the flame front's minimum points as an indicator of the bed volume, the bed volume is changed by alternating the fuel feeding speed. However, there is a high time delay before the changes are seen in the frame front location. Freshly inserted waste needs to travel through the whole grate before the changes are visible. In opposite, when the waste starts to devolatilize and produce visible flame, the soft sensor sees the

changes in the area of the flame. Likewise, response time is higher in the primary air flow. When more air is supplied, the combustion intensity increases that should reflect the area of the flame. Contrarily, primary air flow increases devolatilization of the porous material that is a slower process thus changes are seen slower in the flame front location. However, these aspects should be further investigated. The Figure 8.7 shows the time series of the signals.

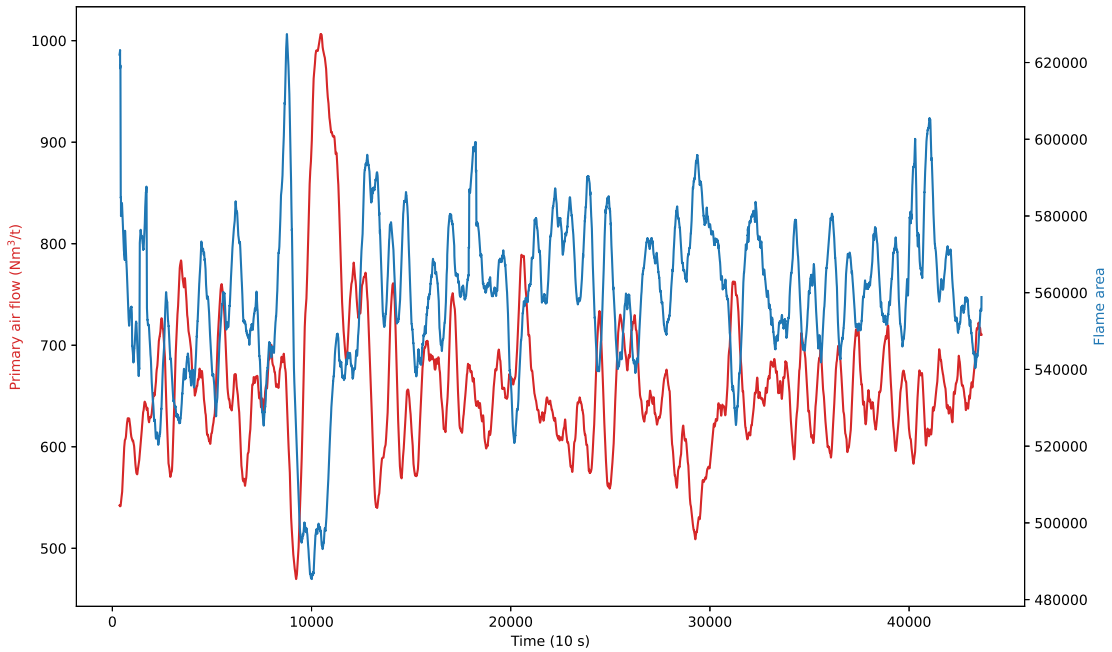

Figure 8.7. *Primary air flow and flame area.*

Results from the Granger causality tests demonstrate that the developed model predicts the state of the process. When looking at the minimum, maximum and average points, the H_0 is rejected in most of the signals that have absolute correlation coefficients more than 0.4. The flame area has a higher number of signals where the null hypothesis cannot be rejected compared to the flame position features but there are still many process variables that have statistically significant P values, such as primary air flow, flue gas O_2 content and combustion chamber temperature, to name a few.

There seems to be a high conclusion that the extracted features help forecast the collected process parameters. Since the extracted features Granger-causes process measurements, both the lags and their respective past values are statistically significant. The changes in the process conditions are seen before the conventional process measurements. These results are in line with the previous studies assumptions that the flame front and area improve the knowledge of the combustion in the grate [5, 31].

The results of our analysis are somewhat like Garami *et al.* [20] findings from the biomass grate boiler. In their study, they estimated that the minimum point of the flame front was

leading the collected process measurements 5–22 min depending on the signal [20]. Our analysis calculated the lags to be in the range of 11–35 min.

For the cross-correlation coefficients, Garami *et al*. calculated over 0.8 for the O_2 flue gas content and flue gas temperature. For the combustion chamber temperature, they reported absolute coefficient of around 0.6 and for NO_x and CO emissions over 0.3. [20] Based on our analysis, absolute coefficients are 0.52, 0.58, 0.50, 0.43 and 0.44 respectively. Results indicate that the flame front location estimates other combustion parameters in the waste grate boiler as well.

Even though there are differences in the correlation coefficient values, there are similar findings as well. Garami *et al*. study explained the relationship between the flame front location and previously mentioned process values by the process dynamics [20]. Comparing the results, our study has similar relationships between these measurements as well. This provides that our solution detects the same combustion phenomena. It needs to be noted that the Garami *et al*. measured the length of the flame front from the fuel feeding port compared to our study where it is compared to the end of the grate. This explains the opposite relationships in the results of this study.

It must be pointed out that the precise comparison to Garami *et al*. cross-correlation and lag results is impractical. Both studies process the signals differently before calculating the lag and correlation coefficients. Having to estimate ten-second intervals from the metadata of the videos affected our signal pre-processing and most likely the reported lag values. Similarly, moving average removes temporary fluctuations thus correlation is based on longer-term trends. The second highest deviation in the results comes from the camera installation and data collection. Our camera had to be installed to an inclined degree at the end of the grate that affects the perceived location of the flame front.

The grate boiler structure and instrumentation affect the results as well. Grate boiler dimensioning depends heavily on the usage of the power plant and the fuel. Even though the boilers would have a similar structure it does not mean that the instrumentation is identical. The instrumentation of the boiler is project-specific and differs plant by plant. The power plants sensors may be placed into different places even though they try to measure the same variable. Furthermore, even though the control loops are designed to achieve similar outcomes, the strategy and parameter tuning cause variations. Since the setups and operation are not identical, the differences in the reported values needs to recognised.

Based on the cross-correlation and Granger causality test results, the proposed system produces reliable information of the combustion and its relevant process parameters. The extracted area of the flame seems to provide the fastest information about the changes in the combustion while the flame front is the best in estimating other important process parameters. The detected phenomena by our proposed computer vision model's are

explained by the combustion process knowledge and dynamics. The data analysis results are in line with the previous studies. Additionally, the proposed method is the first of its kind, to our knowledge, where computer vision extracts combustion flame from the grate boiler. These findings confirm that our model provides additional information on the combustion process. It seems that the grate utility and control schemes can be optimised with the supplementary information that the model provides.

The Table 8.1 shows the main results between the extracted features and the state variables of the primary control loops which were available in our data set. For each state variable, the most correlating feature was selected to the table. The table contains the maximum lag values, cross-correlation coefficients and null hypothesis results for these signals. Based on these values, it seems that our method is reliably providing information from the main combustion characteristics.

Extracted feature	**Signal name**	m_{max}	$\hat{R}_{xy}$	**Reject H_0?**
Flame area	Flue gas O_2 content	325	-0.60	Yes
	Live steam flow	-176	0.59	Yes
	Thermal load	-185	0.59	No
	Flue gas CO content	529	-0.54	No
	Fuel feeding speed	11 131	-0.51	-
	Feedwater temperature	-6339	0.42	-
Minimum point	Primary air flow	135	0.71	Yes
	Secondary air flow	122	-0.62	Yes
	Chamber temperature	207	-0.58	Yes
	Live steam pressure	-68	-0.53	Yes
Y-intercept coefficient (b)	Live steam temperature	78	-0.48	Yes

Table 8.1. *Main data analysis results for the primary control loop state variables.*

The literature review found that the earlier studies follow the generic approach model, which is presented in the Figure 4.1, solving their computer vision tasks. Furthermore, the study noticed that many previous studies have applied the same algorithms, such as Otsu for segmentation, which have been proven to work in the previous studies. Based on these findings, the same approach method and algorithms was applied in the developed model as well which further strengthens their applicability for solving combustion diagnostics problems.

In addition to well-proven methods, the study discovered that some earlier studies have reported poor segmentation capabilities. To overcome these challenges, the literature

review found out that some state-of-the-art algorithms, as an example DBSCAN, provide better performance in some circumstances. To our knowledge, these methods had not been previously tested in combustion processes. Based on our visual examination, this method provided reliable information compared to other methods.

The developed model has some limitations. One of the situations where the flame front location and area are not detected accurately is illustrated in the Figure 8.8. The flue gasses circulate close to the rear wall blocking the visibility of the camera.

Figure 8.8. *Flue gasses intercepting camera vision.*

One can argue that the flame front is too far on the grate. Based on the surveys, the process operators try to keep the flame front at the fourth grate level and there should not be too much combustion happening at the last grate level. As seen in the figure, the combustion is partly occurring at the fifth grate level. Comparing to the Figure 6.1 there is a clear difference in the image quality and combustion itself. The expanding flame front and its disturbance to the detect features are seen from the trend figures as well where the largest peaks and troughs are like in the Figure 6.9.

Even though the flue gasses prohibit the accurate recognition of the flame front and flame area, our proposed method detects the flame front moving towards the last grate level as seen from the trend lines. It is possible to develop that the model provides alarms to process operators to take corrective actions before the combustion spreads too far. Another solution would be to detect flame front with MWIR camera which image quality is not affected by the flue gasses and flame. However, these aspects should be researched

further before drawing exact conclusions.

There are some limitations in this study that needs to be recognised when reviewing the results of the quantitative research. The collected research material limits the depth of the study. Due to the schedule of our measurement campaign, we could not collect long-duration video material from each imaging location thus the study had to base the analysis on the available data. Furthermore, the measurement equipment and applied configurations need to be taken into account when considering the reliability and validity of the data collection.

The collected data set from the power plant limits the study. The data set did not include every available process measurement in our data collection. Bias from our judgemental sampling affects how comprehensive the data set is and therefore the depth of the data analysis as well. Sampling rate and data prepossessing methods have also affected the data set and the results.

The developed application had to be developed under several limitations. One of them was the size of the video material that was utilised to develop and verify the model. The thorough robustness of the model is hard to evaluate since we covered only a small amount of boiler operation conditions during the measurement campaign. The second concerns the boundary conditions of the software. The developed application was optimised for the Valmet imaging systems while some of the proposed parameters of the model were tuned particularly for the specific grate boiler environment. Based on our analysis, we do not know how well our model performs in the other grate boilers, in the other view angles position or with other parameter tuning.

8.2 Process state variables

Based on our findings, the important process state variables of the grate boiler power plant are live steam pressure and temperature, feedwater volume, combustion power, furnace chamber pressure and electric power. According to the surveys and literature review, combustion power has the highest impact on the process. Combustion power state variables depend on the model representation as Nielsen *et al.* [31] argued.

Based on our findings, fuel particle size, calorific value, conductivity, moisture content, mass flow rate, airflow rate, temperature and heat transfer coefficients are important state variables modelling stoichiometric reactions of the combustion. As shown in Section 2.2, many factors contribute to the combustion reactions. These variables and thermodynamical equations allow to build an accurate model.

Creating an applicable model with all the state variables is impractical for a couple of reasons. The first one is about the complexity and computational requirements of the model. The literature review found out that these models are resource-intensive and

practically infeasible for real-time controllers. The second issue comes from the data collection. Measuring all these state variables accurately cannot be achieved without expensive instrumentation.

Approximation of the formerly described state variables is possible from the easier measurable variables. The more data is collected from the process the more accurate state representation is created. This statement is supported by Kadlec *et al.* [48] and Ballester and García-Armingol [49] studies.

Based on our findings, the conventional state variables from combustion power are primary and secondary air flow, grate movement speed, flue gas O_2 content, combustion chamber temperature and pressure. Both surveys and literature review indicate that these variables are important for combustion control purposes. Based on our literature review, some of the state-of-the-art models apply additional measurements, such as fuel quality, flame location, bed inventory and bed temperatures like Strobel *et al.* [21] and Martin *et al.* [22] studies show.

It must be noted that the other state variables are also important for the power plant. The power plant cannot for example produce electricity or heat without the live steam and feedwater. However, our study presents that these state variables are well-known or they are estimated reliably. The study does not claim that there are no room for improvements for these variables but based on our findings, the highest impact on the power plant's efficiency is achieved by making a more accurate state representation of the combustion and control it. Both literature review and surveys support this statement.

8.3 Combustion characteristics

Combustion characteristics that are automatically detectable from the video feed recognised in the study are divided into geometric, radiation, physico-chemical and fluid mechanics types as shown in the Table 3.1. Both literature review and surveys support this finding. This is not a remarkable finding since these characteristics have been proven to affect the combustion conditions as found out in the literature review. However, it is worth noting that the power plant specialists were concerned about each of the parameter types. Evaluating surveys shows that the respondents of the surveys are aware of the combustion characteristic, how they affect the process and address that they should be monitored. This opens the possibility of computer vision-based control and monitoring applications.

Based on our findings, the flame area, shape and position are the most interesting characteristics from the geometrical parameters. Our data analysis and the literature review support this. From the flame position, the grate boiler specialists were mostly concerned with the flame front and they actively try to control its location. Flame front location seems

to contain essential information about the combustion and the control loops can utilise that information as Strobel *et al*. [21] showed. Furthermore, our data analysis showed the correlation between the flame area and process measurements. Based on our literature review, there are no earlier studies about the area of the flame in the grate boilers but it has been shown to be an important parameter in the other combustion processes like Fleury *et al*. [57] found out. This together with our data analysis findings seems to prove that the flame area is an important combustion characteristic that should be either controlled or monitored. The proposed method for measuring both quantities is explained in Chapter 6.

Combustion uniformity and process changes are monitorable from the flame intensity. Both surveys and literature review support this. Process operators were interested in observing the intensity of the flame between the grate lines. The literature review found out that the colour of the flame provides information about the combustion like Szatvanyi *et al*. [62] demonstrated. Measuring intensity is easy since the camera imaging sensor provides it automatically. Intensity provides measurable parameters, such as luminous area, uniformity or centroid of the flame like Wang *et al*. [12] and Li *et al*. [58] showed. However, what exact variables to measure depends on the wanted outcome and needs to be decided based on the requirements of the application.

Results show that the temperature is measurable from many spots. Judging from the number of the recurring locations in the surveys, the most suitable location would be from the end of the grate or above the bed. This location provides the largest field of vision to the combustion. Likewise, this provides detection of the local hot spots or combustion symmetry. Another consideration is at the beginning of the grate but this would require a separate camera. It was also left unclear how much additional benefit this would bring to the combustion monitoring since all the respondents did not mention this location.

Based on the literature review, the temperature is measurable directly from the video feed or with an external probe. The literature review found that Wien's approximation of the Planck formula was the most adopted approach for creating 2D temperature maps straight from the video feed. This seems to be a promising technique for real-time measurements but the accuracy and complexity of the measurement needs to be considered. Jiang *et al*. [63] demonstrated that the measurement accuracy of this method is not as accurate as of the thermal probe while Sun *et al*. [10] showed that the temperature readings are highly influenced by the camera calibrations. Depending on the requirements of the application these things need to be addressed. However, there are studies, such as Smart *et al*. [18] where image-based temperature measurements have shown to be practically viable.

Optical flow techniques can estimate flame motion and mixing of the air. Our literature review showed that flame flow movement is possible from MWIR video feed with optical flow techniques, such as Toth *et al*. [28] study. Considering from this perspective, there is

possible potential to measure this variable but more research from the topic is required.

An important finding of the study was the automatic recognition of the unburned material. Managers and process operators of the surveys mentioned many times that unburned materials cause issues in the grate and ash hopper. Even though unburned material moving to the hopper is not directly related to the combustion they have a role in the power plant's continuous operation as discussed in the surveys. Minimising the unplanned shutdowns of the power plant caused by the clogged ash hopper helps to improve the power plant's operability and output. Here automatic detection of the big objects helps process operators in decision making. The video feed provides essential information both to control systems and human operators like Ballester and García-Armingol [49] argued.

Our literature review did not find earlier studies where computer vision has been directly utilised for detecting unburned material purposes but this does not mean that it would be impossible. Object detection is a classical computer vision technique that is usable in this case. Detection is possible with segmentation algorithms tuned for solid objects, such as active contours as Marques and Jorge [56] discussed. Another solution would be to monitor flame boundaries. If there is some big unburning object in the grate, the flame boundaries warp around the object. Comparing flame boundaries to the reference lines is one way to approximate big objects moving through the grate. There are many methods to achieve flame boundary detection as discussed in Subsections 4.1.3 and 4.1.4.

The qualitative side of the study needs to be considered when evaluating the results. The study used surveys which affected the reliability of the results. Questionnaire layout and design are influenced by the researcher's subjective viewpoints and experience. This can restrict the covered topics or emphasise some too much. Another point is the sample size. Surveys were collected with discretionary sampling where the researcher's judgement influence the reliability. The sample size was relatively small and presents only the opinions of few people. It did not contain the opinions of every target audience who work with the grate boilers, such as boiler manufacturers. Likewise, we need to consider respondents subjective biases, such as background, expertise, motive and honesty when considering the accuracy and generalisability of the results.

This study qualitative analysis is prone to subjective biases. Content analysis requires analysing the underlying meaning and semantic relationships between the words which are influenced by the researcher's subjective interpretation. Even though we reflected survey findings to our literature review the quality and reliability of the analysis are dependable on the original data set and self-reported conclusions. Nevertheless, it needs to be reminded that the scope of the thesis was to identify new development ideas rather than drawing general conclusions that hold in every situation. Judging from this aspect, the study was able to identify new perspectives, provide concrete examples of combustion characteristics and demonstrate how they are measurable.

9. CONCLUSION

The main objective of this study was to develop a computer vision-based soft sensor that automatically determines flame front and area from the video feed taken from the combustion chamber of the grate boiler. The second objective of the study was to examine what other combustion characteristics a visible or infrared light camera can measure. This chapter summarises and reflects on the study. The first section provides answers to the research questions. The second section evaluates the scientific contribution and significance of the study. The final section discusses future research opportunities.

9.1 Main findings

The first research question was *which process state variables are important in grate boiler control systems?* According to the results, the most important state variables are related to modelling combustion. The identified variables are focused on representing the fuel quality or the physical and chemical reactions of the combustion. These variables are important since they help to build a more accurate state representation for control purposes. Based on the results, the other state models and their control loops have an effect on the overall functionality of the grate boiler. However, the highest impact for efficiency is achieved by improving the combustion state representation and controls.

The next research question was *which combustion characteristics can be detected from the video that can be integrated to automation systems?* According to the findings, the detectable characteristics with cameras include flame geometrical parameters, such as position, shape and motion; radiational, such as flame intensity and brightness; temperature and big unburned material. These characteristics are the ones that the control systems utilise or process specialists actively monitor from combustion. Therefore, the most potential benefits are in improving tools for monitoring and control combustion with these measurements. The process specialists and control applications both benefit from the additional information camera systems provide. Process operators would gain new ways to monitor the process more efficiently with added features, such as automatic alarms or easily interpretable numerical values, while more advanced control strategies can be developed based on the extracted data. These would assist grate boiler operators to discover solutions for their combustion issues and find optimal combustion conditions.

Therefore, the focus should be on these factors when analysing the research and development requirements of the camera systems.

The third research question was *how process variables can be measured automatically using infrared or visible light cameras?* The study found out that formerly described variables are possible to detect with computer vision. Depending on the characteristic, the study describes various methods how to measure them. It was found out that not all formerly described characteristic has been previously measured in grate boilers. However, the literature review discovered well-known and applied approaches in other combustion processes that are applicable in grate combustion. The study analysed a general approach model that helps systematically to build computer vision applications in combustion processes. Based on the literature review, some of the approaches and characteristics, such as flame front position, have been proven to be useful in the grate boiler environment while some, such as the movement of the combustion flame, have not yet been verified in this environment. The study provided a model to measure the area of the combustion flame and proved with data analysis that it is an important characteristic to measure from the grate combustion.

The final research question was *how to determine flame front and area with computer vision?* Chapter 6 describes the data-driven computer vision model that determines the flame features from the video feed. The model was evaluated against the process data that provided insight into the model with promising results. The results demonstrate that the model produces important information on combustion. The model correlates well with process measurements and predicts their changes. The area of the flame correlated the most with flue gas O_2 content while flame front location correlated with air flows and combustion chamber temperature. This information can be used for control and diagnostic purposes. Prior research supports our results. In addition, the model utilises some state-of-the-art approaches which have not been applied in combustion process applications. These methods overcome some of the problems reported in the earlier studies. Therefore, the study implemented both an academically and practically feasible data-driven soft sensor.

The results of the study and proposed model are somewhat applicable in grate combustion and camera systems. However, a couple of limitations needs to be addressed that affect the generalisability of the results. The first limitation of the study comes from the applied research method that was a single case study. The collected data and results are reflected on data available from only one power plant thus the conclusions cannot be fully generalised to other contexts. To gain broader insight and new knowledge of researched phenomenon studies with larger sample sizes are required.

In the data analysis phase, applied data analysis methods were limited for the model evaluation. The study analysed data with a couple of regression and time series analysis

tools but other factors need to be considered. The performance of the model, accuracy and computational complexity are just some of the examples that need to be taken into account when analysing the usefulness of the proposed approach in the real-life environment. These were out of the thesis scope but something that should be considered when evaluating the results in the other contexts.

As for the final limitation, the number of earlier studies from the topic needs to be addressed. Evaluating computer vision applications in combustion processes is a large topic but there are not many studies focusing on grate boiler environments. By taking into account every combustion process, the domain-specific information of the grate boiler is lost which influences the results. More detailed information is attainable by focusing on the scope of the study.

9.2 Contributions and implications

This study has both practical and scientific significance. The study assists Valmet to evaluate research and development requirements for their imaging systems based on the real-life challenges that an industrial grate boiler is facing. Furthermore, the study presented an objective and systematic review of the state-of-the-art control and monitoring computer vision applications. The study demonstrated the usefulness of the measured flame characteristic through data analysis and process knowledge. Managers and specialists working with grate boilers can adopt the results of the thesis to evaluate technological opportunities and complement their understanding of the combustion process.

The study supplements computer vision research in a combustion environment. The study investigated some of the modern computer vision methods that had been proven successful in other contexts and applied them in the model. Some prior studies present black-box models that are difficult to analyse. Our model is introduced as the white-box model that is explained openly and development choices are demonstrated distinctly. The model is easily interpretable and allows transparent analysis of the model which allows further development of the model if required. Likewise, the study demonstrated the practicality of the model which is an important part of assessing the feasibility of the research.

The proposed model makes a useful contribution to the grate boilers. The model can be extended to other grate boilers, such as biomass boilers or boilers with different structures. The combustion characteristics are likely relatively similar in these processes. Furthermore, retrofitting the proposed method to the combustion chamber that has a camera installed is possible. The system costs are reasonably low since the development was done with open-source libraries and a common office laptop that does not have high computational power. This would facilitate grate boiler operators to gain new monitoring tools for the combustion process. Given the supplementary information of the combus-

tion parameters the model provides, the results suggest that the proposed system can be utilised in advanced process controls to provide more efficient combustion. This would presumably help power plants to achieve higher productivity with lower emissions.

This research further strengthens the grate combustion research. State variables, measurable combustion characteristics and computer vision models have been researched previously and the results of the study support these findings well. Moreover, the study reinforces earlier studies since a case study helps to examine new viewpoints and increase the practical usefulness of the research. The study provides contemporary and useful insight into the research phenomena from the grate boiler and WTE point of view. The study demonstrates a comprehensive evaluation between the combustion parameters and computer vision model, which findings are explained through the process dynamics. The study showed a relationship between the measured characteristics and process measurements which is helpful in evaluating the performance of the combustion. Based on the literature review and knowledge, no earlier studies have conducted Granger causality analysis or evaluated flame area from the grate combustion with computer vision. This increases the significance of the study. The results support the earlier research about stoichiometric reactions the findings bring deeper insight about the process.

9.3 Future research

We identified a set of research topics that can be investigated in the future. The first subject is to integrate the developed computer vision soft sensor into automation systems. Based on the findings, the model produces data that is utilisable in the control loops for improving controllability or in monitoring systems for providing better insight for the process operators. As Ballester and García-Armingol [49] discussed, more research is required to find practical applications and usefulness for the systems. One possibility would be to integrate the model to Nielsen *et al.* [31] proposed control strategy and evaluate the gained benefits.

Another future research topic would be to do more extensive data analysis. The study showed that there is some relationship between the flame front and area to conventional process measurements. However, the usefulness of the model through data exploitation is something that should be further researched to enrich the conclusions. As an example, studies could focus to research relationships and operation conditions of the characteristics with more extensive video material and process data. Furthermore, it is possible to research influence between these variables with factor analysis, to name a few future approaches. This would help to develop advanced control and monitoring applications for more efficient energy production by understanding grate combustion more thoroughly.

The study and its findings provide an opportunity for studies with larger samples. Ideas and topics addressed in the study should be investigated with a wider sample to gain

a broader overview of the research phenomena. On the one hand, future studies can include surveys with more power plant operators, grate boiler manufacturers, process controllers and other specialists who work with grate boilers. On the other hand, the proposed model can be tested in other grate boilers using different fuel mixes or operating conditions, to name a few. These approaches would help to deepen the understanding of the research phenomena and combine practical data.

The next research opportunity includes conducting market research. Earlier studies have concentrated more on the technological aspects and the maturity level of the technology has been proven. At the same time, there are little to no earlier studies where the computer vision for combustion diagnostics have been researched from the business perspectives of the companies. Development cost, payback time, consumer interest, product differentiation, usability and system integration are just some of the aspects that should be researched when evaluating computer vision-based applications and gained benefits from the technology supplier's perspective which Valmet represents. Market research helps to evaluate grate boiler challenges from a larger perspective.

As for the final identified research opportunity, future research can concentrate on camera technologies. We limited our computer vision development to the visual light camera due to resource constraints but we believe that the model is adaptable to the infrared camera too. Furthermore, there would be research interest to analyse infrared cameras even further. Because an infrared camera sees the waste pile of the bed through the flame, there is a possibility that it is detectable from the image. This gives essential information about the combustion. Another topic includes investigating mobile cameras as an inspection tool. As the measurement campaign showed, there is some use for the mobile camera as an inspection tool. A camera assists monitoring boiler lifetime and components during its operation. This information helps to evaluate maintenance needs but more research is required.

REFERENCES

[1] Neuwahl, F., Cusano, G., Gómez Benavides, J., Holbrook, S. and Roudier, S. Best Available Techniques (BAT) reference document for waste incineration: Industrial Emissions Directive 2010/75/EU (Integrated Pollution Prevention and Control). eng. EUR 29971 (2019). ISSN: 1831-9424. URL: https://publications.jrc.ec.europa.eu/repository/handle/JRC118637 (visited on Jan. 4, 2021).

[2] Vesanto, P., Ruonala, S. and Nuutila, M. *Jätteenpolton parhaan käytettävissä olevan tekniikan (BAT) vertailuasiakirjan käyttö suomalaisessa toimintaympäristössä. Jätteenpolton BREF 2006*. fin. Suomen ympäristökeskus, 2006. ISBN: 952-11-2309-5. URL: https://helda.helsinki.fi/bitstream/handle/10138/38712/SY_27_2006.pdf (visited on Feb. 20, 2021).

[3] Lombardi, L., Carnevale, E. and Corti, A. A review of technologies and performances of thermal treatment systems for energy recovery from waste. eng. *Waste management (Elmsford)* 37 (2015), pp. 26–44. ISSN: 0956-053X. URL: https://www.sciencedirect.com/science/article/pii/S0956053X14005273 (visited on Jan. 4, 2021).

[4] Patel, C., Lettieri, P. and Germanà, A. Techno-economic performance analysis and environmental impact assessment of small to medium scale SRF combustion plants for energy production in the UK. eng. *Process safety and environmental protection* 90.3 (2012), pp. 255–262. ISSN: 0957-5820. URL: https://www.sciencedirect.com/science/article/pii/S0957582011000607 (visited on Mar. 14, 2021).

[5] Yin, C., Rosendahl, L. A. and Kær, S. K. Grate-firing of biomass for heat and power production. eng. *Progress in energy and combustion science* 34.6 (2008), pp. 725–754. ISSN: 0360-1285. URL: https://www.sciencedirect.com/science/article/pii/S0360128508000245 (visited on Jan. 30, 2021).

[6] Rosendahl, L. *Biomass combustion science, technology and engineering*. eng. 1st edition. Woodhead Publishing series in energy, number 40. Cambridge, UK: Woodhead Publishing Limited, 2013. ISBN: 0-85709-743-1. URL: https://ebookcentral.proquest.com/lib/tampere/detail.action?pq-origsite=primo&docID=1574947 (visited on Mar. 12, 2021).

[7] Fodor, Z. and Klemeš, J. J. Waste as alternative fuel – Minimising emissions and effluents by advanced design. eng. *Process safety and environmental protection* 90.3 (2012), pp. 263–284. ISSN: 0957-5820. URL: https://www.sciencedirect.

com/science/article/pii/S0957582011000991#bib0340 (visited on Apr. 14, 2021).

[8] Mikus, M., Dziedzic, K. and Jurczyk, M. FLUE GAS CLEANING IN MUNICIPAL WASTE-TO-ENERGY PLANTS – PART I. *INFRASTRUCTURE AND ECOLOGY OF RURAL AREAS* IV (Oct. 2016), pp. 1179–1193. DOI: 10.14597/infraeco.2016.4.1.086. URL: https://www.researchgate.net/publication/313846308_FLUE_GAS_CLEANING_IN_MUNICIPAL_WASTE-TO-ENERGY_PLANTS_-_PART_I (visited on Jan. 4, 2021).

[9] Munir, S., Nimmo, W. and Gibbs, B. The effect of air staged, co-combustion of pulverised coal and biomass blends on NOx emissions and combustion efficiency. eng. *Fuel (Guildford)* 90.1 (2011), pp. 126–135. ISSN: 0016-2361. URL: https://www.sciencedirect.com/science/article/pii/S0016236110004114 (visited on Mar. 14, 2021).

[10] Sun, D., Lu, G., Zhou, H. and Yan, Y. Flame stability monitoring and characterization through digital imaging and spectral analysis. eng. *Measurement science & technology* 22.11 (2011), pp. 114007–. ISSN: 0957-0233. URL: https://iopscience.iop.org/article/10.1088/0957-0233/22/11/114007 (visited on Jan. 10, 2021).

[11] Beér, J. Combustion technology developments in power generation in response to environmental challenges. eng. *Progress in energy and combustion science* 26.4 (2000), pp. 301–327. ISSN: 0360-1285. URL: https://www.sciencedirect.com/science/article/pii/S0360128500000071 (visited on Mar. 14, 2021).

[12] Wang, Y., Yu, Y., Zhu, X. and Zhang, Z. Pattern recognition for measuring the flame stability of gas-fired combustion based on the image processing technology. *Fuel* 270 (2020), p. 117486. ISSN: 0016-2361. DOI: https://doi.org/10.1016/j.fuel.2020.117486. URL: http://www.sciencedirect.com/science/article/pii/S0016236120304816 (visited on Jan. 10, 2021).

[13] Lu, G., Gilabert, G. and Yan, Y. Vision based monitoring and characterisation of combustion flames. eng. *Journal of physics. Conference series* 15.1 (2005), pp. 194–200. ISSN: 1742-6596.

[14] Zhou, H., Tang, Q., Yang, L., Yan, Y., Lu, G. and Cen, K. Support vector machine based online coal identification through advanced flame monitoring. eng. *Fuel (Guildford)* 117 (2014), pp. 944–951. ISSN: 0016-2361. URL: https://www.sciencedirect.com/science/article/pii/S0016236113009824 (visited on Jan. 14, 2021).

[15] Huang, Y., Yan, Y. and Riley, G. Vision-based measurement of temperature distribution in a 500-kW model furnace using the two-colour method. eng. *Measurement : journal of the International Measurement Confederation* 28.3 (2000), pp. 175–183. ISSN: 0263-2241. URL: https://www.sciencedirect.com/science/article/pii/S0263224100000105#BIB1 (visited on Jan. 12, 2021).

[16] Tanaś, J. and Kotyra, A. Application of optical flow algorithms and flame image sequences analysis in combustion process diagnostics. eng. *Photonics Applications in Astronomy, Communications, Industry, and High-Energy Physics Experiments*. Vol. 10031. SPIE, 2016, pp. 1003151-1003151–6. ISBN: 9781510604858.

[17] Chen, J., Chan, L. L. T. and Cheng, Y.-C. Gaussian process regression based optimal design of combustion systems using flame images. eng. *Applied energy* 111 (2013), pp. 153–160. ISSN: 0306-2619. URL: https://www.sciencedirect.com/science/article/pii/S0306261913003310 (visited on Jan. 11, 2021).

[18] Smart, J., Lu, G., Yan, Y. and Riley, G. Characterisation of an oxy-coal flame through digital imaging. eng. *Combustion and flame* 157.6 (2010), pp. 1132–1139. ISSN: 0010-2180. URL: https://www.sciencedirect.com/science/article/pii/S0010218009003095 (visited on Jan. 12, 2021).

[19] Tóth, P., Garami, A. and Csordás, B. Image-based deep neural network prediction of the heat output of a step-grate biomass boiler. eng. *Applied energy* 200 (2017), pp. 155–169. ISSN: 0306-2619. URL: https://www.sciencedirect.com/science/article/pii/S0306261917305822 (visited on Jan. 10, 2021).

[20] Garami, A., Csordás, B., Palotás, Á. and Tóth, P. Reaction zone monitoring in biomass combustion. eng. *Control engineering practice* 74 (2018), pp. 95–106. ISSN: 0967-0661. URL: https://www.sciencedirect.com/science/article/pii/S096706611830025X (visited on Jan. 10, 2021).

[21] Strobel, R., Waldner, M. H. and Gablinger, H. Highly efficient combustion with low excess air in a modern energy-from-waste (EfW) plant. eng. *Waste management (Elmsford)* 73 (2018), pp. 301–306. ISSN: 0956-053X. URL: https://www.sciencedirect.com/science/article/pii/S0956053X17304907 (visited on Mar. 17, 2021).

[22] Martin, J. J., Koralewska, R. and Wohlleben, A. Advanced solutions in combustion-based WtE technologies. eng. *Waste management (Elmsford)* 37 (2015), pp. 147–156. ISSN: 0956-053X. URL: https://www.sciencedirect.com/science/article/pii/S0956053X1400381X#s0020 (visited on Apr. 15, 2021).

[23] Cui, F., Ji, S. and Xu, Q. Design of Flame End Points Detection System for Refuse Incineration Based on ARM and DSP. eng. *Wireless Communications, Networking and Applications*. Lecture Notes in Electrical Engineering. New Delhi: Springer India, 2015, pp. 1243–1253. ISBN: 9788132225799. URL: https://link.springer.com/chapter/10.1007%2F978-81-322-2580-5_113#enumeration (visited on Jan. 9, 2021).

[24] Fleury, A., Trigo, F., Pacífico, A. and Martins, F. An inference model for combustion diagnostics in an experimental oil furnace. eng. *Expert systems* 35.2 (2018), e12245–n/a. ISSN: 0266-4720. URL: https://onlinelibrary.wiley.com/doi/full/10.1111/exsy.12245 (visited on Jan. 11, 2021).

[25] Allen, M., Butler, C., Johnson, S., Lo, E. and Russo, F. An imaging neural network combustion control system for utility boiler applications. *Combustion and Flame* 94.1 (1993), pp. 205–214. ISSN: 0010-2180. DOI: https://doi.org/10.1016/0010-2180(93)90031-W. URL: http://www.sciencedirect.com/science/article/pii/001021809390031W (visited on Jan. 14, 2021).

[26] Chen, J., Chang, Y.-H., Cheng, Y.-C. and Hsu, C.-K. Design of image-based control loops for industrial combustion processes. eng. *Applied energy* 94 (2012), pp. 13–21. ISSN: 0306-2619. URL: https://www.sciencedirect.com/science/article/pii/S0306261911008865 (visited on Jan. 10, 2021).

[27] Zhang, R., Cheng, S. and Guo, C. Detection Method for Pulverized Coal Injection and Particles in the Tuyere Raceway Using Image Processing. eng. *ISIJ international* 58.2 (2018), pp. 244–252. ISSN: 0915-1559. URL: https://www.jstage.jst.go.jp/article/isijinternational/58/2/58_ISIJINT-2017-433/_html/-char/en (visited on Jan. 19, 2021).

[28] Toth, P., Zhan, Z., Fu, Z., Palotas, A. B., Eddings, E. G. and Ring, T. A. The potential of on-line optical flow measurement in the control and monitoring of pilot-scale oxy-coal flames. eng. *Experiments in fluids* 55.5 (2014), pp. 1–13. ISSN: 0723-4864. URL: https://link-springer-com.libproxy.tuni.fi/article/10.1007/s00348-014-1727-3 (visited on Apr. 27, 2021).

[29] *Valmet. About us - Valmet in brief*. URL: https://www.valmet.com/about-us/valmet-in-brief/ (visited on Sept. 3, 2021).

[30] *Valmet. Boiler Diagnostic Systems*. Jan. 14, 2021. URL: https://www.valmet.com/automation/analyzers-measurements/boiler-diagnostics (visited on Jan. 14, 2021).

[31] Nielsen, R., Vinther, K., Rundvik, H., Ekstedt, E., Windahl, J. and Velut, S. *Grate boiler modelling for soft sensor based control*. .Final report of project P43455-1 of Swedish Energy Agency. 2018:490. Stockholm, Sweden: Energiforsk, Oct. 2018. ISBN: 978-91-7673-490-2. URL: https://energiforsk.se/program/branslebaserad-el-och-varmeproduktion-sebra/rapporter/grate-boiler-modeling-for-soft-sensor-based-control-2018-490/ (visited on Apr. 15, 2021).

[32] Umweltbundesamt. Draft of a German Report for the creation of a BREF document "waste incineration". (2001). URL: http://files.gamta.lt/aaa/Tipk/tipk/4_kiti%20GPGB/63.pdf (visited on Jan. 4, 2021).

[33] Castaldi, M. and Klinghoffer, N. *Waste to Energy Conversion Technology*. eng. 2013, pp. 3–14. ISBN: 0857096362. URL: https://ebookcentral.proquest.com/lib/tampere/detail.action?pq-origsite=primo&docID=1574937 (visited on Jan. 4, 2021).

[34] Vakkilainen, E. *Fluidized Bed Boilers for Biomass*. eng. 2017. URL: https://ebookcentral.proquest.com/lib/tampere/detail.action?pq-origsite=primo&docID=4696959 (visited on Jan. 5, 2021).

[35] Ragland, K. W. and Bryden, K. M. *Combustion Engineering*. eng. Bosa Roca: Taylor & Francis Group, 2011. ISBN: 9781420092509. URL: https://ebookcentral.proquest.com/lib/tampere/detail.action?docID=1446577 (visited on Jan. 7, 2021).

[36] Raiko, R. *Poltto ja palaminen*. fin. 2nd ed. Helsinki: Teknillistieteelliset akatemiat, 2002. ISBN: 951-666-604-3.

[37] Huhtinen, M. *Höyrykattilatekniikka*. fin. 5th ed. Helsinki: Edita, 2000. ISBN: 951-37-3360-2.

[38] Rayaprolu, K. *Boilers: A Practical Reference*. eng. Baton Rouge: CRC Press, 2013. ISBN: 1466500530. URL: https://www.taylorfrancis.com/books/mono/10.1201/b12977/boilers-kumar-rayaprolu (visited on Jan. 7, 2021).

[39] Paces, N. and Kozek, M. Modeling of a grate-firing biomass furnace for real-time application. eng. *IMCIC 2011 - 2nd International Multi-Conference on Complexity, Informatics and Cybernetics, Proceedings*. Vol. 1. 2011, pp. 357–362. ISBN: 9781936338207. URL: https://www.researchgate.net/publication/266490889_Modeling_of_a_Grate-Firing_Biomass_Furnace_for_Real-Time_Application (visited on Feb. 24, 2021).

[40] Vilenius, S. M. *Arinakattilan hyötysuhteen määritys jätteen energiahyödyntämisessä*. fin. Kemian ja biotekniikan laitos - Department of Chemistry and Bioengineering, 2015. URL: https://trepo.tuni.fi/bitstream/handle/123456789/22818/Vilenius.pdf (visited on Feb. 21, 2021).

[41] Sarkar, D. K. *Thermal power plant : design and operation*. eng. Amsterdam: Elsevier, 2015. ISBN: 9780128017555. URL: https://ebookcentral.proquest.com/lib/tampere/reader.action?docID=2193598 (visited on Mar. 11, 2021).

[42] Joronen, T., Majanne, Y. and Kovács, J. *Voimalaitosautomaatio*. fin. SAS julkaisusarja, 33. Helsinki: Suomen automaatioseura, 2007. ISBN: 978-952-5183-32-0.

[43] Milovanović, Z. N., Dumonjić-Milovanović, S. R., Milašinović, A. N. and Knežević, D. M. Efficiency of operation of 300 mw condensing thermal power blocks with supercritical steam parameters in sliding pressure mode. eng. *Thermal science* 22.Suppl. 5 (2018), S1371–S1382. ISSN: 0354-9836. URL: https://www.sciencedirect.com/science/article/pii/S0956053X17304907 (visited on Mar. 15, 2021).

[44] Seeber, R., Gölles, M., Dourdoumas, N. and Horn, M. Reference shaping for model-based control of biomass grate boilers. eng. *Control engineering practice* 82 (2019), pp. 173–184. ISSN: 0967-0661. URL: https://www.sciencedirect.com/science/article/pii/S0967066118306373 (visited on Apr. 11, 2021).

[45] Bauer, R., Gölles, M., Brunner, T., Dourdoumas, N. and Obernberger, I. Modelling of grate combustion in a medium scale biomass furnace for control purposes. eng. *Biomass & bioenergy* 34.4 (2010), pp. 417–427. ISSN: 0961-9534. URL: https://www.sciencedirect.com/science/article/pii/S096195340900244X (visited on Apr. 12, 2021).

[46] Miljković, B., Pešenjanski, I. and Vićević, M. Mathematical modelling of straw combustion in a moving bed combustor: A two dimensional approach. eng. *Fuel (Guildford)* 104 (2013), pp. 351–364. ISSN: 0016-2361. URL: https://www.sciencedirect.com/science/article/pii/S0016236112006539 (visited on Apr. 12, 2021).

[47] Kortela, J. and Jämsä-Jounela, S.-L. Fuel-quality soft sensor using the dynamic superheater model for control strategy improvement of the BioPower 5 CHP plant. eng. *International journal of electrical power & energy systems* 42.1 (2012), pp. 38–48. ISSN: 0142-0615. URL: https://www.sciencedirect.com/science/article/pii/S0142061512000567 (visited on Apr. 13, 2021).

[48] Kadlec, P., Gabrys, B. and Strandt, S. Data-driven Soft Sensors in the process industry. eng. *Computers & chemical engineering* 33.4 (2009), pp. 795–814. ISSN: 0098-1354. URL: https://www.sciencedirect.com/science/article/pii/S0098135409000076 (visited on Apr. 11, 2021).

[49] Ballester, J. and García-Armingol, T. Diagnostic techniques for the monitoring and control of practical flames. eng. *Progress in energy and combustion science* 36.4 (2010), pp. 375–411. ISSN: 0360-1285. URL: https://www.sciencedirect.com/science/article/pii/S0360128509000689 (visited on Jan. 9, 2021).

[50] Shang, C., Yang, F., Huang, D. and Lyu, W. Data-driven soft sensor development based on deep learning technique. eng. *Journal of process control* 24.3 (2014), pp. 223–233. ISSN: 0959-1524. URL: https://www.sciencedirect.com/science/article/pii/S0959152414000365 (visited on Apr. 13, 2021).

[51] Lin, B. and Jørgensen, S. B. Soft sensor design by multivariate fusion of image features and process measurements. eng. *Journal of process control* 21.4 (2011), pp. 547–553. ISSN: 0959-1524. URL: https://www.sciencedirect.com/science/article/pii/S0959152411000096 (visited on Jan. 14, 2021).

[52] Matthes, J., Waibel, P. and Keller, H. Detection of empty grate regions in firing processes using infrared cameras. June 2012. DOI: 10.21611/qirt.2012.210. URL: https://www.researchgate.net/publication/268201856_Detection_of_empty_grate_regions_in_firing_processes_using_infrared_cameras (visited on Jan. 13, 2021).

[53] Pappa, N., Kumar, K. S., Nambi, U. S. and Sujatha, K. Monitoring Power Station Boilers Using ANN and Image Processing. eng. *Advanced materials research*. Vol. 631-632. 2013, pp. 1154–1159. ISBN: 9783037855874.

[54] Hernández, R. and Ballester, J. Flame imaging as a diagnostic tool for industrial combustion. *Combustion and Flame* 155.3 (2008), pp. 509–528. ISSN: 0010-2180. DOI: https://doi.org/10.1016/j.combustflame.2008.06.010. URL: https://www.sciencedirect.com/science/article/pii/S0010218008001983 (visited on Jan. 10, 2021).

[55] Wu, Q. Computer image processing and neural network technology for boiler thermal energy diagnosis. eng. *Thermal science* 24.5 Part B (2020), pp. 3059–3068. ISSN: 0354-9836. URL: https://www.researchgate.net/publication/339544688_Computer_image_processing_and_neural_network_technology_for_boiler_thermal_energy_diagnosis (visited on Jan. 9, 2021).

[56] Marques, J. S. and Jorge, P. M. Visual inspection of a combustion process in a thermoelectric plant. eng. *Signal processing* 80.8 (2000), pp. 1577–1589. ISSN: 0165-1684. URL: https://www.sciencedirect.com/science/article/pii/S0165168400000578 (visited on Jan. 10, 2021).

[57] Fleury, A., Trigo, F. and Martins, F. A new approach based on computer vision and non-linear Kalman filtering to monitor the nebulization quality of oil flames. eng. *Expert systems with applications* 40.12 (2013), pp. 4760–4769. ISSN: 0957-4174. URL: https://www.sciencedirect.com/science/article/pii/S0957417413001243 (visited on Jan. 14, 2021).

[58] Li, W., Wang, D. and Chai, T. Burning state recognition of rotary kiln using ELMs with heterogeneous features. eng. *Neurocomputing (Amsterdam)* 102 (2013), pp. 144–153. ISSN: 0925-2312. URL: https://www.sciencedirect.com/science/article/pii/S0925231212004201 (visited on Jan. 14, 2021).

[59] Han, P., Zhang, X., Zhen, C. and Wang, B. Boiler Flame Image Classification Based on Hidden Markov Model. eng. *2006 IEEE International Symposium on Industrial Electronics*. Vol. 1. IEEE, 2006, pp. 575–578. ISBN: 9781424404964. URL: https://ieeexplore.ieee.org/document/4077991 (visited on Jan. 14, 2021).

[60] Zhen, C., Han, P. and Niu, Y. Research on image processing for furnace flame and reconstruct on temperature field. eng. *SMC'03 Conference Proceedings. 2003 IEEE International Conference on Systems, Man and Cybernetics. Conference Theme - System Security and Assurance (Cat. No.03CH37483)*. Vol. 1. IEEE, 2003, 678–683 vol.1. ISBN: 9780780379527. URL: https://ieeexplore.ieee.org/document/1243893 (visited on Jan. 9, 2019).

[61] Zhang, R., Cheng, Y., Li, Y., Zhou, D. and Cheng, S. Image-Based Flame Detection and Combustion Analysis for Blast Furnace Raceway. eng. *IEEE transactions on instrumentation and measurement* 68.4 (2019), pp. 1120–1131. ISSN: 0018-9456. URL: https://ieeexplore.ieee.org/document/8626147 (visited on Jan. 10, 2021).

[62] Szatvanyi, G., Duchesne, C. and Bartolacci, G. Multivariate Image Analysis of Flames for Product Quality and Combustion Control in Rotary Kilns. eng. *Industrial & engineering chemistry research* 45.13 (2006), pp. 4706–4715. ISSN: 0888-5885. URL: https://pubs.acs.org/doi/abs/10.1021/ie051336q (visited on Jan. 14, 2021).

[63] Jiang, Z.-W., Luo, Z.-X. and Zhou, H.-C. A simple measurement method of temperature and emissivity of coal-fired flames from visible radiation image and its application in a CFB boiler furnace. eng. *Fuel (Guildford)* 88.6 (2009), pp. 980–987. ISSN: 0016-2361. URL: https://www.sciencedirect.com/science/article/pii/S0016236108005206 (visited on Jan. 11, 2021).

[64] RUAO, M., COSTA, M. and CARVALHO, M. G. A NOx diagnostic system based on a spectral ultraviolet/visible imaging device. eng. *Fuel (Guildford)* 78.11 (1999), pp. 1283–1292. ISSN: 0016-2361. URL: https://www.sciencedirect.com/science/article/pii/S001623619900037X#BIB4 (visited on Jan. 10, 2021).

[65] Silva, R., Fleury, A., Martins, F., Ponge-Ferreira, W. and Trigo, F. Identification of the state-space dynamics of oil flames through computer vision and modal techniques. eng. *Expert systems with applications* 42.5 (2015), pp. 2421–2428. ISSN: 0957-4174. URL: https://www.sciencedirect.com/science/article/pii/S095741741400654X (visited on Jan. 14, 2021).

[66] Sawicki, D. Determining of combustion process state based on flame images analysis. eng. *Photonics Applications in Astronomy, Communications, Industry, and High-Energy Physics Experiments*. Vol. 10031. SPIE, 2016, 100311Y-100311Y–7. ISBN: 9781510604858.

[67] Bae, H., Kim, S., Wang, B.-H., Lee, M. H. and Harashima, F. Flame detection for the steam boiler using neural networks and image information in the Ulsan steam power generation plant. eng. *IEEE transactions on industrial electronics (1982)* 53.1 (2006), pp. 338–348. ISSN: 0278-0046. URL: https://ieeexplore.ieee.org/document/1589393 (visited on Jan. 10, 2021).

[68] Li, N., Lu, G., Li, X. and Yan, Y. Prediction of NOx Emissions from a Biomass Fired Combustion Process Based on Flame Radical Imaging and Deep Learning Techniques. eng. *Combustion science and technology* 188.2 (2016), pp. 233–246. ISSN: 0010-2202. URL: https://www.tandfonline.com/doi/full/10.1080/00102202.2015.1102905 (visited on Jan. 14, 2021).

[69] Chen, J., Hsu, T.-Y., Chen, C.-C. and Cheng, Y.-C. Monitoring combustion systems using HMM probabilistic reasoning in dynamic flame images. eng. *Applied energy*. Applied Energy 87.7 (2010), pp. 2169–2179. ISSN: 0306-2619. URL: https://www.sciencedirect.com/science/article/pii/S0306261909004954 (visited on Jan. 14, 2021).

[70] Szeliski, R. *Computer Vision Algorithms and Applications*. eng. 2nd ed. draft 2021. Texts in Computer Science. London: Springer, 2021. ISBN: 1-84882-935-3. URL: http://szeliski.org/Book/ (visited on Feb. 16, 2021).

[71] Pietikäinen, M. and Silvén, O. *Tekoälyn haasteet – koneoppimisesta ja konenäöstä tunnetekoälyyn*. fin. Center for Machine Vision and Signal Analysis (CMVS). Oulu: Oulun yliopisto, 2019. ISBN: 978-952-62-2482-4. URL: http://jultika.oulu.fi/Record/isbn978-952-62-2482-4 (visited on Feb. 16, 2021).

[72] Garami, A. and Tóth, P. Flame image processing and artificial intelligence as a diagnostic tool for industrial biomass combustion. English. *Materials Science and Engineering* 43.1 (2018). Copyright - Copyright University of Miskolc 2018; Last updated - 2020-03-11, pp. 31–41. ISSN: 2063-6792. URL: https://www.proquest.com/scholarly-journals/flame-image-processing-artificial-intelligence-as/docview/2375706486/se-2 (visited on Jan. 9, 2021).

[73] Sawicki, D. FLAME MONITORING USING IMAGE CLASSIFICATION. eng. *Informatics, Control, Measurement in Economy and Environment Protection* 6.1 (2016), pp. 37–40. ISSN: 2083-0157. URL: https://ph.pollub.pl/index.php/iapgos/article/view/1161/928 (visited on Jan. 11, 2021).

[74] Sbarbaro, D., Zawadsky, A. and Farias, O. Monitoring and characterization of combustion flames by generalized Hebbian learning. eng. *Proceedings of the 2002 International Joint Conference on Neural Networks. IJCNN'02 (Cat. No.02CH37290)*. Vol. 1. IEEE, 2002, 82–85 vol.1. ISBN: 9780780372788. URL: https://ieeexplore.ieee.org/document/1005447 (visited on Jan. 14, 2021).

[75] Otsu, N. A Threshold Selection Method from Gray-Level Histograms. eng. *IEEE transactions on systems, man, and cybernetics* 9.1 (1979), pp. 62–66. ISSN: 0018-9472. URL: https://ieeexplore.ieee.org/document/4310076 (visited on Mar. 23, 2021).

[76] Wu, Y., Song, Y. and Zhou, H. State identification of boiler combustion flame images based on gray entropy multiple thresholding and support vector machine. eng. *Zhōnggúo diànjī gōngchéng xúebào* 33.20 (2013), pp. 66–73. ISSN: 0258-8013.

[77] Shen, J., Hao, X., Liang, Z., Liu, Y., Wang, W. and Shao, L. Real-Time Superpixel Segmentation by DBSCAN Clustering Algorithm. eng. *IEEE transactions on image processing* 25.12 (2016), pp. 5933–5942. ISSN: 1057-7149. URL: https://ieeexplore.ieee.org/document/7588062 (visited on Apr. 11, 2021).

[78] Ester, M., Kriegel, H.-P., Sander, J. and Xu, X. A density-based algorithm for discovering clusters in large spatial databases with noise. *Proceedings of the Second International Conference on Knowledge Discovery and Data Mining*. AAAI Press, 1996, pp. 226–231. URL: https://citeseerx.ist.psu.edu/viewdoc/summary?doi=10.1.1.121.9220 (visited on Apr. 4, 2021).

[79] Grana, C., Borghesani, D. and Cucchiara, R. Optimized Block-Based Connected Components Labeling With Decision Trees. eng. *IEEE transactions on image processing* 19.6 (2010), pp. 1596–1609. ISSN: 1057-7149. URL: https://ieeexplore-ieee-org.libproxy.tuni.fi/document/5428863 (visited on May 14, 2021).

[80] WANG, F., WANG, X. J., MA, Z. Y., YAN, J. H., CHI, Y., WEI, C. Y., NI, M. J. and CEN, K. F. The research on the estimation for the NOx emissive concentration of the pulverized coal boiler by the flame image processing technique. eng. *Fuel (Guildford)* 81.16 (2002), pp. 2113–2120. ISSN: 0016-2361. URL: https://www.sciencedirect.com/science/article/pii/S0016236113009824 (visited on Jan. 14, 2021).

[81] Canny, J. A Computational Approach to Edge Detection. eng. *IEEE transactions on pattern analysis and machine intelligence* PAMI-8.6 (1986), pp. 679–698. ISSN: 0162-8828. URL: https://ieeexplore.ieee.org/document/4767851 (visited on Apr. 4, 2021).

[82] Omiotek, Z. and Kotyra, A. Flame Image Processing and Classification Using a Pre-Trained VGG16 Model in Combustion Diagnosis. eng. *Sensors (Basel, Switzerland)* 21.2 (2021), pp. 500–. ISSN: 1424-8220. URL: https://search-proquest-com.libproxy.tuni.fi/docview/2478305672?pq-origsite=primo&accountid=14242 (visited on Apr. 28, 2021).

[83] Brox, T., Bruhn, A., Papenberg, N. and Weickert, J. High accuracy optical flow estimation based on a theory for warping. eng. *Lecture notes in computer science* 3024 (2004), pp. 25–36. ISSN: 0302-9743.

[84] Castiñeira, D., Rawlings, B. C. and Edgar, T. F. Multivariate Image Analysis (MIA) for Industrial Flare Combustion Control. eng. *Industrial & engineering chemistry research* 51.39 (2012), pp. 12642–12652. ISSN: 0888-5885. URL: https://pubs.acs.org/doi/abs/10.1021/ie3003039 (visited on Jan. 14, 2021).

[85] Howell, J. R. *Thermal Radiation Heat Transfer*. eng. Boca Raton, FL, 2010. URL: https://ebookcentral.proquest.com/lib/tampere/detail.action?pq-origsite=primo&docID=1447246 (visited on Sept. 6, 2021).

[86] Qiu, T., Liu, M., Zhou, G., Wang, L. and Gao, K. An Unsupervised Classification Method for Flame Image of Pulverized Coal Combustion Based on Convolutional Auto-Encoder and Hidden Markov Model. eng. *Energies (Basel)* 12.13 (2019), pp. 2585–. ISSN: 1996-1073. URL: https://search-proquest-com.libproxy.tuni.fi/docview/2316876467?accountid=14242&pq-origsite=primo (visited on May 5, 2021).

[87] Lu, G., Yan, Y., Huang, Y. and Reed, A. An Intelligent Vision System for Monitoring and Control of Combustion Flames. eng. *Measurement and control (London)* 32.6 (1999), pp. 164–168. ISSN: 0020-2940.

[88] Tanaś, J., Kotyra, A. and Shegebaeva, J. Diagnostics of combustion process based on flame images analysis and genetic programming. eng. *Photonics Applications*

in Astronomy, Communications, Industry, and High-Energy Physics Experiments. Vol. 9662. SPIE, 2015, pp. 966229-966229–5. ISBN: 9781628418804.

[89] Bertucco, L., Fichera, A., Nunnari, G. and Pagano, A. A cellular neural networks approach to flame image analysis for combustion monitoring. eng. *Proceedings of the 2000 6th IEEE International Workshop on Cellular Neural Networks and their Applications (CNNA 2000) (Cat. No.00TH8509)*. IEEE, 2000, pp. 455–459. ISBN: 9780780363441. URL: https://ieeexplore.ieee.org/document/877371/ (visited on Jan. 14, 2021).

[90] Lu, G., Yan, Y., Huang, Y. and Reed, A. An Intelligent Vision System for Monitoring and Control of Combustion Flames. eng. *Measurement and control (London)* 32.6 (1999), pp. 164–168. ISSN: 0020-2940. URL: https://journals.sagepub.com/doi/10.1177/002029409903200601 (visited on Jan. 14, 2021).

[91] Seraj, M. and Shooredeli, M. A. Data-driven predictor and soft-sensor models of a cement grate cooler based on neural network and effective dynamics. eng. *2017 Iranian Conference on Electrical Engineering (ICEE)*. IEEE, 2017, pp. 726–731. ISBN: 1509059636. URL: https://ieeexplore.ieee.org/document/7985134 (visited on Jan. 9, 2019).

[92] Zhou, H., Li, Y. and Cen, K. Online blend-type identification during co-firing coal and biomass using SVM and flame emission spectrum in a pilot-scale furnace. eng. *IET renewable power generation* 13.2 (2019), pp. 253–261. ISSN: 1752-1416. URL: https://advance-lexis-com.libproxy.tuni.fi/api/document?collection=news&id=urn:contentItem:5V8B-DJW1-F034-6004-00000-00 (visited on May 14, 2021).

[93] Lou, C., Li, W.-H., Zhou, H.-C. and Salinas, C. T. Experimental investigation on simultaneous measurement of temperature distributions and radiative properties in an oil-fired tunnel furnace by radiation analysis. eng. *International journal of heat and mass transfer* 54.1 (2011), pp. 1–8. ISSN: 0017-9310. URL: https://www.sciencedirect.com/science/article/pii/S0017931010005703 (visited on July 1, 2021).

[94] Yin, R. K. *Case study research : design and methods*. eng. 3. ed. Applied social research methods series ; vol. 5. Thousand Oaks (Calif.): Sage, 2003. ISBN: 0-7619-2552-X.

[95] Williamson, K. *Research Methods for Students, Academics and Professionals: Information Management and Systems*. eng. Topics in Australasian Library and Information Studies. Witney: Elsevier Science & Technology, 2002. ISBN: 9781876938420. URL: https://web-a-ebscohost-com.libproxy.tuni.fi/ehost/detail/detail?vid=0&sid=ed938735-7e07-44e8-9b2a-65811eaf80a6%40sdc-v-sessmgr03 (visited on Apr. 25, 2021).

[96] Stephanie, T., Elisabeth, T.-K., Franz, W. and Dagmar, J. *Waste management*. Vol. 8. Thomé-Kozmiensky Verlag GmbH, 2018. 614 p. ISBN: 978-3-944310-42-8.

URL: https://www.vivis.de/2018/10/waste-management-volume-8/350/ (visited on Feb. 3, 2021).

[97] *Tammervoima. Tampere Waste-to-Energy plant*. Jan. 1, 2018. URL: https://tammervoima.fi/wp-content/uploads/2020/10/tammervoima_english_2018_final_web.pdf (visited on May 9, 2021).

[98] *Tampereen sähkölaitoksen vuosikertomus. Vihreitä askeleita – 2015*. Mar. 1, 2016. URL: https://www.sahkolaitos.fi/globalassets/tiedostot/ohjeet-ja-opasteet/sahkolaitos/vuosiraportit-ja-tilinpaatokset/vuosikertomus-2015.pdf (visited on May 9, 2021).

[99] *Steinmüller Babcock Environment. References Tampere - Finland*. Feb. 1, 2020. URL: https://www.steinmueller-babcock.com/references/tampere-finland/ (visited on Jan. 30, 2021).

[100] *Valmet DNA. Information Management*. URL: https://www.valmet.com/automation/distributed-control-system/information-management/ (visited on May 19, 2021).

[101] Bengtsson, M. How to plan and perform a qualitative study using content analysis. eng. *NursingPlus open* 2 (2016), pp. 8–14. ISSN: 2352-9008. URL: https://www.sciencedirect.com/science/article/pii/S2352900816000029 (visited on May 30, 2021).

[102] Julius, O. and Smith, I. *Mathematics of the Discrete Fourier Transform (DFT), with Audio Applications – Second Edition*. eng. 2nd edition. W3k Publishing, 2007. ISBN: 9780974560748. URL: https://ccrma.stanford.edu/~jos/st/Unbiased_Cross_Correlation.html (visited on May 10, 2021).

[103] Alessio, S. M. *Digital Signal Processing and Spectral Analysis for Scientists Concepts and Applications*. eng. Cham, 2016. URL: https://link-springer-com.libproxy.tuni.fi/book/10.1007%2F978-3-319-25468-5 (visited on May 10, 2021).

[104] Hamilton, J. D. *Time series analysis*. eng. Princeton (N.J.), 1994. URL: http://www.ru.ac.bd/stat/wp-content/uploads/sites/25/2019/03/504_02_Hamilton_Time-Series-Analysis.pdf (visited on May 12, 2021).

[105] Granger, C. W. J. Investigating Causal Relations by Econometric Models and Cross-spectral Methods. eng. *Econometrica* 37.3 (1969), pp. 424–438. ISSN: 0012-9682.

[106] *OpenCV. About*. Mar. 23, 2021. URL: https://opencv.org/about/ (visited on Mar. 23, 2021).

APPENDIX A: DATA SHEETS OF CAMERAS

Valmet Furnace IR Camera for the Power Utility Industry

- Inspect Waterwall Conditions
- Faster Detection of Water Leaks
- Evaluate Slag Buildup
- Reduced Downtime from Feedback on Internal Boiler Conditions
- Better Operator Safety with Real-Time Monitoring

Valmet

Typical Pneumatic and Electrical Connections for Valmet Furnace Camera

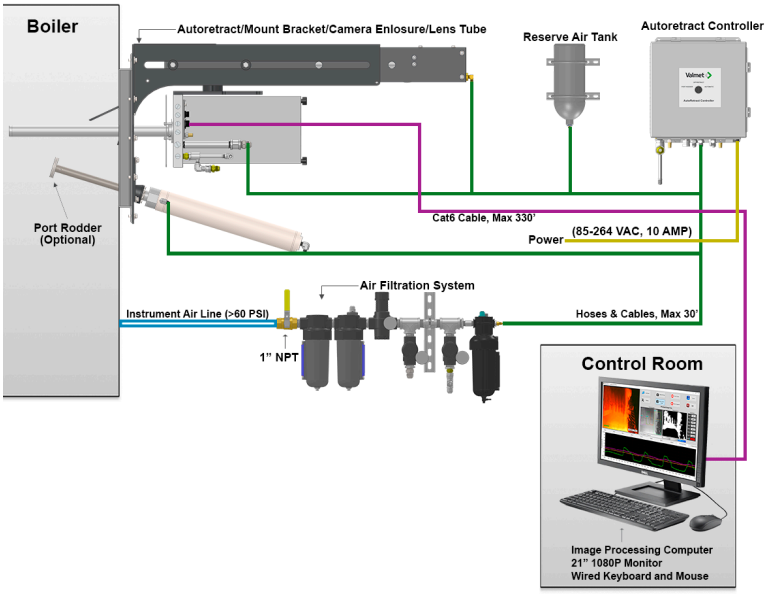

Specifications

Universal Enclosure:

- Dimensions 8.5 x 10.5 x 20.5” (216 x 267 x 521 mm)
- Weight 32 lbs (14.5 kg)
- Electrical 85~240 VAC, 50/60 Hz, < 2 Amps
- IP Video & Temp Analog – NTSC / Digital – MJPEG & H.264

Imaging Module:

- Frame Rate 30 Hz
- Resolution 640 x 480
- Video Output NTSC
- Operating Temp 0 to 130°F (–18 to 54°C)
- Auto Correction Automatic Gain, Automatic Level

Lens Tube: SL 64/35 (64° Field of View, 20” Effective L)

- Dimensions D 1-5/8 x L 35” (D 41 x L 889 mm)
- Weight 6.5 lbs (3 kg)
- Focal Range 12” (305 mm) to Infinity

Air Filter System:

- Dimensions 6 x 16 x 28” (152 x 406 x 711 mm)
- Weight 20 lbs (9 kg)

AutoRetract (AR): 24” Typical

- Dimensions 15 x 26.2 x 69.5“ (381x665x1765 mm)
- Weight 95 lbs (43 kg)
- Electrical 85~240 VAC, 50/60 Hz

AR Controller:

- Dimensions 12 x 10–12 x 5–6” (305 x 254–305 x 127–152 mm)
- Weight 32-38 lbs (14.5-17 kg) [based on model]

Cooling Air Supply: Plant Service Air, Regulated

- Pressure > 60 psig (4.1 bar)
- Consumption At 60 psi Inlet Pressure, <60 SCFM (1699 l/min)
- Inlet Air Temp < 130°F (54°C)

For more information, contact your local Valmet office. www.valmet.com

Valmet Visible Thermal Imaging System

Valmet Visible Thermal Imaging System is a rugged, air-cooled, HD visible camera paired with a high resolution thermal sensor for real-time product temperature measurements. Designed for comprehensive observation and analysis of kiln environments, the Valmet Visible Thermal Imaging System provides unparalleled image quality from start up to full load conditions.

Benefits

- Improved monitoring resulting in reduced operating costs
- Combustion optimization resulting in fuel savings
- Allows for visual evaluation of flame shape and size
- Reduced maintenance costs
- Greater visibility during start-up and at full load
- Product temperature alerts
- Historical temperature data trends

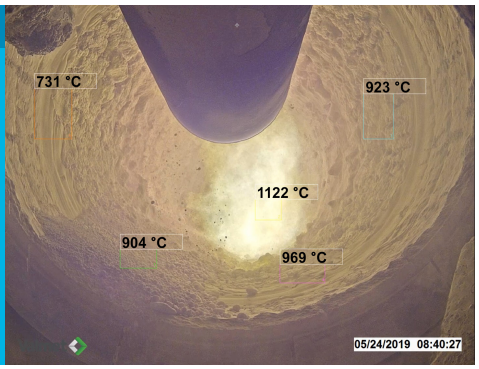

Reliability

Valmet Visible Thermal Imaging Systems are engineered for durability and longevity inside of hot, dusty environments, providing a low maintenance solution to many complex process challenges. Digital only data transmission improves reliability of video streams and nearly eliminates unwanted noise or image signal degradation.

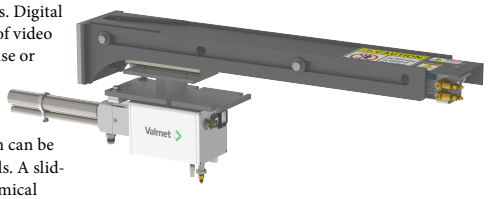

Configuration flexibility

The Valmet Visible Thermal Imaging System can be configured to meet your project budget needs. A sliding rail mount provides a reliable, yet economical mounting solution with a small installation footprint. Additionally, the camera system can be purchased with an automated retraction system, which will retract the system on loss of power or air pressure, protecting the camera unit from unintentional damage in the event of cooling air loss.

Technical specifications and layout

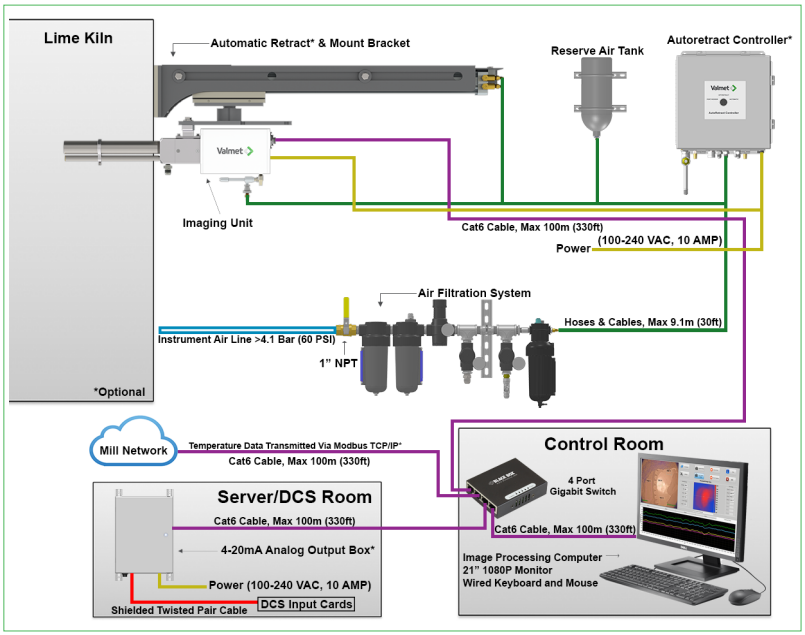

Dimensions	Camera enclosure Air filter	216 x 140 x 140 mm (8 1/2" x 5 1/2" x 5 1/2") 152 x 406 x 711 mm (6" x 16" x 28")
Standard camera tube with thermal probe	HD visible / Thermal 64/24	64º FOV, D 80 x L 610 mm (3 1/8" x 24")
Lens performance	Focal range	305 mm (12") to infinity
Camera unit	Framerate Detector Display resolution Gain/level Video format	30 Hz CMOS, 1920x1200 pixels 1400x1050 Automatic gain, automatic level H.264, motion jpeg
Thermal probe	Sensor array size Object temperature range Sensor framerate	1024 pixels 20 ºC to >1000 ºC (68 ºF to >1832 ºF) 60 Hz
Weights	24" Camera unit with thermal probe	7.14 kg (15.75 lbs)
Environmental	Imaging unit/camera Air filter system	-18 ºC to 54 ºC (0 ºF to 130 ºF) (non-condensing) Note: >54 ºC (>130 ºF) may require additional cooling hardware 0 ºC to 79 ºC (32 ºF to 175 ºF)
Electrical	Camera and thermal probe unit	85~240 VAC 50/60 Hz 0.8 A SCCR: 5 kA
Cooling air	Air supply Pressure Consumption	Plant (service) air (good), instrument air (best) 4.14 bar (60 psi) <1699 l/min (60 SCFM) @ 5.5 bar (80 psi) inlet pressure

For more information, contact your local Valmet office. www.valmet.com

APPENDIX B: COLLECTED PROCESS VALUES

Tag code	Tag description	Tag unit
TV1LBA10FF901:av	F LVE-STM BLR	kg/s
TV1LBA10CP902:av	P AVG LVE-STM BLR	bar (g)
TV1LBA20CT001:av	PÄÄHÖYRY LÄMPÖTILA	℃
TV1LBA10CT901:av	T AVG LVE-STM BLR	℃
TV1LAB20CT001:av	SYÖTTÖVESI LÄMPÖTILA	℃
TV1CHV10CE401YR01:av	ACTIVE POWER	MW
TV1LBF10CF001:av	PÄÄHÖYRY R1 VIRTAUS	kg/s
TV1LBF30CF001:av	PÄÄHÖYRY R2 R3 VIRTAUS	kg/s
TV1HAH23DT901:pos	CLC TEMP DNSTR SH 2	%
TV1LBA10DT901:pos	CLC TEMP LVE-STM	%
TV1LBA10DP002:me	CLC PRES LVE-STM BY ACC	bar (g)
TV1LBA10DP002:spa	CLC PRES LVE-STM BY ACC	bar (g)
TV1LBA10DP002:pos	CLC PRES LVE-STM BY ACC	Nm^3/h
TV1HLA30FF901:av	F TOT PRI-AIR GRT-ZN	Nm^3/h
TV1HLA31DF901:me	F PRI-AIR GRT-LFT ZN 1	Nm^3/h
TV1HLA31DF901:spa	F PRI-AIR GRT-LFT ZN 1	Nm^3/h
TV1HLA31DF901:pos	F PRI-AIR GRT-LFT ZN 1	%
TV1HLA41DF901:me	F PRI-AIR GRT-RGHT ZN 1	Nm^3/h
TV1HLA41DF901:spa	F PRI-AIR GRT-RGHT ZN 1	Nm^3/h
TV1HLA41DF901:pos	F PRI-AIR GRT-RGHT ZN 1	%
TV1HLA32DF901:me	F PRI-AIR GRT-LFT ZN 2	Nm^3/h
TV1HLA32DF901:spa	F PRI-AIR GRT-LFT ZN 2	Nm^3/h
TV1HLA32DF901:pos	F PRI-AIR GRT-LFT ZN 2	%

TV1HLA42DF901:me	F PRI-AIR GRT-RGHT ZN 2	Nm^3/h
TV1HLA42DF901:spa	F PRI-AIR GRT-RGHT ZN 2	Nm^3/h
TV1HLA42DF901:pos	F PRI-AIR GRT-RGHT ZN 2	%
TV1HLA33DF901:me	F PRI-AIR GRT-LFT ZN 3	Nm^3/h
TV1HLA33DF901:spa	F PRI-AIR GRT-LFT ZN 3	Nm^3/h
TV1HLA33DF901:pos	F PRI-AIR GRT-LFT ZN 3	%
TV1HLA43DF901:me	F PRI-AIR GRT-RGHT ZN 3	Nm^3/h
TV1HLA43DF901:spa	F PRI-AIR GRT-RGHT ZN 3	Nm^3/h
TV1HLA43DF901:pos	F PRI-AIR GRT-RGHT ZN 3	%
TV1HLA34DF901:me	F PRI-AIR GRT-LFT ZN 4	Nm^3/h
TV1HLA34DF901:spa	F PRI-AIR GRT-LFT ZN 4	Nm^3/h
TV1HLA34DF901:pos	F PRI-AIR GRT-LFT ZN 4	%
TV1HLA44DF901:me	F PRI-AIR GRT-RGHT ZN 4	Nm^3/h
TV1HLA44DF901:spa	F PRI-AIR GRT-RGHT ZN 4	Nm^3/h
TV1HLA44DF901:pos	F PRI-AIR GRT-RGHT ZN 4	%
TV1HLA35DF901:me	F PRI-AIR GRT-LFT ZN 5	Nm^3/h
TV1HLA35DF901:spa	F PRI-AIR GRT-LFT ZN 5	Nm^3/h
TV1HLA35DF901:pos	F PRI-AIR GRT-LFT ZN 5	%
TV1HLA45DF901:me	F PRI-AIR GRT- RGHT ZN 5	Nm^3/h
TV1HLA45DF901:spa	F PRI-AIR GRT- RGHT ZN 5	Nm^3/h
TV1HLA45DF901:pos	F PRI-AIR GRT- RGHT ZN 5	%
TV1HNA10DQ901:me	CLC O2 FLU-GAS	Vol% dry
TV1HNA10DQ901:spa	CLC O2 FLU-GAS	Vol% dry
TV1HNA10DQ901:pos	CLC O2 FLU-GAS	Nm^3/h
TV1HLA80DF901:me	F TOT SECY-AIR	Nm^3/h
TV1HLA80DF901:spa	F TOT SECY-AIR	Nm^3/h
TV1HLA80DF901:pos	F TOT SECY-AIR	%
TV1HLA81FF901:av	SEK.ILMAN VIRTAUS ETUSEIN	Nm^3/h
TV1HLA82FF901:av	SEK.ILMAN VIRTAUS	Nm^3/h
TV1HHC10DT901:me	CLC BRN-OUT-TEMP	℃

TV1HHC10DT901:spa	CLC BRN-OUT-TEMP	℃
TV1HHC10DT901:pos	CLC BRN-OUT-TEMP	Nm^3/t
TV1HHY01DQ001:me	CLC FIRING	Nm^3/t
TV1HHY01DQ001:spa	CLC FIRING	Nm^3/t
TV1HHY01DQ001:pos	CLC FIRING	mm/s
TV1HHY01DQ001XQ20:av	SP FEEDER SPEED	mm/s
TV1HFB30DF001YQ01:av	CLC SPD WST FDR LFT	mm/s
TV1HFB30DG001:pos	CLC SPD WSTR FDR LFT	%
TV1HFB30CG001:av	G WST-FDR LFT	mm
TV1HFB40DG001:pos	CLC SPD WSTR FDR RGHT	%
TV1HFB40CG001:av	G WST-FDR RGHT	mm
TV1HHY01DQ001XQ21:av	SP GRATE SPEED ZONE 1	mm/s
TV1HHC31DF001YQ01:av	CLC SPD GRT LFT TRK-ZN 1	mm/s
TV1HHC31DG001:pos	CLC SPD GRT LFT TRK-ZN 1	%
TV1HHC31CG001:av	G GRT LFT ZN 1	mm
TV1HHC41DG001:pos	CLC SPD GRT RGHT TRK-ZN 1	%
TV1HHC41CG001:av	G GRT RGHT ZN 1	mm
TV1HHY01DQ001XQ22:av	SP GRATE SPEED ZONE 2	mm/s
TV1HHC32DF001YQ01:av	CLC SPD GRT LFT TRK-ZN 2	mm/s
TV1HHC32DG001:pos	CLC SPD GRT LFT TRK-ZN 2	%
TV1HHC32CG001:av	G GRT LFT ZN 2	mm
TV1HHC42DG001:pos	CLC SPD GRT RGHT TRK-ZN 2	%
TV1HHC42CG001:av	G GRT RGHT ZN 2	mm
TV1HHY01DQ001XQ23:av	SP GRATE SPEED ZONE 3	mm/s
TV1HHC33DF001YQ01:av	CLC SPD GRT LFT TRK-ZN 3	mm/s
TV1HHC33DG001:pos	CLC SPD GRT LFT TRK-ZN 3	%
TV1HHC33CG001:av	G GRT LFT ZN 3	mm
TV1HHC43DG001:pos	CLC SPD GRT RGHT TRK-ZN 3	%
TV1HHC43CG001:av	G GRT RGHT ZN 3	mm
TV1HHY01DQ001XQ24:av	SP GRATE SPEED ZONE 4	mm/s

TV1HHC34DF001YQ01:av	CLC SPD GRT LFT TRK-ZN 4	mm/s
TV1HHC34DG001:pos	CLC SPD GRT LFT TRK-ZN 4	%
TV1HHC34CG001:av	G GRT LFT ZN 4	mm
TV1HHC44DG001:pos	CLC SPD GRT RGHT TRK-ZN 4	%
TV1HHC44CG001:av	G GRT RGHT ZN 4	mm
TV1HHY01DQ001XQ25:av	SP GRATE SPEED ZONE 5	mm/s
TV1HHC35DF001YQ01:av	CLC SPD GRT LFT TRK-ZN 5	mm/s
TV1HHC35DG001:pos	CLC SPD GRT LFT TRK-ZN 5	%
TV1HHC35CG001:av	G GRT LFT ZN 5	mm
TV1HHC45DG001:pos	CLC SPD GRT RGHT TRK-ZN 5	%
TV1HHC45CG001:av	G GRT RGHT ZN 5	mm
TV1HHC10CT901:av	TULIPESÄ SK T-KA YLÄR	℃
TV1HBK10FT901:av	T FLU-GAS 2 SEC 850℃	℃
TV1HBK10CT901:av	T AV FLU-GAS CELG 1ST PAS	℃
TV1HBK30CT001:av	T FLU-GAS UPSTR 3RD PASS	℃
TV1HBK30CT002:av	T FLU-GAS DNSTR 3RD PASS	℃
TV1HFB10CU911:av	THRM LD	MW
TV1HJA10DU902XQ01:av	CLC HT-INP AUX-BRN 1	MW
TV1HJA20DU902XQ01:av	CLC HT-INP AUX-BRN 2	MW
TV1HNA10DQ907:me	CLC NO2 BLR OUTL	mg/Nm^3 (dry)
TV1HNA10DQ907:spa	CLC NO2 BLR OUTL	mg/Nm^3 (dry)
TV1HNA10DQ907:pos	CLC NO2 BLR OUTL	l/h
TV1HSK15CF001:av	F NH3-W SNCR-INJ	l/h
TV1HNE00CF001:av	CEMS SAVUKAASUN VIRTAUS	m^3/h
TV1HNA20CQ001:av	Crude gas meas HCL	mg/Nm^3
TV1HNA20CQ002:av	Crude gas meas SO2	mg/Nm^3
TV1HNA20CQ003:av	Crude gas meas Nox	mg/Nm^3
TV1HNA20CQ005:av	Crude gas meas CO	mg/Nm^3
TV1HNE10CQ003FRL	CO-pit, raja	mg/m^3 (n)
TV1HNE10CQ004FRL	SO2-pit, raja	mg/m^3 (n)

TV1HNE10CQ012FRL	NH3-pit, raja	mg/m^3 (n)
TV1HNE10CQ008FRL	HCl-pit, raja	mg/m^3 (n)
TV1HNE10CQ007FRL	HF-pit, raja	mg/m^3 (n)
TV1HNE10CQ002FRL	NOx-pit, raja	mg/m^3 (n)
TV1HNE10CQ002N:av	SAVUKAASUN NOX (NO2)	ppm
TV1HNE10CQ009FRL	TOC-pit, raja	mg/m^3 (n)

Table B.1. *Collected process values.*

APPENDIX C: SURVEY QUESTIONNAIRE

Jesse Salmi

Jätteenpolton kysely

Introduction omitted as confidential information.

1. **Kerro hieman itsestäsi. Mikä on toimenkuvasi yrityksessä ja kuinka kauan olet ollut siinä? Kuinka tuttua jätteenpoltto on sinulle yleisesti?**

2. **Mitkä tekijät tuottavat suurimpia haasteita jätteenpoltossa ja kattilan toiminnassa?**

3. **Miten ohjaatte kattilaa automaatiojärjestelmän kautta?**
   a. **Miten hallitsette palamisprosessia?**
   b. **Millaisia ongelmia tilanteita kattilassa/palamisessa ilmenee ja miten toimitte niissä? Kerro esimerkkejä tilanteista**

4. **Miten hyödynnätte arinan kamerajärjestelmää kattilan ajamisessa?**

5. **Miten kamerajärjestelmiä voisi parantaa, jotta niistä olisi enemmän apua teille?**

6. **Miten kattilan toiminta vaikuttaa laitoksen muiden osien kuntoon?**

7. **Miten pystytte vaikuttamaan kattilan kuntoon polttoprosessia ohjaamalla?**

Palautetta kysymyksistä. Oliko jokin kohta epäselvä, jota olisi voinut tarkentaa?

Muuta lisättävää / vapaa sana

Kiitokset kyselyyn osallistumisestasi!

APPENDIX D: SIGNAL ANALYSIS RESULTS

Signal name	m_{max}	$\hat{R}_{xy}$	P_{xy}	P_{yx}
CLC FIRING:me	135	0.70731	1.69631e-09	6.06270e-05
F PRI-AIR GRT-LFT ZN 5:me	144	0.6652	6.85089e-11	5.24226e-06
CLC PRES LVE-STM BY ACC:pos	147	0.66481	7.53082e-19	1.03825e-02
F PRI-AIR GRT-LFT ZN 3:spa	147	0.6648	1.27926e-17	3.25158e-04
F PRI-AIR GRT-RGHT ZN 3:spa	147	0.6648	1.27926e-17	3.25158e-04
F PRI-AIR GRT-LFT ZN 4:spa	147	0.66479	1.33477e-16	6.74986e-04
F PRI-AIR GRT-RGHT ZN 4:spa	147	0.66479	1.33477e-16	6.74986e-04
F PRI-AIR GRT-LFT ZN 1:spa	147	0.66477	3.84760e-15	8.08207e-03
F PRI-AIR GRT- RGHT ZN 5:spa	147	0.66477	3.80837e-15	8.01852e-03
F PRI-AIR GRT-LFT ZN 5:spa	147	0.66477	3.84760e-15	8.08207e-03
F PRI-AIR GRT-RGHT ZN 1:spa	147	0.66477	3.84760e-15	8.08207e-03
F PRI-AIR GRT-RGHT ZN 2:spa	147	0.66475	1.88830e-14	1.46445e-02
F PRI-AIR GRT-LFT ZN 2:spa	147	0.66475	1.88830e-14	1.46445e-02
F PRI-AIR GRT-LFT ZN 4:me	143	0.6647	1.58977e-13	3.66497e-03
F PRI-AIR GRT-RGHT ZN 4:me	144	0.66449	2.54966e-12	9.99763e-06
F PRI-AIR GRT- RGHT ZN 5:me	144	0.66416	2.14146e-07	2.19398e-07
F PRI-AIR GRT-RGHT ZN 1:me	143	0.66413	1.42550e-09	1.21839e-06
F PRI-AIR GRT-RGHT ZN 3:me	144	0.66398	2.18167e-11	4.83245e-06
F PRI-AIR GRT-LFT ZN 1:me	143	0.66397	1.29688e-15	9.64901e-09
F TOT PRI-AIR GRT-ZN:av	144	0.66389	3.24036e-12	1.55584e-04
F PRI-AIR GRT-LFT ZN 3:me	144	0.66338	5.54546e-11	1.93548e-01
F PRI-AIR GRT-LFT ZN 2:me	145	0.66315	8.11039e-10	4.28583e-09
F PRI-AIR GRT-RGHT ZN 2:me	145	0.66305	1.94572e-13	1.01372e-06

SEK.ILMAN VIRTAUS:av	122	-0.62032	7.72529e-10	2.89416e-05
CLC O2 FLU-GAS:pos	118	-0.6201	6.70959e-10	1.21135e-02
F TOT SECY-AIR:spa	119	-0.62	3.26177e-07	1.28236e-02
F TOT SECY-AIR:me	122	-0.61992	2.10197e-10	1.45752e-03
SEK.ILMAN VIRTAUS ETUSEIN:av	122	-0.61941	7.76916e-12	9.48166e-04
F TOT SECY-AIR:pos	122	-0.61077	2.31423e-10	4.81286e-04
TULIPESÄ SK T-KA YLÄR:av	207	-0.58116	6.77167e-04	5.04385e-03
Crude gas meas HCL:av	-8772	0.54513	#	#
Crude gas meas SO2:av	-8860	0.5422	#	#
CLC PRES LVE-STM BY ACC:me	-66	-0.53107	6.00130e-13	5.58924e-05
P AVG LVE-STM BLR:av	-68	-0.52956	1.44718e-13	1.15720e-02
CLC O2 FLU-GAS:me	27	0.51895	3.02369e-03	3.35398e-01
F PRI-AIR GRT-LFT ZN 5:pos	141	0.50731	5.04599e-09	8.14495e-05
F LVE-STM BLR:av	-336	-0.5068	1.16585e-04	1.07663e-19
THRM LD:av	-349	-0.50457	2.36962e-04	1.08907e-07
CLC FIRING:spa	11031	-0.50432	#	#
CLC BRN-OUT-TEMP:pos	11031	-0.50397	#	#
CLC BRN-OUT-TEMP:me	170	-0.50268	8.31872e-12	4.94099e-05
F PRI-AIR GRT- RGHT ZN 5:pos	142	0.49891	3.68436e-05	5.21565e-07
F PRI-AIR GRT-LFT ZN 4:pos	100	0.48235	6.69788e-06	1.90784e-03
SP FEEDER SPEED:av	10970	0.47473	#	#
CLC FIRING:pos	10978	0.47357	#	#
SP GRATE SPEED ZONE 3:av	10925	0.46716	#	#
SP GRATE SPEED ZONE 1:av	10925	0.46715	#	#
SP GRATE SPEED ZONE 2:av	10925	0.46715	#	#
SP GRATE SPEED ZONE 4:av	10925	0.46712	#	#
PÄÄHÖYRY R2 R3 VIRTAUS:av	7864	-0.45494	#	#
CEMS SAVUKAASUN VIRTAUS:av	146	0.45436	9.49774e-04	1.41596e-04
PÄÄHÖYRY LÄMPÖTILA:av	67	0.45197	2.18711e-05	9.24215e-03
F PRI-AIR GRT-RGHT ZN 4:pos	107	0.4492	3.21330e-06	1.33453e-02

T AVG LVE-STM BLR:av	61	0.44912	5.58832e-05	5.79643e-03
PÄÄHÖYRY R1 VIRTAUS:av	8010	-0.44156	#	#
Crude gas meas CO:av	206	0.43687	5.54741e-01	1.86971e-01
F NH3-W SNCR-INJ:av	10251	-0.43465	#	#
CLC NO2 BLR OUTL:pos	10246	-0.43403	#	#
SAVUKAASUN NOX (NO2):av	73	-0.43097	1.05261e-05	4.74042e-03
ACTIVE POWER:av	7874	0.43063	#	#
SP GRATE SPEED ZONE 5:av	-574	-0.39881	8.25934e-04	4.81773e-01
CLC TEMP DNSTR SH 2:pos	-527	-0.39822	3.37536e-04	7.53882e-10
SYÖTTÖVESI LÄMPÖTILA:av	-6503	-0.38096	#	#
F PRI-AIR GRT-RGHT ZN 3:pos	92	0.37315	2.81003e-07	1.23454e-02
CLC TEMP LVE-STM:pos	-1398	-0.37145	3.61286e-01	1.81502e-02
T FLU-GAS 2 SEC 850℃:av	-9572	-0.36963	#	#
Crude gas meas Nox:av	62	-0.35558	5.63037e-01	1.71898e-01
T AV FLU-GAS CELG 1ST PAS:av	-9585	-0.35151	#	#
F PRI-AIR GRT-RGHT ZN 2:pos	-1455	-0.34995	4.49334e-02	1.22737e-02
CLC SPD GRT LFT TRK-ZN 3:pos	10738	-0.3488	#	#
G GRT LFT ZN 2:av	-19637	-0.34775	#	#
F PRI-AIR GRT-RGHT ZN 1:pos	-1483	-0.32464	3.78943e-02	4.03456e-02
F PRI-AIR GRT-LFT ZN 2:pos	-19789	0.32379	#	#
F PRI-AIR GRT-LFT ZN 3:pos	18784	-0.31845	#	#
T FLU-GAS UPSTR 3RD PASS:av	-1149	-0.30995	1.50580e-31	6.29372e-01
F PRI-AIR GRT-LFT ZN 1:pos	-1482	-0.30955	6.13604e-02	1.79150e-01
T FLU-GAS DNSTR 3RD PASS:av	-441	-0.3092	9.54692e-01	6.97685e-01
CLC NO2 BLR OUTL:me	20169	0.30841	#	#
CLC SPD WSTR FDR RGHT:pos	-358	0.30796	1.21491e-09	7.77161e-11
NOx-pit raja	16360	0.30652	#	#
G GRT RGHT ZN 3:av	20823	-0.30219	#	#
TOC-pit raja	16360	0.29589	#	#
HCl-pit raja	16360	0.29585	#	#

NH3-pit raja	16360	0.29584	#	#
HF-pit raja	16360	0.29583	#	#
SO2-pit raja	16360	0.29562	#	#
CO-pit raja	16360	0.29549	#	#
G GRT LFT ZN 5:av	20755	0.28794	#	#
CLC SPD GRT RGHT TRK-ZN 4:pos	-428	-0.28418	2.49451e-01	4.35235e-02
CLC SPD GRT LFT TRK-ZN 4:pos	14657	-0.27896	#	#
G GRT LFT ZN 3:av	21638	-0.27846	#	#
G GRT RGHT ZN 5:av	12339	-0.27273	#	#
G GRT RGHT ZN 2:av	-18932	-0.26876	#	#
CLC SPD GRT RGHT TRK-ZN 1:pos	20996	0.26603	#	#
CLC SPD GRT LFT TRK-ZN 2:av	-20843	-0.25722	#	#
CLC SPD GRT LFT TRK-ZN 1:av	-20843	-0.25722	#	#
CLC SPD WST FDR LFT:av	-20843	-0.25722	#	#
CLC SPD GRT LFT TRK-ZN 3:av	-20843	-0.25722	#	#
CLC SPD GRT LFT TRK-ZN 4:av	-20843	-0.25722	#	#
CLC SPD GRT RGHT TRK-ZN 2:pos	-19622	0.25201	#	#
G GRT LFT ZN 1:av	16200	0.25067	#	#
CLC SPD GRT LFT TRK-ZN 2:pos	-130	-0.23298	2.94009e-02	8.30528e-08
CLC SPD GRT RGHT TRK-ZN 3:pos	-70	-0.20866	7.72374e-04	1.31803e-01
G GRT RGHT ZN 1:av	-1327	-0.1997	5.87593e-01	6.43866e-01
CLC SPD GRT LFT TRK-ZN 1:pos	13547	-0.19491	#	#
CLC SPD WSTR FDR LFT:pos	12122	-0.18925	#	#
CLC SPD GRT RGHT TRK-ZN 5:pos	12055	-0.18323	#	#
CLC SPD GRT LFT TRK-ZN 5:pos	19778	-0.13081	#	#
G GRT LFT ZN 4:av	-4452	-0.12249	#	#
G GRT RGHT ZN 4:av	18554	0.11994	#	#
G WST-FDR LFT:av	11111	-0.11132	#	#
G WST-FDR RGHT:av	11020	-0.10457	#	#

Table D.1. *Results with extracted flame front minimum point.*

Signal name	m_{max}	$\hat{R}_{xy}$	P_{xy}	P_{yx}
F PRI-AIR GRT-LFT ZN 5:pos	142	0.5784	2.52263e-04	1.82140e-06
F PRI-AIR GRT- RGHT ZN 5:pos	140	0.57672	3.77351e-04	1.85230e-05
F PRI-AIR GRT-LFT ZN 4:pos	118	0.53066	8.58377e-07	9.54863e-03
F PRI-AIR GRT-RGHT ZN 4:pos	135	0.53065	1.93215e-07	7.18970e-08
F PRI-AIR GRT-LFT ZN 5:me	105	0.50705	1.56313e-03	5.40474e-05
F PRI-AIR GRT-LFT ZN 3:me	105	0.50692	1.14026e-02	3.64010e-06
F PRI-AIR GRT-RGHT ZN 4:me	105	0.50692	1.22078e-04	2.29268e-06
F PRI-AIR GRT-LFT ZN 2:me	105	0.50601	1.21935e-05	2.38553e-03
F TOT PRI-AIR GRT-ZN:av	105	0.50587	1.30375e-03	2.05095e-05
F PRI-AIR GRT- RGHT ZN 5:me	105	0.50579	2.85464e-05	2.21846e-05
F PRI-AIR GRT-RGHT ZN 2:me	105	0.50538	4.03813e-04	1.10524e-05
F PRI-AIR GRT-LFT ZN 4:me	104	0.50534	1.99484e-03	1.14504e-02
F PRI-AIR GRT-LFT ZN 5:spa	107	0.50524	1.38528e-10	4.39294e-04
F PRI-AIR GRT-RGHT ZN 1:spa	107	0.50524	1.38528e-10	4.39294e-04
F PRI-AIR GRT- RGHT ZN 5:spa	107	0.50524	1.38797e-10	4.43003e-04
F PRI-AIR GRT-LFT ZN 1:spa	107	0.50524	1.38528e-10	4.39294e-04
F PRI-AIR GRT-LFT ZN 2:spa	107	0.50521	9.02662e-11	1.55563e-02
F PRI-AIR GRT-RGHT ZN 2:spa	107	0.50521	9.02662e-11	1.55563e-02
CLC PRES LVE-STM BY ACC:pos	107	0.50518	6.58130e-11	8.80749e-05
F PRI-AIR GRT-LFT ZN 4:spa	107	0.50515	1.65464e-09	1.53814e-02
F PRI-AIR GRT-RGHT ZN 4:spa	107	0.50515	1.65464e-09	1.53814e-02
F PRI-AIR GRT-RGHT ZN 3:spa	107	0.50515	1.33084e-10	1.60041e-03
F PRI-AIR GRT-LFT ZN 3:spa	107	0.50515	1.33084e-10	1.60041e-03
F PRI-AIR GRT-RGHT ZN 3:me	105	0.50502	3.19326e-07	3.91196e-05
F PRI-AIR GRT-LFT ZN 1:me	104	0.50464	1.10860e-05	7.52042e-06
F PRI-AIR GRT-RGHT ZN 1:me	104	0.50456	2.31271e-02	8.87604e-05
F PRI-AIR GRT-LFT ZN 3:pos	144	0.48309	6.90893e-07	2.85919e-06
F PRI-AIR GRT-RGHT ZN 3:pos	125	0.47712	1.45730e-05	3.18202e-04
CLC FIRING:me	81	0.45584	3.70203e-02	1.51990e-04

F PRI-AIR GRT-RGHT ZN 2:pos	158	0.45017	4.65798e-05	5.00681e-04
CLC NO2 BLR OUTL:me	21420	-0.43172	#	#
G GRT RGHT ZN 5:av	7047	0.42241	#	#
TULIPESÄ SK T-KA YLÄR:av	174	-0.42089	5.16022e-06	1.73865e-03
Crude gas meas CO:av	1940	-0.41728	5.24590e-22	1.00000e+00
PÄÄHÖYRY LÄMPÖTILA:av	55	0.40354	1.07522e-01	5.91836e-05
T AVG LVE-STM BLR:av	47	0.40207	3.63495e-02	4.65522e-02
CLC BRN-OUT-TEMP:me	170	-0.39757	1.57375e-08	8.92955e-06
CEMS SAVUKAASUN VIRTAUS:av	100	0.38394	1.33762e-05	1.75071e-04
F TOT SECY-AIR:pos	-19665	0.37165	#	#
SEK.ILMAN VIRTAUS ETUSEIN:av	-19662	0.37033	#	#
F TOT SECY-AIR:spa	-19666	0.37018	#	#
CLC O2 FLU-GAS:pos	-19666	0.37006	#	#
F TOT SECY-AIR:me	-19662	0.36989	#	#
SEK.ILMAN VIRTAUS:av	-19662	0.36943	#	#
SP GRATE SPEED ZONE 5:av	402	0.34984	4.87102e-03	1.51085e-01
NH3-pit raja:TV1HNE10CQ012FRL	16343	0.34697	#	#
TOC-pit raja:TV1HNE10CQ009FRL	16343	0.34697	#	#
HF-pit raja:TV1HNE10CQ007FRL	16343	0.34696	#	#
HCl-pit raja:TV1HNE10CQ008FRL	16343	0.34696	#	#
SO2-pit raja:TV1HNE10CQ004FRL	16343	0.34674	#	#
CO-pit raja:TV1HNE10CQ003FRL	16343	0.34668	#	#
NOx-pit raja:TV1HNE10CQ002FRL	16343	0.34659	#	#
CLC TEMP LVE-STM:pos	106	0.34593	1.36833e-04	1.75620e-03
CLC PRES LVE-STM BY ACC:me	-115	-0.34091	1.95114e-10	4.53733e-03
P AVG LVE-STM BLR:av	-117	-0.33923	8.14760e-06	1.27760e-02
F PRI-AIR GRT-LFT ZN 2:pos	20208	0.3367	#	#
CLC NO2 BLR OUTL:pos	-19676	0.33372	#	#
F NH3-W SNCR-INJ:av	-19668	0.33372	#	#
T AV FLU-GAS CELG 1ST PAS:av	11575	-0.32822	#	#

F PRI-AIR GRT-LFT ZN 1:pos	178	0.32225	6.20135e-05	1.30983e-04
Crude gas meas Nox:av	2072	0.31747	#	#
SAVUKAASUN NOX (NO2):av	2053	0.3118	#	#
G GRT LFT ZN 5:av	-17994	0.30871	#	#
T FLU-GAS 2 SEC 850°C:av	18942	-0.30638	#	#
T FLU-GAS UPSTR 3RD PASS:av	239	0.29851	3.46872e-02	2.84784e-01
CLC O2 FLU-GAS:me	1906	-0.29628	5.64098e-05	3.13319e-01
F PRI-AIR GRT-RGHT ZN 1:pos	174	0.29295	4.86262e-04	5.33688e-07
Crude gas meas SO2:av	-8963	0.29215	#	#
CLC BRN-OUT-TEMP:pos	1667	-0.29092	6.98405e-217	1.00000e+00
CLC FIRING:spa	1667	-0.29085	8.80747e-216	1.00000e+00
Crude gas meas HCL:av	-8871	0.28935	#	#
PÄÄHÖYRY R1 VIRTAUS:av	-21527	0.28871	#	#
PÄÄHÖYRY R2 R3 VIRTAUS:av	-21432	0.28643	#	#
CLC SPD GRT LFT TRK-ZN 3:pos	10721	-0.28144	#	#
SP GRATE SPEED ZONE 4:av	1602	0.28142	9.30110e-01	4.65379e-01
SP GRATE SPEED ZONE 3:av	1602	0.28128	9.28459e-01	4.95261e-01
SP GRATE SPEED ZONE 2:av	1602	0.28128	9.34118e-01	5.02511e-01
SP GRATE SPEED ZONE 1:av	1602	0.28128	9.34118e-01	5.02511e-01
SP FEEDER SPEED:av	10110	0.28066	#	#
ACTIVE POWER:av	-21429	-0.27914	#	#
CLC FIRING:pos	10116	0.27908	#	#
G GRT LFT ZN 2:av	-19510	-0.26959	#	#
SYÖTTÖVESI LÄMPÖTILA:av	-20353	0.2635	#	#
T FLU-GAS DNSTR 3RD PASS:av	7163	-0.26174	#	#
CLC TEMP DNSTR SH 2:pos	-18206	0.26034	#	#
F LVE-STM BLR:av	-18821	0.25479	#	#
THRM LD:av	-18959	0.25473	#	#
CLC SPD GRT LFT TRK-ZN 2:pos	19963	-0.22878	#	#
CLC SPD GRT RGHT TRK-ZN 4:pos	1380	0.21739	4.70010e-01	7.14081e-03

G GRT RGHT ZN 2:av	16180	-0.21368	#	#
CLC SPD GRT RGHT TRK-ZN 1:pos	-2126	0.20579	#	#
CLC SPD GRT LFT TRK-ZN 4:pos	19230	-0.20126	#	#
CLC SPD GRT RGHT TRK-ZN 2:pos	-4727	0.19713	#	#
G GRT RGHT ZN 1:av	-1475	-0.1958	8.81609e-01	9.26427e-01
G GRT RGHT ZN 3:av	20626	-0.19562	#	#
G GRT LFT ZN 1:av	15303	0.19236	#	#
CLC SPD GRT RGHT TRK-ZN 3:pos	-86	-0.18957	2.77089e-04	1.00977e-02
CLC SPD GRT LFT TRK-ZN 1:pos	756	-0.18875	1.51927e-01	6.01495e-01
G GRT LFT ZN 3:av	21571	-0.17806	#	#
CLC SPD GRT RGHT TRK-ZN 5:pos	-5914	0.17374	#	#
CLC SPD WSTR FDR RGHT:pos	11112	-0.16971	#	#
CLC SPD WSTR FDR LFT:pos	969	-0.12679	1.42763e-02	6.38308e-03
G GRT LFT ZN 4:av	21460	-0.12317	#	#
G GRT RGHT ZN 4:av	-19589	-0.11844	#	#
CLC SPD GRT LFT TRK-ZN 5:pos	430	-0.10793	3.31975e-05	5.48420e-02
CLC SPD GRT LFT TRK-ZN 2:av	-19173	-0.10425	#	#
CLC SPD GRT LFT TRK-ZN 1:av	-19173	-0.10425	#	#
CLC SPD GRT LFT TRK-ZN 3:av	-19173	-0.10425	#	#
CLC SPD GRT LFT TRK-ZN 4:av	-19173	-0.10425	#	#
CLC SPD WST FDR LFT:av	-19173	-0.10425	#	#
G WST-FDR LFT:av	10130	-0.0686	#	#
G WST-FDR RGHT:av	10920	-0.0656	#	#

Table D.2. *Results with extracted flame front maximum point.*

Signal name	m_{max}	$\hat{R}_{xy}$	P_{xy}	P_{yx}
CLC FIRING:me	171	0.54915	8.23990e-05	3.14782e-07
F PRI-AIR GRT-RGHT ZN 4:me	189	0.53174	2.82583e-07	1.74491e-04
F PRI-AIR GRT-LFT ZN 5:me	187	0.53131	1.23073e-08	1.27254e-07

F PRI-AIR GRT-LFT ZN 4:me	188	0.53096	2.11164e-06	6.94604e-05
F PRI-AIR GRT-LFT ZN 3:me	188	0.5302	1.68361e-04	7.20102e-08
F TOT PRI-AIR GRT-ZN:av	188	0.53009	1.59927e-06	3.64990e-07
F PRI-AIR GRT-LFT ZN 5:spa	190	0.52987	2.34073e-17	1.05569e-02
F PRI-AIR GRT-LFT ZN 1:spa	190	0.52987	2.34073e-17	1.05569e-02
F PRI-AIR GRT-RGHT ZN 1:spa	190	0.52987	2.34073e-17	1.05569e-02
F PRI-AIR GRT- RGHT ZN 5:spa	190	0.52987	2.33415e-17	1.05714e-02
CLC PRES LVE-STM BY ACC:pos	190	0.52985	1.69181e-09	1.86633e-02
F PRI-AIR GRT-RGHT ZN 3:spa	190	0.52985	1.05276e-13	7.38872e-04
F PRI-AIR GRT-LFT ZN 2:spa	190	0.52985	6.43354e-16	1.10392e-02
F PRI-AIR GRT-LFT ZN 3:spa	190	0.52985	1.05276e-13	7.38872e-04
F PRI-AIR GRT-RGHT ZN 2:spa	190	0.52985	6.43354e-16	1.10392e-02
F PRI-AIR GRT- RGHT ZN 5:me	187	0.52984	2.94238e-06	9.08852e-07
F PRI-AIR GRT-LFT ZN 4:spa	190	0.52983	6.07533e-12	6.51101e-03
F PRI-AIR GRT-RGHT ZN 4:spa	190	0.52983	6.07533e-12	6.51101e-03
F PRI-AIR GRT-LFT ZN 2:me	188	0.52981	5.82823e-07	4.32391e-08
F PRI-AIR GRT-LFT ZN 1:me	187	0.52944	1.02547e-07	4.46845e-06
F PRI-AIR GRT-RGHT ZN 3:me	187	0.52938	4.88812e-03	6.28372e-09
F PRI-AIR GRT-RGHT ZN 1:me	186	0.52924	1.36704e-06	1.90966e-07
F PRI-AIR GRT-RGHT ZN 2:me	188	0.52876	5.45153e-07	3.05474e-08
F PRI-AIR GRT-LFT ZN 5:pos	204	0.52207	4.02545e-09	6.02587e-03
F PRI-AIR GRT-LFT ZN 4:pos	191	0.51691	4.18113e-06	6.52894e-04
F PRI-AIR GRT- RGHT ZN 5:pos	203	0.51419	1.36516e-07	2.10509e-05
F PRI-AIR GRT-RGHT ZN 4:pos	204	0.49616	1.18980e-04	7.46369e-05
CEMS SAVUKAASUN VIRTAUS:av	169	0.47822	8.89071e-03	2.72848e-05
PÄÄHÖYRY LÄMPÖTILA:av	92	0.47461	1.84811e-03	3.72617e-04
T AVG LVE-STM BLR:av	85	0.47186	1.11419e-05	2.88371e-03
TULIPESÄ SK T-KA YLÄR:av	244	-0.4397	1.69070e-04	4.46344e-01
CLC PRES LVE-STM BY ACC:me	-66	-0.43967	9.70075e-03	2.51979e-03
P AVG LVE-STM BLR:av	-68	-0.43786	1.55583e-02	8.18030e-03

SP FEEDER SPEED:av	-408	-0.43523	5.62854e-21	4.24323e-01
Crude gas meas HCL:av	-8802	0.43471	#	#
CLC FIRING:pos	-404	-0.43455	6.22027e-16	1.89289e-01
CLC O2 FLU-GAS:me	84	0.42279	1.52501e-07	9.21049e-03
F PRI-AIR GRT-RGHT ZN 3:pos	181	0.42091	5.70337e-03	3.38558e-05
F NH3-W SNCR-INJ:av	18402	-0.41921	#	#
CLC NO2 BLR OUTL:pos	18397	-0.41884	#	#
SEK.ILMAN VIRTAUS:av	141	-0.41783	1.41873e-07	4.22074e-08
CLC O2 FLU-GAS:pos	138	-0.41736	2.80713e-04	4.40506e-06
F TOT SECY-AIR:spa	138	-0.41725	3.65318e-03	7.55604e-10
F TOT SECY-AIR:me	141	-0.41719	1.30415e-07	9.43637e-08
SEK.ILMAN VIRTAUS ETUSEIN:av	141	-0.41642	5.20279e-07	1.93419e-06
SP GRATE SPEED ZONE 4:av	-481	-0.41388	6.34185e-02	7.20064e-01
SP GRATE SPEED ZONE 2:av	-481	-0.41377	7.23400e-02	7.11342e-01
SP GRATE SPEED ZONE 1:av	-481	-0.41377	7.23400e-02	7.11342e-01
SP GRATE SPEED ZONE 3:av	-481	-0.41375	6.52103e-02	7.04523e-01
F TOT SECY-AIR:pos	141	-0.41015	2.73050e-05	1.33893e-07
F PRI-AIR GRT-LFT ZN 3:pos	208	0.40213	5.10494e-03	3.24917e-04
Crude gas meas SO2:av	-8854	0.40113	#	#
CLC BRN-OUT-TEMP:pos	-328	0.39981	6.08333e-139	5.59598e-15
CLC FIRING:spa	-328	0.39976	4.53191e-132	8.46349e-12
SP GRATE SPEED ZONE 5:av	-526	-0.39783	3.43876e-03	9.69651e-01
F LVE-STM BLR:av	-334	-0.39321	1.50859e-06	4.02296e-16
CLC BRN-OUT-TEMP:me	230	-0.39012	3.34902e-12	1.95071e-04
Crude gas meas CO:av	276	0.38703	9.99920e-01	3.37632e-01
G GRT RGHT ZN 5:av	7076	0.38495	#	#
THRM LD:av	-345	-0.38113	9.99991e-01	2.92420e-02
T AV FLU-GAS CELG 1ST PAS:av	-514	-0.36052	2.16806e-49	1.55404e-03
PÄÄHÖYRY R2 R3 VIRTAUS:av	7862	-0.35267	#	#
SYÖTTÖVESI LÄMPÖTILA:av	2856	-0.35154	#	#

NOx-pit raja:TV1HNE10CQ002FRL	16373	0.35142	#	#
SAVUKAASUN NOX (NO2):av	143	-0.34977	5.24660e-04	2.23861e-05
F PRI-AIR GRT-RGHT ZN 2:pos	217	0.34527	1.46060e-02	5.78547e-04
TOC-pit raja:TV1HNE10CQ009FRL	16373	0.34283	#	#
NH3-pit raja:TV1HNE10CQ012FRL	16373	0.34282	#	#
HCl-pit raja:TV1HNE10CQ008FRL	16373	0.3428	#	#
HF-pit raja:TV1HNE10CQ007FRL	16373	0.34278	#	#
SO2-pit raja:TV1HNE10CQ004FRL	16373	0.34271	#	#
CO-pit raja:TV1HNE10CQ003FRL	16373	0.34207	#	#
Crude gas meas Nox:av	19536	0.34123	#	#
PÄÄHÖYRY R1 VIRTAUS:av	7998	-0.33511	#	#
G GRT LFT ZN 2:av	-19599	-0.32464	#	#
CLC SPD GRT RGHT TRK-ZN 4:pos	-402	-0.32346	2.99812e-01	4.64359e-02
ACTIVE POWER:av	7866	0.32155	#	#
T FLU-GAS 2 SEC 850℃:av	18973	-0.31333	#	#
CLC TEMP LVE-STM:pos	-1254	-0.30257	3.70549e-05	9.00851e-01
CLC SPD GRT LFT TRK-ZN 3:pos	21243	-0.30145	#	#
CLC TEMP DNSTR SH 2:pos	-476	-0.30072	7.52429e-02	6.22436e-05
CLC NO2 BLR OUTL:me	21434	-0.29926	#	#
F PRI-AIR GRT-LFT ZN 2:pos	20295	0.28986	#	#
T FLU-GAS DNSTR 3RD PASS:av	7207	-0.27639	#	#
T FLU-GAS UPSTR 3RD PASS:av	18987	-0.27052	#	#
CLC SPD GRT LFT TRK-ZN 4:pos	20153	-0.26908	#	#
G GRT LFT ZN 5:av	-17990	0.26882	#	#
F PRI-AIR GRT-RGHT ZN 1:pos	18793	-0.25639	#	#
G GRT LFT ZN 1:av	16229	0.25558	#	#
F PRI-AIR GRT-LFT ZN 1:pos	6987	-0.25333	#	#
CLC SPD GRT LFT TRK-ZN 2:pos	-116	-0.25235	1.63136e-03	1.89496e-03
CLC SPD WSTR FDR RGHT:pos	-369	0.24811	2.74315e-03	3.17583e-05
G GRT RGHT ZN 2:av	-21474	-0.24069	#	#

CLC SPD GRT RGHT TRK-ZN 1:pos	11281	0.22456	#	#
CLC SPD GRT RGHT TRK-ZN 2:pos	16775	-0.22265	#	#
G GRT RGHT ZN 3:av	20808	-0.2174	#	#
CLC SPD GRT RGHT TRK-ZN 3:pos	-94	-0.21661	3.31229e-05	6.58408e-03
G GRT LFT ZN 3:av	21626	-0.20499	#	#
G GRT RGHT ZN 1:av	-1446	-0.20364	9.84099e-01	9.88856e-01
CLC SPD GRT LFT TRK-ZN 1:pos	857	-0.18774	7.88000e-02	6.40089e-01
CLC SPD GRT LFT TRK-ZN 1:av	-12002	-0.17467	#	#
CLC SPD GRT LFT TRK-ZN 2:av	-12002	-0.17467	#	#
CLC SPD GRT LFT TRK-ZN 4:av	-12002	-0.17467	#	#
CLC SPD GRT LFT TRK-ZN 3:av	-12002	-0.17467	#	#
CLC SPD WST FDR LFT:av	-12002	-0.17467	#	#
CLC SPD WSTR FDR LFT:pos	12165	-0.15613	#	#
CLC SPD GRT RGHT TRK-ZN 5:pos	2097	0.15501	#	#
G GRT RGHT ZN 4:av	18554	0.13667	#	#
G GRT LFT ZN 4:av	-4512	-0.13344	#	#
CLC SPD GRT LFT TRK-ZN 5:pos	19814	-0.11836	#	#
G WST-FDR LFT:av	18805	-0.10315	#	#
G WST-FDR RGHT:av	-308	0.08247	6.34284e-08	1.33135e-08

Table D.3. *Results with extracted flame front average point.*

Signal name	m_{max}	$\hat{R}_{xy}$	P_{xy}	P_{yx}
CLC FIRING:me	159	-0.56861	1.87638e-06	1.59870e-06
F PRI-AIR GRT-RGHT ZN 4:me	174	-0.54459	5.72119e-06	1.08159e-06
F PRI-AIR GRT-LFT ZN 5:me	173	-0.54412	1.70003e-08	4.75488e-12
F PRI-AIR GRT-LFT ZN 4:me	173	-0.54389	7.55732e-07	1.95016e-04
F TOT PRI-AIR GRT-ZN:av	173	-0.5429	5.92478e-06	2.14932e-08
F PRI-AIR GRT-LFT ZN 3:me	174	-0.54287	2.35569e-04	7.78231e-08
F PRI-AIR GRT- RGHT ZN 5:spa	175	-0.54275	1.10300e-16	6.92948e-02

F PRI-AIR GRT-RGHT ZN 1:spa	175	-0.54275	1.10341e-16	6.89802e-02
F PRI-AIR GRT-LFT ZN 5:spa	175	-0.54275	1.10341e-16	6.89802e-02
F PRI-AIR GRT-LFT ZN 1:spa	175	-0.54275	1.10341e-16	6.89802e-02
F PRI-AIR GRT-RGHT ZN 3:spa	175	-0.54273	7.34281e-15	1.13597e-01
F PRI-AIR GRT-LFT ZN 3:spa	175	-0.54273	7.34281e-15	1.13597e-01
CLC PRES LVE-STM BY ACC:pos	175	-0.54273	2.69773e-19	3.15814e-02
F PRI-AIR GRT-LFT ZN 4:spa	175	-0.54272	2.69480e-14	5.08204e-02
F PRI-AIR GRT-RGHT ZN 4:spa	175	-0.54272	2.69480e-14	5.08204e-02
F PRI-AIR GRT-LFT ZN 2:spa	175	-0.54272	7.30807e-18	1.55554e-01
F PRI-AIR GRT-RGHT ZN 2:spa	175	-0.54272	7.30807e-18	1.55554e-01
F PRI-AIR GRT- RGHT ZN 5:me	173	-0.54262	1.52504e-04	4.60899e-07
F PRI-AIR GRT-LFT ZN 2:me	173	-0.54256	1.26158e-04	6.38233e-05
F PRI-AIR GRT-LFT ZN 1:me	172	-0.54225	2.02161e-09	3.24536e-06
F PRI-AIR GRT-RGHT ZN 3:me	173	-0.54223	2.44933e-08	2.79031e-06
F PRI-AIR GRT-RGHT ZN 1:me	172	-0.54217	9.16648e-04	3.42543e-09
F PRI-AIR GRT-RGHT ZN 2:me	173	-0.54152	1.74146e-07	1.04005e-07
F PRI-AIR GRT-LFT ZN 5:pos	189	-0.52187	1.21177e-08	3.51503e-06
F PRI-AIR GRT-LFT ZN 4:pos	167	-0.51948	1.59779e-05	9.58802e-03
F PRI-AIR GRT- RGHT ZN 5:pos	188	-0.51372	5.82404e-03	4.06747e-05
F PRI-AIR GRT-RGHT ZN 4:pos	185	-0.49625	9.50988e-08	7.49079e-06
CEMS SAVUKAASUN VIRTAUS:av	155	-0.48944	1.75698e-03	2.13480e-05
PÄÄHÖYRY LÄMPÖTILA:av	84	-0.48426	6.97673e-02	7.23000e-07
T AVG LVE-STM BLR:av	78	-0.48153	1.91280e-02	9.04913e-05
SP FEEDER SPEED:av	-414	0.45795	1.88748e-25	6.58941e-01
CLC PRES LVE-STM BY ACC:me	-72	0.4578	1.62893e-17	1.52757e-02
CLC FIRING:pos	-411	0.45701	7.46039e-11	2.17558e-01
Crude gas meas HCL:av	-8815	-0.45652	#	#
P AVG LVE-STM BLR:av	-74	0.45602	1.32666e-24	4.68521e-02
TULIPESÄ SK T-KA YLÄR:av	234	0.45125	3.35445e-02	9.78606e-02
CLC O2 FLU-GAS:me	77	-0.44577	2.44838e-07	3.81806e-02

F NH3-W SNCR-INJ:av	18393	0.44378	#	#
CLC NO2 BLR OUTL:pos	18387	0.44339	#	#
SEK.ILMAN VIRTAUS:av	135	0.43589	1.17266e-06	1.31982e-05
CLC O2 FLU-GAS:pos	131	0.43551	7.58944e-07	1.77800e-03
F TOT SECY-AIR:spa	131	0.4354	1.50490e-06	1.54326e-03
F TOT SECY-AIR:me	135	0.43534	5.11584e-05	4.74469e-05
SP GRATE SPEED ZONE 4:av	-488	0.43526	8.00555e-02	4.57926e-01
SP GRATE SPEED ZONE 1:av	-488	0.43516	8.52786e-02	4.03124e-01
SP GRATE SPEED ZONE 2:av	-488	0.43516	8.52786e-02	4.03124e-01
SP GRATE SPEED ZONE 3:av	-488	0.43513	8.37803e-02	3.95895e-01
SEK.ILMAN VIRTAUS ETUSEIN:av	134	0.43466	1.62992e-05	1.40651e-03
F TOT SECY-AIR:pos	134	0.42738	1.17373e-06	5.53266e-05
Crude gas meas SO2:av	-8865	-0.42192	#	#
CLC BRN-OUT-TEMP:pos	-333	-0.42115	1.35306e-132	6.26101e-13
CLC FIRING:spa	-333	-0.4211	2.29378e-137	5.41668e-13
F PRI-AIR GRT-RGHT ZN 3:pos	153	-0.41981	3.67135e-03	9.79071e-03
SP GRATE SPEED ZONE 5:av	-533	0.4152	3.59650e-02	9.04362e-01
F LVE-STM BLR:av	-340	0.41392	7.35638e-12	3.48883e-23
Crude gas meas CO:av	264	-0.4056	8.75918e-01	2.47364e-01
THRM LD:av	-352	0.40082	9.83667e-01	9.03906e-02
CLC BRN-OUT-TEMP:me	215	0.39742	1.56839e-11	1.13120e-02
F PRI-AIR GRT-LFT ZN 3:pos	190	-0.39499	7.28939e-07	1.15296e-06
G GRT RGHT ZN 5:av	7073	-0.38498	#	#
T AV FLU-GAS CELG 1ST PAS:av	-513	0.37242	1.47418e-38	6.54971e-04
SAVUKAASUN NOX (NO2):av	128	0.37112	2.74036e-08	1.25222e-02
PÄÄHÖYRY R2 R3 VIRTAUS:av	7860	0.3663	#	#
SYÖTTÖVESI LÄMPÖTILA:av	2856	0.36329	#	#
Crude gas meas Nox:av	19538	-0.36279	#	#
NOx-pit raja:TV1HNE10CQ002FRL	16365	-0.35433	#	#
PÄÄHÖYRY R1 VIRTAUS:av	7991	0.34931	#	#

TOC-pit raja:TV1HNE10CQ009FRL	16364	-0.34493	#	#
NH3-pit raja:TV1HNE10CQ012FRL	16364	-0.34492	#	#
HCl-pit raja:TV1HNE10CQ008FRL	16364	-0.3449	#	#
HF-pit raja:TV1HNE10CQ007FRL	16364	-0.34488	#	#
SO2-pit raja:TV1HNE10CQ004FRL	16364	-0.34482	#	#
CO-pit raja:TV1HNE10CQ003FRL	16364	-0.34417	#	#
F PRI-AIR GRT-RGHT ZN 2:pos	203	-0.33909	4.41036e-05	1.69908e-04
ACTIVE POWER:av	7863	-0.33445	#	#
CLC SPD GRT RGHT TRK-ZN 4:pos	-404	0.33294	1.31613e-01	2.86035e-02
G GRT LFT ZN 2:av	-19599	0.32364	#	#
T FLU-GAS 2 SEC 850℃:av	-525	0.32138	1.54286e-40	1.71531e-03
CLC TEMP LVE-STM:pos	-1265	0.31724	1.47583e-01	1.66522e-01
CLC SPD GRT LFT TRK-ZN 3:pos	21243	0.31556	#	#
CLC TEMP DNSTR SH 2:pos	-492	0.31379	3.97611e-02	1.09923e-07
F PRI-AIR GRT-LFT ZN 2:pos	20285	-0.29108	#	#
CLC NO2 BLR OUTL:me	21425	0.28743	#	#
T FLU-GAS DNSTR 3RD PASS:av	7197	0.28269	#	#
CLC SPD GRT LFT TRK-ZN 4:pos	20147	0.27899	#	#
T FLU-GAS UPSTR 3RD PASS:av	3812	0.27742	#	#
F PRI-AIR GRT-RGHT ZN 1:pos	18779	0.26314	#	#
F PRI-AIR GRT-LFT ZN 1:pos	6984	0.26176	#	#
CLC SPD GRT LFT TRK-ZN 2:pos	-115	0.26106	1.42037e-04	1.75474e-03
G GRT LFT ZN 1:av	16215	-0.26092	#	#
CLC SPD WSTR FDR RGHT:pos	-372	-0.25971	4.04225e-03	6.74770e-04
G GRT LFT ZN 5:av	-17988	-0.25	#	#
G GRT RGHT ZN 2:av	20133	-0.24627	#	#
CLC SPD GRT RGHT TRK-ZN 2:pos	16773	0.23288	#	#
CLC SPD GRT RGHT TRK-ZN 1:pos	11281	-0.22327	#	#
G GRT RGHT ZN 3:av	20808	0.22209	#	#
CLC SPD GRT RGHT TRK-ZN 3:pos	16029	0.21897	#	#

G GRT LFT ZN 3:av	21626	0.21283	#	#
G GRT RGHT ZN 1:av	-1437	0.2068	9.99978e-01	8.59912e-01
CLC SPD GRT LFT TRK-ZN 2:av	-12018	0.18567	#	#
CLC SPD GRT LFT TRK-ZN 1:av	-12018	0.18567	#	#
CLC SPD GRT LFT TRK-ZN 4:av	-12018	0.18567	#	#
CLC SPD GRT LFT TRK-ZN 3:av	-12018	0.18567	#	#
CLC SPD WST FDR LFT:av	-12018	0.18567	#	#
CLC SPD GRT LFT TRK-ZN 1:pos	13535	0.18288	#	#
CLC SPD WSTR FDR LFT:pos	12121	0.16247	#	#
CLC SPD GRT RGHT TRK-ZN 5:pos	2056	-0.15688	#	#
G GRT RGHT ZN 4:av	18556	-0.13567	#	#
G GRT LFT ZN 4:av	-4515	0.13491	#	#
CLC SPD GRT LFT TRK-ZN 5:pos	19811	0.12432	#	#
G WST-FDR LFT:av	18765	0.10704	#	#
G WST-FDR RGHT:av	-302	-0.08602	2.56885e-06	1.78285e-08

Table D.4. *Results with extracted flame front coefficient* b*.*

Signal name	m_{max}	$\hat{R}_{xy}$	P_{xy}	P_{yx}
F PRI-AIR GRT-LFT ZN 2:pos	228	0.45146	7.79969e-05	3.76349e-12
THRM LD:av	250	0.42482	5.24827e-03	8.77438e-02
CLC NO2 BLR OUTL:me	-19779	0.42046	#	#
F LVE-STM BLR:av	279	0.416	4.45132e-02	1.70598e-05
CLC BRN-OUT-TEMP:pos	12701	0.39386	#	#
CLC FIRING:spa	12701	0.39384	#	#
T AV FLU-GAS CELG 1ST PAS:av	-19529	-0.3929	#	#
CLC TEMP DNSTR SH 2:pos	709	0.39041	4.66804e-03	9.39497e-10
T FLU-GAS UPSTR 3RD PASS:av	536	0.3817	5.37903e-02	2.68367e-01
Crude gas meas HCL:av	-8448	-0.3769	#	#
SP GRATE SPEED ZONE 1:av	12559	-0.37437	#	#

SP GRATE SPEED ZONE 2:av	12559	-0.37437	#	#
SP GRATE SPEED ZONE 3:av	12558	-0.37437	#	#
SP GRATE SPEED ZONE 4:av	12558	-0.37427	#	#
CLC O2 FLU-GAS:me	667	-0.36976	1.13367e-10	6.58571e-09
T FLU-GAS DNSTR 3RD PASS:av	628	0.36731	1.56920e-03	1.15643e-02
PÄÄHÖYRY R1 VIRTAUS:av	-16283	-0.36699	#	#
F PRI-AIR GRT-LFT ZN 1:pos	245	0.36633	1.09825e-06	1.48222e-07
SYÖTTÖVESI LÄMPÖTILA:av	-6396	0.36549	#	#
SP FEEDER SPEED:av	12645	-0.36215	#	#
CLC FIRING:pos	12645	-0.3565	#	#
PÄÄHÖYRY R2 R3 VIRTAUS:av	-16320	-0.3563	#	#
ACTIVE POWER:av	-7432	-0.35388	#	#
Crude gas meas SO2:av	-7000	-0.34872	#	#
CLC FIRING:me	39	-0.34449	2.35254e-02	2.73912e-03
F PRI-AIR GRT- RGHT ZN 5:pos	-11152	0.34333	#	#
SEK.ILMAN VIRTAUS ETUSEIN:av	61	0.34193	9.26660e-02	1.55299e-03
CLC O2 FLU-GAS:pos	58	0.34154	8.67979e-04	1.51916e-03
F TOT SECY-AIR:spa	58	0.34153	1.45057e-03	5.80226e-05
F TOT SECY-AIR:me	61	0.3415	7.66791e-02	6.71862e-03
SEK.ILMAN VIRTAUS:av	61	0.34096	3.61726e-02	1.24660e-02
F PRI-AIR GRT-LFT ZN 5:pos	-11161	0.33804	#	#
CLC TEMP LVE-STM:pos	410	0.33493	8.33734e-05	6.70781e-05
F TOT SECY-AIR:pos	61	0.33279	5.29992e-02	1.02798e-03
F PRI-AIR GRT-LFT ZN 3:pos	-11149	0.33042	#	#
F PRI-AIR GRT- RGHT ZN 5:me	19381	0.32849	#	#
F PRI-AIR GRT-RGHT ZN 2:me	19383	0.32825	#	#
F PRI-AIR GRT-LFT ZN 5:me	19383	0.32822	#	#
F PRI-AIR GRT-RGHT ZN 2:spa	19384	0.32749	#	#
F PRI-AIR GRT-LFT ZN 2:spa	19384	0.32749	#	#
F PRI-AIR GRT-LFT ZN 1:me	19381	0.32738	#	#

F PRI-AIR GRT-LFT ZN 5:spa	19384	0.32737	#	#
F PRI-AIR GRT- RGHT ZN 5:spa	19384	0.32737	#	#
F PRI-AIR GRT-RGHT ZN 1:spa	19384	0.32737	#	#
F PRI-AIR GRT-LFT ZN 1:spa	19384	0.32737	#	#
F PRI-AIR GRT-RGHT ZN 3:spa	19384	0.32734	#	#
F PRI-AIR GRT-LFT ZN 3:spa	19384	0.32734	#	#
F PRI-AIR GRT-LFT ZN 4:spa	19384	0.32734	#	#
F PRI-AIR GRT-RGHT ZN 4:spa	19384	0.32734	#	#
CLC PRES LVE-STM BY ACC:pos	19384	0.3273	#	#
F PRI-AIR GRT-RGHT ZN 1:me	19381	0.32701	#	#
F PRI-AIR GRT-LFT ZN 4:me	19382	0.32695	#	#
F TOT PRI-AIR GRT-ZN:av	19382	0.32695	#	#
F PRI-AIR GRT-LFT ZN 2:me	19383	0.32673	#	#
F PRI-AIR GRT-RGHT ZN 3:me	19383	0.32672	#	#
F PRI-AIR GRT-LFT ZN 3:me	19382	0.32636	#	#
F PRI-AIR GRT-RGHT ZN 4:me	19379	0.32537	#	#
CEMS SAVUKAASUN VIRTAUS:av	-17293	0.32414	#	#
F PRI-AIR GRT-RGHT ZN 2:pos	-11045	0.32265	#	#
NOx-pit raja:TV1HNE10CQ002FRL	-14927	0.32132	#	#
F PRI-AIR GRT-RGHT ZN 3:pos	-11116	0.31629	#	#
NH3-pit raja:TV1HNE10CQ012FRL	-14905	0.31562	#	#
HCl-pit raja:TV1HNE10CQ008FRL	-14905	0.31557	#	#
HF-pit raja:TV1HNE10CQ007FRL	-14905	0.31557	#	#
TOC-pit raja:TV1HNE10CQ009FRL	-14905	0.31557	#	#
CO-pit raja:TV1HNE10CQ003FRL	-14905	0.31524	#	#
SO2-pit raja:TV1HNE10CQ004FRL	-14904	0.31481	#	#
F PRI-AIR GRT-RGHT ZN 4:pos	-11159	0.3142	#	#
T FLU-GAS 2 SEC 850℃:av	-19503	-0.31277	#	#
F PRI-AIR GRT-RGHT ZN 1:pos	270	0.31134	3.44516e-05	2.13111e-10
F PRI-AIR GRT-LFT ZN 4:pos	-11147	0.30803	#	#

CLC BRN-OUT-TEMP:me	-19189	0.30661	#	#
CLC PRES LVE-STM BY ACC:me	-20255	-0.30303	#	#
P AVG LVE-STM BLR:av	-20254	-0.30245	#	#
F NH3-W SNCR-INJ:av	18240	0.29933	#	#
CLC NO2 BLR OUTL:pos	18233	0.29907	#	#
CLC SPD GRT LFT TRK-ZN 3:pos	-20312	-0.29669	#	#
Crude gas meas Nox:av	14852	-0.29008	#	#
G GRT RGHT ZN 1:av	-20909	0.28913	#	#
SP GRATE SPEED ZONE 5:av	10984	-0.28878	#	#
SAVUKAASUN NOX (NO2):av	19177	-0.28358	#	#
Crude gas meas CO:av	94	-0.28122	1.77231e-04	1.58816e-01
G GRT RGHT ZN 5:av	-17813	0.27487	#	#
TULIPESÄ SK T-KA YLÄR:av	-15257	-0.26881	#	#
CLC SPD GRT RGHT TRK-ZN 1:pos	-21208	-0.24062	#	#
G GRT LFT ZN 5:av	316	0.23771	1.98569e-17	3.39658e-10
PÄÄHÖYRY LÄMPÖTILA:av	-5630	-0.22796	#	#
T AVG LVE-STM BLR:av	-6617	-0.22737	#	#
CLC SPD WST FDR LFT:av	-16623	0.21956	#	#
CLC SPD GRT LFT TRK-ZN 2:av	-16623	0.21956	#	#
CLC SPD GRT LFT TRK-ZN 4:av	-16623	0.21956	#	#
CLC SPD GRT LFT TRK-ZN 1:av	-16623	0.21956	#	#
CLC SPD GRT LFT TRK-ZN 3:av	-16623	0.21956	#	#
G GRT LFT ZN 3:av	-16541	0.21494	#	#
CLC SPD GRT RGHT TRK-ZN 4:pos	12558	-0.21297	#	#
G GRT LFT ZN 1:av	10444	-0.20751	#	#
CLC SPD GRT LFT TRK-ZN 4:pos	13920	0.20706	#	#
CLC SPD GRT RGHT TRK-ZN 5:pos	-2993	-0.19918	#	#
CLC SPD GRT RGHT TRK-ZN 3:pos	-18835	-0.19306	#	#
CLC SPD GRT LFT TRK-ZN 1:pos	21354	0.18742	#	#
CLC SPD WSTR FDR RGHT:pos	12612	0.1776	#	#

G GRT LFT ZN 2:av	-21100	-0.17715	#	#
CLC SPD GRT LFT TRK-ZN 2:pos	-6466	0.17639	#	#
G GRT LFT ZN 4:av	-19293	0.17216	#	#
G GRT RGHT ZN 3:av	-4659	-0.16598	#	#
G GRT RGHT ZN 2:av	-13331	0.16164	#	#
CLC SPD GRT RGHT TRK-ZN 2:pos	13730	0.15623	#	#
CLC SPD WSTR FDR LFT:pos	11456	0.1555	#	#
G GRT RGHT ZN 4:av	-1346	-0.09658	1.26758e-05	1.32420e-04
CLC SPD GRT LFT TRK-ZN 5:pos	21638	0.09627	#	#
G WST-FDR LFT:av	12243	0.09389	#	#
G WST-FDR RGHT:av	12383	0.07907	#	#

Table D.5. *Results with extracted flame front coefficient* a*.*

Signal name	m_{max}	$\hat{R}_{xy}$	P_{xy}	P_{yx}
CLC FIRING:me	406	-0.67912	6.79396e-03	4.91777e-04
Crude gas meas HCL:av	-8627	-0.6213	#	#
Crude gas meas SO2:av	-8717	-0.60583	#	#
CLC O2 FLU-GAS:me	325	-0.59969	1.07321e-04	2.67876e-06
CEMS SAVUKAASUN VIRTAUS:av	431	-0.59309	5.76981e-04	2.59908e-01
F PRI-AIR GRT-LFT ZN 4:me	435	-0.5891	9.90974e-03	1.25943e-03
F PRI-AIR GRT-RGHT ZN 4:me	433	-0.58837	1.01992e-04	9.95752e-04
F PRI-AIR GRT-RGHT ZN 3:spa	435	-0.58817	7.17191e-02	1.07000e-41
F PRI-AIR GRT-LFT ZN 3:spa	435	-0.58817	7.17191e-02	1.07000e-41
CLC PRES LVE-STM BY ACC:pos	435	-0.58817	9.53388e-02	9.75969e-35
F PRI-AIR GRT-LFT ZN 4:spa	435	-0.58815	2.70500e-02	8.98539e-37
F PRI-AIR GRT-RGHT ZN 4:spa	435	-0.58815	2.70500e-02	8.98539e-37
F PRI-AIR GRT-LFT ZN 1:spa	435	-0.58797	1.18161e-01	1.97003e-34
F PRI-AIR GRT-LFT ZN 5:spa	435	-0.58797	1.18161e-01	1.97003e-34
F PRI-AIR GRT-RGHT ZN 1:spa	435	-0.58797	1.18161e-01	1.97003e-34

F PRI-AIR GRT-RGHT ZN 2:spa	435	-0.58797	6.10807e-02	1.35336e-32
F PRI-AIR GRT- RGHT ZN 5:spa	435	-0.58797	1.18363e-01	1.98238e-34
F PRI-AIR GRT-LFT ZN 2:spa	435	-0.58797	6.10807e-02	1.35336e-32
F PRI-AIR GRT-LFT ZN 5:me	434	-0.58776	2.80820e-05	2.34981e-02
F PRI-AIR GRT-LFT ZN 3:me	434	-0.58759	2.30743e-04	6.18148e-04
F PRI-AIR GRT-LFT ZN 1:me	432	-0.58741	3.64858e-03	5.10079e-03
F TOT PRI-AIR GRT-ZN:av	434	-0.58728	1.47161e-02	7.12103e-04
F PRI-AIR GRT-RGHT ZN 3:me	433	-0.58718	1.88892e-04	5.50075e-04
F PRI-AIR GRT-RGHT ZN 1:me	433	-0.58715	4.97493e-02	1.25965e-01
F PRI-AIR GRT- RGHT ZN 5:me	434	-0.58701	8.01250e-05	8.16330e-03
F LVE-STM BLR:av	-176	0.58657	1.01279e-02	9.01083e-15
F PRI-AIR GRT-LFT ZN 2:me	435	-0.58629	1.75011e-04	1.08411e-02
THRM LD:av	-185	0.58574	3.94967e-06	3.94843e-01
F PRI-AIR GRT-RGHT ZN 2:me	434	-0.58516	6.62647e-03	2.03514e-03
Crude gas meas CO:av	529	-0.53904	9.99970e-01	1.00000e+00
SEK.ILMAN VIRTAUS:av	191	0.53854	1.44376e-06	6.12430e-05
CLC O2 FLU-GAS:pos	187	0.53811	5.96666e-13	6.20106e-08
F TOT SECY-AIR:spa	187	0.53801	2.77144e-10	2.21911e-07
F TOT SECY-AIR:me	190	0.53798	5.09793e-08	1.81527e-04
SEK.ILMAN VIRTAUS ETUSEIN:av	189	0.53731	9.11469e-08	3.42293e-05
CLC FIRING:spa	11212	0.5322	#	#
CLC BRN-OUT-TEMP:pos	11212	0.53189	#	#
F TOT SECY-AIR:pos	192	0.52761	5.15739e-08	4.92394e-07
PÄÄHÖYRY R2 R3 VIRTAUS:av	8030	0.5227	#	#
TULIPESÄ SK T-KA YLÄR:av	353	0.52044	1.72321e-05	8.75792e-08
SP FEEDER SPEED:av	11131	-0.50869	#	#
CLC FIRING:pos	11133	-0.5075	#	#
SP GRATE SPEED ZONE 4:av	11060	-0.50407	#	#
SP GRATE SPEED ZONE 3:av	11060	-0.50407	#	#
SP GRATE SPEED ZONE 1:av	11060	-0.50404	#	#

SP GRATE SPEED ZONE 2:av	11060	-0.50404	#	#
P AVG LVE-STM BLR:av	-40	0.49876	3.73303e-02	6.74906e-02
CLC PRES LVE-STM BY ACC:me	-37	0.49843	1.24083e-01	1.23592e-01
PÄÄHÖYRY R1 VIRTAUS:av	8166	0.49675	#	#
ACTIVE POWER:av	8044	-0.48742	#	#
CLC TEMP DNSTR SH 2:pos	-474	0.48413	1.32474e-03	2.77240e-08
F NH3-W SNCR-INJ:av	18523	0.47183	#	#
CLC NO2 BLR OUTL:pos	18518	0.47121	#	#
SAVUKAASUN NOX (NO2):av	299	0.46464	1.16125e-05	4.61006e-04
SP GRATE SPEED ZONE 5:av	-476	0.45262	4.01108e-01	4.15033e-01
F PRI-AIR GRT-LFT ZN 5:pos	447	-0.45215	8.74129e-04	3.41561e-03
F PRI-AIR GRT- RGHT ZN 5:pos	447	-0.44019	8.81471e-03	1.78506e-02
F PRI-AIR GRT-LFT ZN 4:pos	428	-0.43924	8.86033e-02	5.35992e-04
CLC TEMP LVE-STM:pos	-1143	0.42995	2.31880e-01	4.70193e-02
SYÖTTÖVESI LÄMPÖTILA:av	-6339	0.41944	#	#
F PRI-AIR GRT-RGHT ZN 4:pos	433	-0.40903	2.42462e-04	5.07502e-02
T AV FLU-GAS CELG 1ST PAS:av	-511	0.39216	2.04704e-21	2.30998e-05
Crude gas meas Nox:av	18825	-0.3873	#	#
CLC BRN-OUT-TEMP:me	437	0.3742	4.54802e-04	5.00784e-02
F PRI-AIR GRT-RGHT ZN 3:pos	18999	0.35937	#	#
PÄÄHÖYRY LÄMPÖTILA:av	178	-0.3577	1.00640e-06	6.96465e-06
F PRI-AIR GRT-RGHT ZN 2:pos	-1309	0.35552	4.87680e-03	2.36191e-02
T FLU-GAS DNSTR 3RD PASS:av	-404	0.35426	9.64407e-01	8.30136e-01
CLC SPD GRT LFT TRK-ZN 3:pos	21320	0.35279	#	#
F PRI-AIR GRT-RGHT ZN 1:pos	-647	0.35169	4.46935e-05	6.79909e-03
T AVG LVE-STM BLR:av	161	-0.35024	4.30442e-05	3.42883e-07
T FLU-GAS 2 SEC 850℃:av	-1237	0.34932	7.17722e-18	5.84100e-01
T FLU-GAS UPSTR 3RD PASS:av	-508	0.3473	9.18827e-01	6.92170e-01
F PRI-AIR GRT-LFT ZN 2:pos	-869	0.33816	1.03975e-04	9.40975e-03
F PRI-AIR GRT-LFT ZN 1:pos	-652	0.33751	2.95300e-05	5.60801e-05

CLC NO2 BLR OUTL:me	19912	-0.33475	#	#
F PRI-AIR GRT-LFT ZN 3:pos	18974	0.33326	#	#
G GRT RGHT ZN 3:av	21093	0.32257	#	#
CLC SPD GRT RGHT TRK-ZN 4:pos	-388	0.32218	1.14982e-02	1.86971e-02
CLC SPD GRT LFT TRK-ZN 4:pos	20339	0.30645	#	#
CLC SPD WSTR FDR RGHT:pos	-367	-0.3018	1.09505e-04	2.00493e-05
G GRT RGHT ZN 5:av	12376	0.28341	#	#
G GRT LFT ZN 1:av	16423	-0.27874	#	#
G GRT LFT ZN 2:av	-19636	0.27205	#	#
CLC SPD WST FDR LFT:av	-20651	0.26881	#	#
CLC SPD GRT LFT TRK-ZN 1:av	-20651	0.26881	#	#
CLC SPD GRT LFT TRK-ZN 4:av	-20651	0.26881	#	#
CLC SPD GRT LFT TRK-ZN 3:av	-20651	0.26881	#	#
CLC SPD GRT LFT TRK-ZN 2:av	-20651	0.26881	#	#
G GRT LFT ZN 5:av	11869	0.26486	#	#
G GRT RGHT ZN 2:av	20199	-0.26112	#	#
CLC SPD GRT RGHT TRK-ZN 3:pos	-14	0.25397	7.99821e-08	3.06016e-01
CLC SPD GRT LFT TRK-ZN 2:pos	-296	0.24276	2.53929e-07	9.72418e-07
NOx-pit raja:TV1HNE10CQ002FRL	20773	-0.24201	#	#
CO-pit raja:TV1HNE10CQ003FRL	20778	-0.23319	#	#
TOC-pit raja:TV1HNE10CQ009FRL	20778	-0.23281	#	#
HF-pit raja:TV1HNE10CQ007FRL	20778	-0.2328	#	#
HCl-pit raja:TV1HNE10CQ008FRL	20778	-0.2328	#	#
NH3-pit raja:TV1HNE10CQ012FRL	20778	-0.23271	#	#
SO2-pit raja:TV1HNE10CQ004FRL	20778	-0.23232	#	#
G GRT LFT ZN 3:av	21637	0.22882	#	#
G GRT RGHT ZN 1:av	-12703	-0.2176	#	#
CLC SPD GRT RGHT TRK-ZN 2:pos	16902	0.21675	#	#
CLC SPD GRT RGHT TRK-ZN 5:pos	11930	0.21507	#	#
CLC SPD GRT LFT TRK-ZN 1:pos	17916	0.20845	#	#

CLC SPD GRT RGHT TRK-ZN 1:pos	-333	0.20588	1.52993e-06	2.92973e-04
CLC SPD WSTR FDR LFT:pos	12206	0.20337	#	#
G GRT RGHT ZN 4:av	18658	-0.14344	#	#
CLC SPD GRT LFT TRK-ZN 5:pos	20015	0.13338	#	#
G GRT LFT ZN 4:av	20493	-0.12531	#	#
G WST-FDR LFT:av	18991	0.11444	#	#
G WST-FDR RGHT:av	12184	0.09975	#	#

Table D.6. *Results with extracted flame area.*

Signal name	Description
CLC PRES LVE-STM BY ACC:spa	Live steam pressure setpoint
CLC O2 FLU-GAS:spa	Excessive flue-gas O_2 setpoint
CLC BRN-OUT-TEMP:spa	Burnout temperature setpoint
CLC SPD GRT LFT TRK-ZN 5:av	Left grate zone 5 movement speed
CLC HT-INP AUX-BRN 1:av	First auxiliary burner power
CLC HT-INP AUX-BRN 2:av	Second auxiliary burner power
CLC NO2 BLR OUTL:spa	SNCR ammonia injection setpoint

Table D.7. *Excluded signals.*